FINAL REPORT

A COMPREHENSIVE MODEL TO DETERMINE THE EFFECTS OF TEMPERATURE AND SPECIES FLUCTUATIONS ON REACTION RATES IN TURBULENT REACTING FLOWS*

W. CHINITZ**

*Work supported under Grant No. NAG1 - 18, National Aeronautics and Space Administration, Langley Research Center, High-Speed Aerodynamics Division, Hypersonic Propulsion Branch, Hampton, VA 23665

**Principal Investigator

Table of Contents

INTRODUCTION

The research summarized herein was begun on February 1, 1980 and had a two-fold objective:

1. The development of a computationally-viable model describing the interaction between fluid-mechanical turbulence and finite-rate combustion reactions, principally in high-speed flows; and

2. The development of chemical kinetic mechanisms, complete and global, describing the finite rate reaction of fuels of interest to NASA with air. These fuels included principally hydrogen and silane, although a limited amount of work involved hydrocarbon fuels as well.

During the course of this research, a number of external publications were issued which describe the work accomplished in substantial detail. As a result, in this Final Report relatively little emphasis will be placed upon the accomplishments adequately described elsewhere. Instead, our emphasis here will be upon aspects of the work not adequately described in the open literature.

THE TURBULENCE - REACTION CHEMISTRY INTERACTION MODEL

This model is described in substantial detail in references 1 and 2 and is summarized in reference 3. Basically, the model is of the "assumed pdf" type in which turbulent mean reaction rate terms are expressed in the form

$$\overline{\dot{w}}_{A_1,1} = \left[\int_{-\infty}^{\infty} k_{f,i}(T)\, p(T)\, dT\right]\left[\int_{-\infty}^{\infty}\int_{-\infty}^{\infty} C_{A_1} C_{A_2} \cdot p(C_{A_1}, C_{A_2})\, dC_{A_1}\, dC_{A_2}\right] \tag{1}$$

in which $k_{f,i}$ is the forward reaction rate coefficient for a particular reaction in a kinetic mechanism, p (T) is the probability density function (pdf) of the temperature, C_{A_j} are species concentrations, and p (C_{A_1}, C_{A_2}) is the joint pdf of these concentrations. Non-dimensionalizing the temperature and species concentrations and introducing the Arrhenius equation for $k_{f,i}$ ultimately leads to (refs. 1 - 3)

$$\overline{\dot{w}}_{A_1,1} = \left(Z_t \bar{k}_{f,i}\right) Z_r \bar{C}_{A_1} \bar{C}_{A_2} \tag{2}$$

in which Z_t is termed a temperature amplification ratio and Z_r is the species amplification ratio. Extensive work with a number of temperature pdf's revealed that values of Z_t are

relatively insensitive to its selection; hence, the computationally simple beta pdf was recommended for use. The recommended joint (two-variable pdf) required for the determination of Z_r is the most likely pdf. Typically, Z_t values appear as in Figs. 1 and 2, indicating that Z_t always exceeds unity. Hence, the effect of the turbulent temperature fluctuations is to increase the reaction rate coefficients.

On the other hand, Z_r may be greater than one (Fig. 3), an enhanced mixedness effect, or less than one (Fig. 4), an unmixedness effect, depending upon the sign of the species concentration gradient in the flow field. The assumed signs of those gradients depends upon the elementary reaction considered and upon the presumed location of the "flame front" location depicted in Fig. 5. Table I indicates the signs of the correlation coefficient ρ^* discussed in ref. 2; $\rho^*>0$ implies $Z_r>1$, $\rho^*<0$ implies $0<Z_r<1$. The results in ref. 2 assumed the "flame front" location to be at fuel-to-oxygen) equivalence ratio equal to one; ie, $\phi_{cr} = 1$. Subsequent work revealed that for the case examined in ref. 2, values in appreciably better agreement with the experimental values are obtained for $\phi_{cr} = 0.1$. These results are shown in Figs. 6 - 17.

A study was also undertaken to assess the effects of changes in the constants associated with the generation and dissipation terms in the transport equations discussed in references 4 and 5 and used in reference 2. In particular, the constants C_{ε_1} and C_{ε_2} in the equation for the dissipation of turbulence kinetic energy and Cg_1 and Cg_2 used in all species fluctuations transport

equations and in the transport equation for the temperature fluctuations. The values consistently used heretofore are:

$C_{\varepsilon_1} = 1.43$

$C_{\varepsilon_2} = 1.92$

$Cg_1 = 2.80$

$Cg_2 = 2.00$

with C_{ε_2} modified for the case of axisymmetric flow.

The study of C_{ε_1} and C_{ε_2} was prompted by the conflicting results of two sensitivity analyses each of which dealt with a different flow situation: one, performed on a k-ε turbulence model for imcompressible round-jet flow showed large sensitivity to a one percent change in the empirical coefficients C_{ε_1} and C_{ε_2} in the ε transport equation [Ref. 6]; on the other hand, Pinckney's analysis on a k-ε turbulence model for "turbulent mixing of hydrogen injected from discrete holes in the surface of a rectangular duct" showed little sensitivity to a 10% change in C_{ε_1} and C_{ε_2} [Ref. 7].

For the experimental case in ref. 4, both C_{ε_1} and C_{ε_2} were increased by 1% as in Reference 6. The results* (Figs. 18 and 19) showed no sensitivity to the increase in the constants. That these results agree with Pinckney's findings further confirms the correctness of the standard values for C_{ε_1} and C_{ε_2} for turbulent, compressible flow.

---

* Note that the only parameters used to compare the results are H_2O and O_2 concentrations because pitot pressure and N_2 concentrations have been found to be insensitive to changes in the turbulence model [Ref. 6].

One of the transport equations used in the model is that for temperature fluctuations [Ref. 8]. This is treated analogously to the equations for the transport of fluctuations in fuel and oxidizer, as well as the dissipation rate of turbulent kinetic energy. The fluctuation equation for fuel and oxidizer are both dependent on the constants C_{g1} and C_{g2}, the commonly recommended values of which are given above. However, no references have been located setting forth the equivalent constants (here called C_1 and C_2) in the temperature fluctuation equation; so the code uses $C_1 = C_{g1}$ and $C_2 = C_{g2}$.

An investigation was made of the assumed value of C_2. The model was tested for values of $C_2 = (0.9)C_{g1}$ and $C_2 = (0.1)C_{g2}$. The ten percent decrease in the value of C_2 did not cause any change in the results. However, decreasing the value by one order of magnitude caused significant changes (Fig. 20). Improvement was found from the centerline radially outward until the start of combustion. Here, the mass fraction of oxygen was found to be significantly lower and the mass fraction of water was found to be somewhat higher.

This work suggests that the value of C_2 in the equation for the transport of temperature fluctuations should perhaps not be the same as the value of C_{g2} in the equations for fluctuations of fuel and oxidizer. It is likely that C_1, assigned the value of C_{g1}, should also be revised.

All the transport equations upon which this model is based require initial radial profiles. Initial values for the equation for the temperature fluctuations are required. There has been

no experimental or theoretical work done on this initial profile. In the code as employed in ref. 2, the initial value for the non-dimensional temperature fluctuations is $\overline{t'^2} = 0.003$ for all radial locations at the initial axial location. This is also the value used for the initial profiles in the transport equations for the fluctuations of fuel and oxidizer.

To determine the effects of changing the initial profile, two attempts were made to improve this profile. First, the initial value was raised by one order of magnitude to 0.03 (Fig. 21). This resulted in some improvement near the centerline and slight improvement in the combustion zone.

Evans, et. al. (ref. 4) reported that the initial profiles used in the transport equations for turbulence kinetic energy and its dissipation had a strong influence on their results. Their report gave two possible initial k-ε profiles: one by a theoretical method and the other deduced from experimental measurements and shown in Fig. 22.

The YCHARML code generates k-ε profiles according to the method discussed in ref. 4. These profiles had been used in all previous work, so in this study the "experimental" profiles (next page) were tried using a ϕ_{cr} of 1.0 (Fig. 5) and 0.1 (Fig. 6). As before (ref. 6), it was found that the critical equivalence ratio of 0.1 gave the better results (Fig. 7). However, the experimental initial k-ε profiles did not materially improve the results. From the centerline radially outward to the flame zone, the experimental profiles gave slightly better results, but outside the flame zone, the results were significantly worse.

CHEMICAL KINETICS STUDIES

Two principal results of these studies were the development of a global H_2 - air combustion model, described in reference 9, and a complete silane (SiH_4)-H_2-air mechanism, described in reference 10. The proposed hydrogen-air global combustion model consists of the two "elementary" reactions

$$H_2 + O_2 \xrightarrow{k_{f_1}} 2\ OH$$

$$2\ OH + H_2 \xrightarrow{k_{f_2}} 2\ H_2O$$

with the forward rate coefficients given in the form

$$K_{f_i} = A_i(\phi) T^{N_i} \exp(-E_i/RT) \qquad (3)$$

The recommended values (ref. 9) at one atmosphere pressure are

$A_1(\phi) = (8.917\phi + 31.4\ 33/\phi - 28.950) \times 10^{47}$, $cm^3/mol\text{-}5$

$E_1 = 4865$ cal/mol

$N_1 = 10$

$A_2(\phi) = (2.0 + 1.333/\phi - 0.833\phi) \times 10^{64}$, $cm^3/mol\text{-}5$

$E_2 = 42{,}500$ cal/mol

$N_2 = -13$

To account for the effects of pressures between 0.5 atm and 1.0 atm, A_2 must be revised as follows:

For $\phi \geq 1$

$$A_2 = 8.80 + 5.85/\phi - 3.67\phi - 4.80\,p - 3.20\,p/\phi + 2.00\,p\,\phi$$

For $\phi < 1$

$$A_2 = 0.67\,\phi^{-1.5}\,p^{-0.7}\,(8.80 + 5.85/\phi - 4.80\,p - 3.20\,p/\phi + 2.00\,p\,\phi)$$

The silane-hydrogen-air ignition and combustion studies are detailed in ref. 10.

Current interest in the use of hydrocarbon fuels in SCRAMJET engines requires that methods be sought for reducing the well-documented lengthy ignition delays and reaction times of hydrocarbon fuels. Two possible approaches to reducing these times are: (1) injecting (relatively) small quantities of hydrogen along with the hydrocarbon fuel with the hope that ignition delay times will be more like those for H_2 than for the CxHy; and (2) regeneratively heating the hydrocarbon prior to its injection into the combustion chamber so as to pyrolyze (thermally crack) it, with the expectation that substantial quantities of hydrogen will be among the pyrolysis products. Studies are underway to investigate both possibilities.

Calculated ignition delay times up to 33% (vol.) hydrogen in the fuel are shown in Fig. 26. Calculations have been carried out selecting propane (C_3H_8) as the representative hydrocarbon fuel.

As can be seen in Fig. 26, at 1.0 atm, ϕ = 1.0, the reduction in ignition delay time compared with that for pure C_3H_8 is slight. For example, at T_o = 1000K, $t_{ID} \simeq 0.05$ sec for C_3H_8 and about 0.025 sec for the 33% H_2/67% C_3H_8 mixture. On the other hand, $t_{ID} \approx 10^{-4}$ sec for pure H_2 at T_o = 1000K. It is recognized, however, that 33% H_2 in the fuel mixture represents very little hydrogen by mass. As an example, the mass equivalent of the 20% SiH_4/80% mixture as applied here would result in a fuel mixture of 98.88% H_2/1.12% C_3H_8 by volume. A similarly wide range of H_2/CxHy ratios was utilized in the experiments of Cookson (ref. 11), shown schematically in Fig. 27. His tests, the results of which are in Fig. 28, would span the range from about 3% H_2 to nearly 96% H_2 (by volume) had his "main" fuel been C_3H_8 rather than kerosene. It is interesting to note that using mode A (see Fig. 27), ignition could be achieved at reasonable kerosene injection pressure ratios using relatively small quantities of H_2 (about 3% to 33% by volume), whereas mode B required much more substantial quantities of H_2 (33% - 96% by volume). Hence, calculations were carried out employing hydrogen concentrations exceeding 33% by volume. The effect upon t_{ig} is shown in Fig. 29 (ϕ = 1, p - 1 atm). It is clear that appreciable reductions of t_{ig} do not occur for values of H_2 concentration less than 40%.

In order to arrive at a recommended <u>minimum</u> fuel hydrogen concentration for SCRAMJET engine applications, a cross-plot was made of the data in Fig. 29 and is shown in Fig. 30 at T_o = 1000 K and 1667 K. It is clear, looking at the 1000K curve, that very large

reductions in t_{ig} occur for fuel hydrogen concentrations exceeding 80% by volume (15.4% by weight). Hence, from the ignition viewpoint, fuel hydrogen concentrations exceeding that value are recommended.

Similar t_{ig} behavior occurs for values of equivalence ratio other than stoichiometric, as is shown in Figs. 31 and 32. This tends to reinforce the above recommendation of % H_2 > 80% (vol.).

From the viewpoint of reaction time, t_R, no clear effect of fuel hydrogen concentration was observed for the conditions calculated. The range of t_R values observed for hydrogen concentrations ranging from 0% to 96% is shown in Fig. 33.

The flame stabilizing characteristics of various C_3H_8/H_2 fuels are shown in the blowout limit correlations in Fig. 34. Here again, as may be seen in the cross-plot at $\phi = 1$ in Fig. 35, values of fuel hydrogen concentration exceeding 80% may be said to result in an "appreciable" shift of the stable flame envelope.

On the basis of these studies, fuel hydrogen concentrations exceeding 80% by volume (15.4% by weight) are recommended for SCRAMJET engines employing hydrogen - gaseous hydrocarbon fuel mixtures, provided that the fuel is propane or a higher molecular weight hydrocarbon. No a priori conclusions can be drawn concerning such lower molecular weight fuels as methane, ethane, ethene and acetylene.

In addition to the above studies, an extensive investigation was undertaken dealing with the ranges of applicability of chemical kinetic models of hydrogen-air combustion. A description of these studies is in Appendix A herein.

LIST OF EXTERNALLY-PUBLISHED REPORTS AND PAPERS

1. Use of Silane in SCRAMJET Research, Paper presented at the 17th JANNAF Combustion Meeting, Sept. 22-26, 1980 (with H. L. Beach, Jr., E. A. Mackley and R. C. Rogers).

2. The Effect of Temperature Fluctuations on Reaction Rate Constants in Turbulent Reacting Flows, in "Fluid Mechanics of Combustion Systems", Edited by T. Morel, R. P. Lohmann and J. J. Rackley, ASME, New York, 1981 (with P. Antaki and G. M. Kassar).

3. Using a Global Hydrogen-Air Combustion Model in Turbulent Reacting Flow Calculations, AIAA J., vol. 21, no. 4, April 1983, pp. 586-592 (with R. C. Rogers).

4. An Assessment of Global and Quasi-Global Models of Hydrocarbon and Hydrogen Combustion Kinetics for Reacting Flow Field Calculations, Paper presented at the 1983 JANNAF Propulsion Meeting, Feb. 14 - 18, 1983 (CPIA Publication No. 370).

5. A Model for Reaction Rates in Turbulent Reacting Flows, NASA TM 85746, May 1984 (with J. Evans).

6. Models for Calculating Reaction Rates in Turbulent Reacting Flows, Paper presented at the 1984 JANNAF Propulsion Meeting, Feb. 7 - 9, 1984 (CPIA Publ. No. 401).

7. Theoretical Studies of the Ignition and Combustion of Silane-Hydrogen-Air Mixtures, NASA CR 3876, Feb. 1985.

REFERENCES

1. Chinitz, W., Antaki, P. and Kassar, G.M., "The Effects of Temperature Fluctuations on Reaction Rate Constants in Turbulent Reacting Flows", in "Fluid Mechanics of Combustion Systems," T. Morel, R. P. Lohmann and J. M. Rackley, eds., ASME, New York, 1981.

2. Chinitz, W. and Evans, J. S., "A Model for Reaction Rates in Turbulent Reacting Flows", NASA TM 85746, May 1984.

3. Chinitz, W., "Models for Calculating Reaction Rates in Turbulent Reacting Flows", 1984 JANNAF Propulsion Meeting, Feb. 1984 (CPIA Publ. No. 401).

4. Evans, J. S., Schexnayder, C. J., Jr. and Beach, H. L., Jr., "Application of a Two-Dimensional Parabolic Computer Program to Prediction of Turbulent Reacting Flows", NASA TP 1169, March 1978.

5. Evans, J. S. and Schexnayder, C. J., Jr., "Influence of Chemical Kinetics and Unmixedness on Burning in Supersonic Hydrogen Flames", AIAA J., vol. 18, no. 2, Feb. 1980, pp. 188-193.

6. Raiszadeh, F. and Dwyer, H. A., "A Studywith Sensitivity Analysis of the K - ε Turbulence Model Applied to Jet Flows", AIAA Paper 83-0285, Jan. 1983.

7. Pinckney, S. Z., "Relationship of Initial Assumptions for Turbulence Quantities, K -ε Model Constants and K -ε Development in SHIP", Internal HPB Memo., NASA Langley Rsch Center, July 29, 1983.

8. Chinitz, W., "A Model to Determine the Effect of Temperature Fluctuations on the Reaction Rate Constant in Turbulent Reacting Flows", Internal HPB memo., NASA Langley Rsch Center, August 1979.

9. Rogers, R. C. and Chinitz, W., "Using a Global Hydrogen-Air Combustion Model in Turbulent Reacting Flow Calculations", AIAA J., vol 21, no. 4, April 1983, pp 586 - 592.

10. Chinitz, W., "Theoretical Studies of the Ignition and Combustion of Silane-Hydrogen-Air Mixtures", NASA CR 3876, Feb. 1985.

11. Cookson, R. A., "Mixing and Ignition of Enclosed Supersonic Diffusion Flames", Aerospace Rsch Labs, Wright-Patterson AFB, ARL 73-0070, April 1973.

TABLE 1

Reaction	Sign of the Correlation Coefficient			
	Forward		Reverse	
	$\phi > \phi_{cr}$	$\phi < \phi_{cr}$	$\phi > \phi_{cr}$	$\phi < \phi_{cr}$
1. $H_2+M = H+H+M$			+	+
2. $O_2+M = O+O+M$			+	+
3. $H_2O+M = OH+H+M$			+	+
4. $OH+M = O+H+M$			+	+
5. $H_2O+O = OH+OH$	+	+	+	+
6. $H_2O+H = OH+H_2$	+	+	-	+
7. $O_2+H = OH+O$	+	-	+	+
8. $H_2+O = OH+H$	-	+	+	+

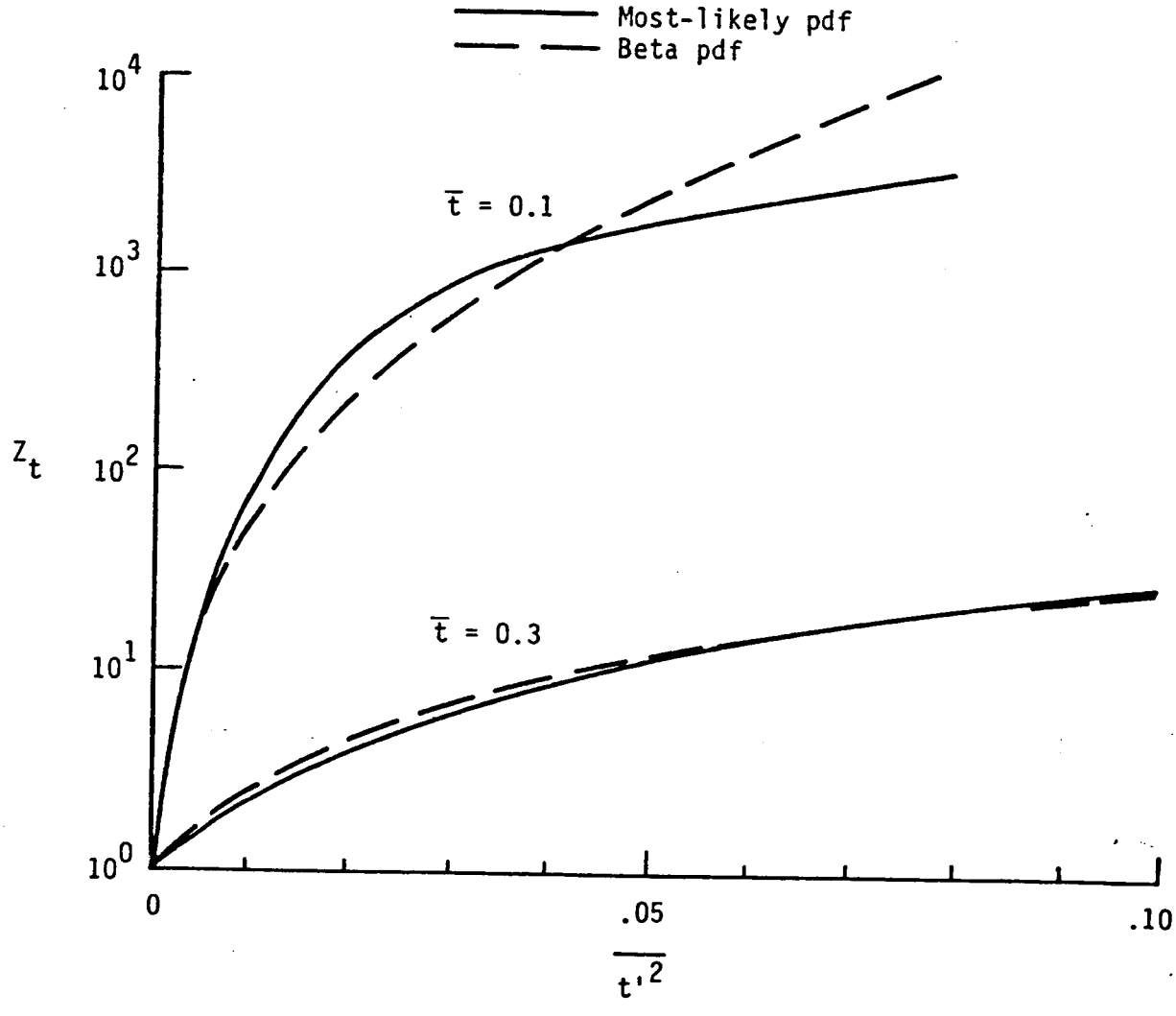

$\bar{t}$ = 0.1 and 0.3.

Figure 1.- Comparison of results for beta pdf and most-likely pdf for case 1.

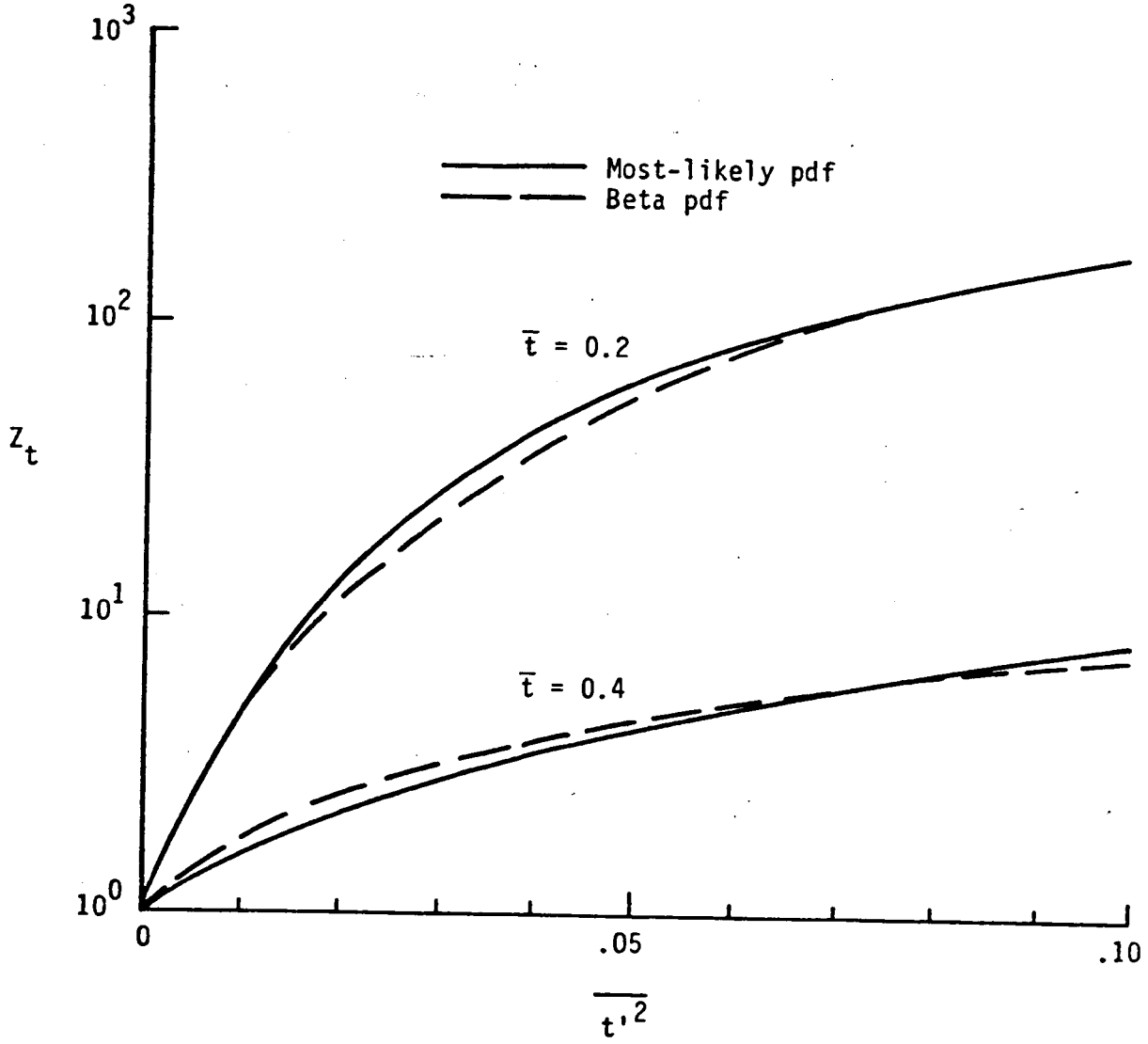

$\bar{t}$ = 0.2 and 0.4.

Figure 2

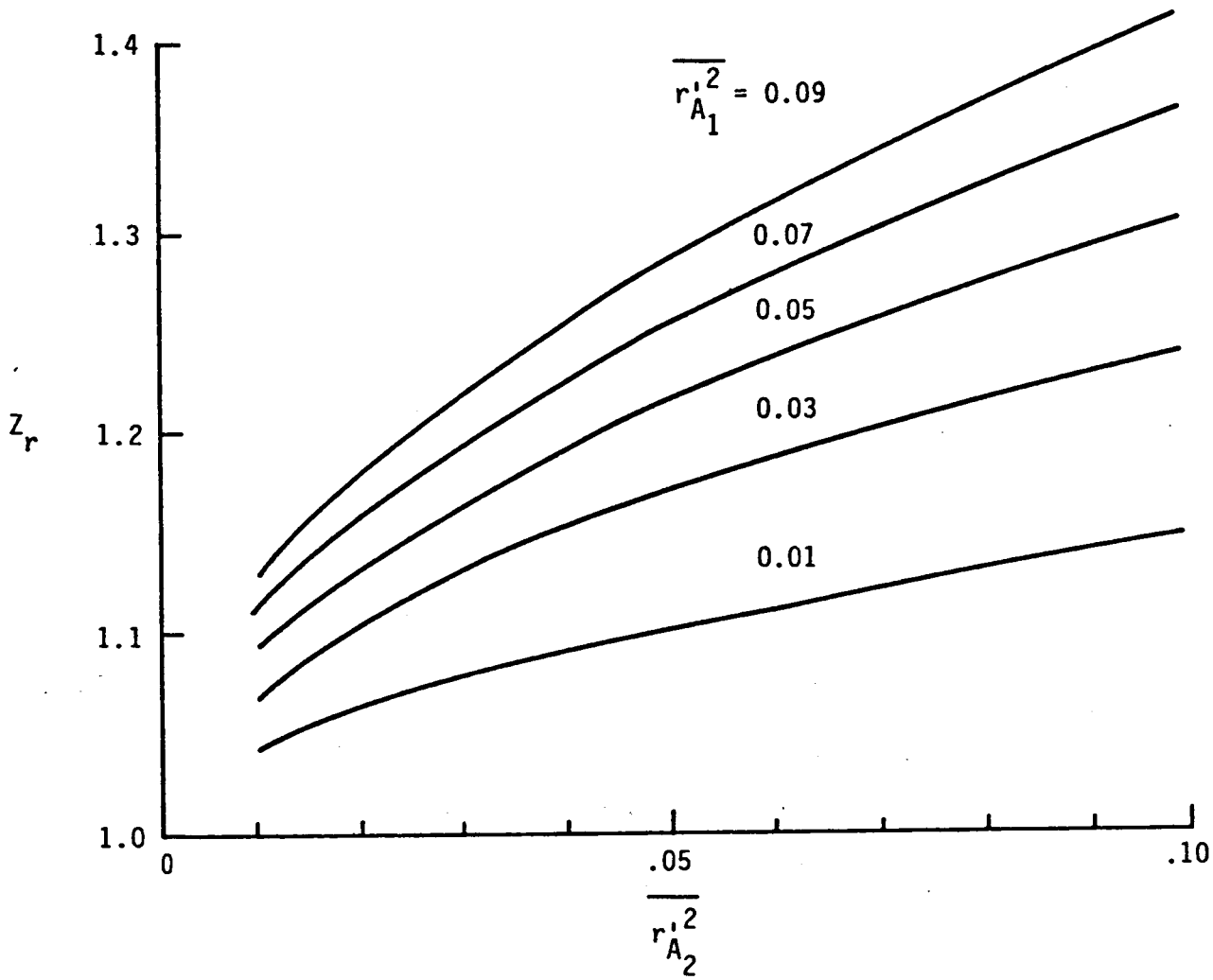

$\bar{r}_{A_1} = 0.4; \quad \bar{r}_{A_2} = 0.6.$

Figure 3

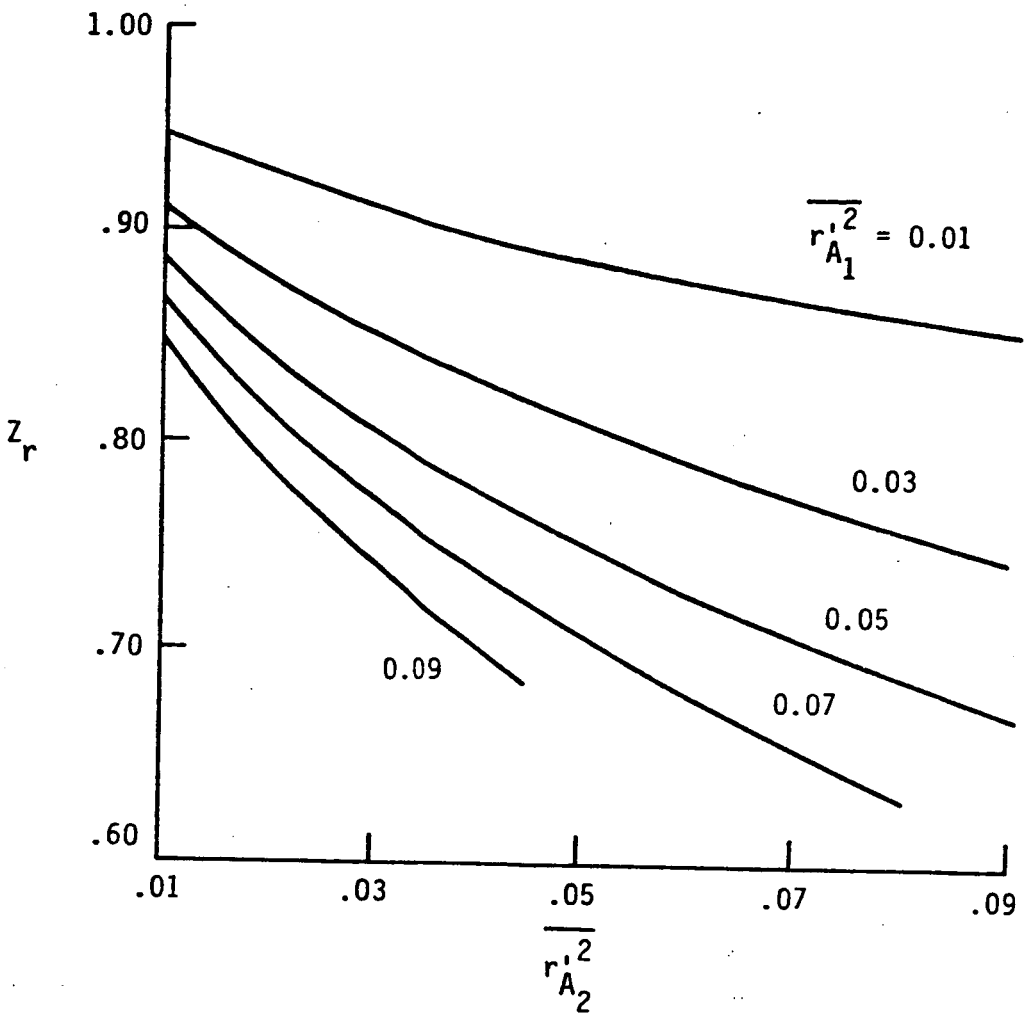

$\bar{r}_{A_1} = 0.2$; $\bar{r}_{A_2} = 0.9$.

Figure 4

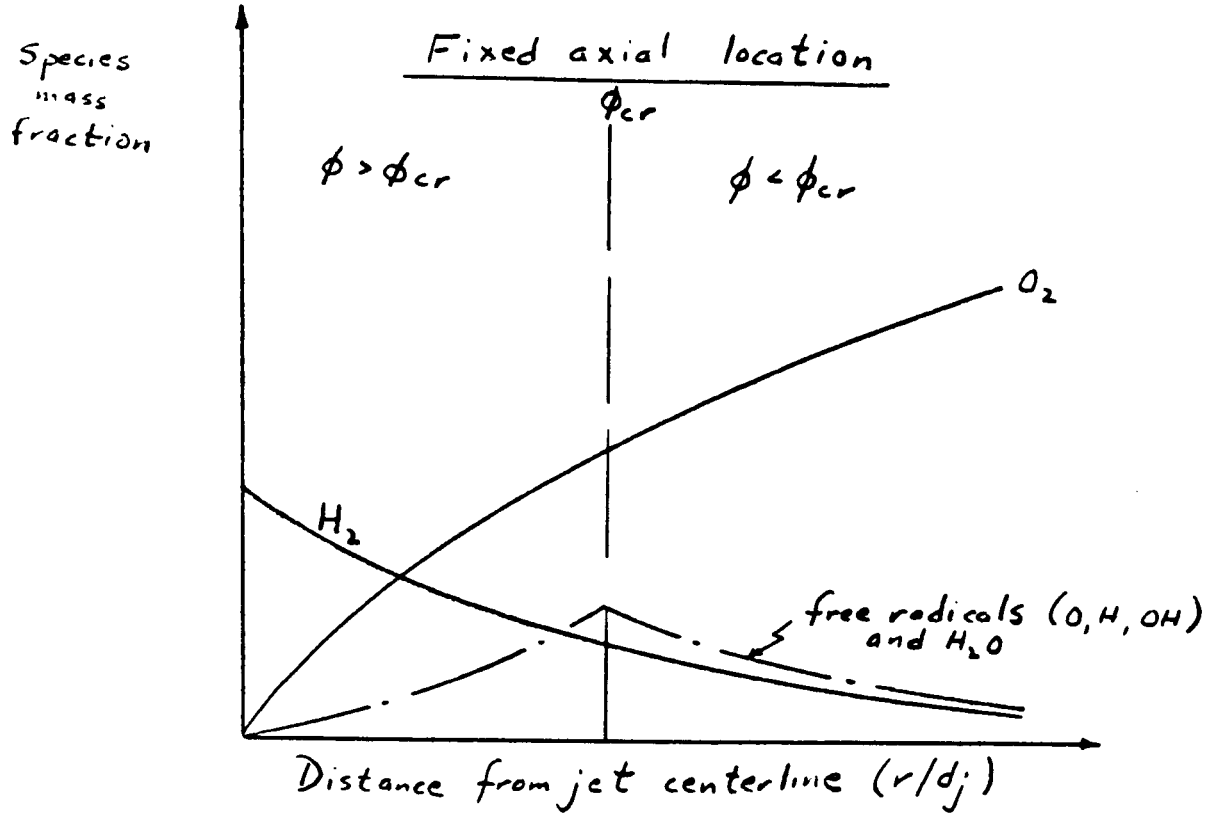

Figure 5. Schematic of the Axisymmetric Flame

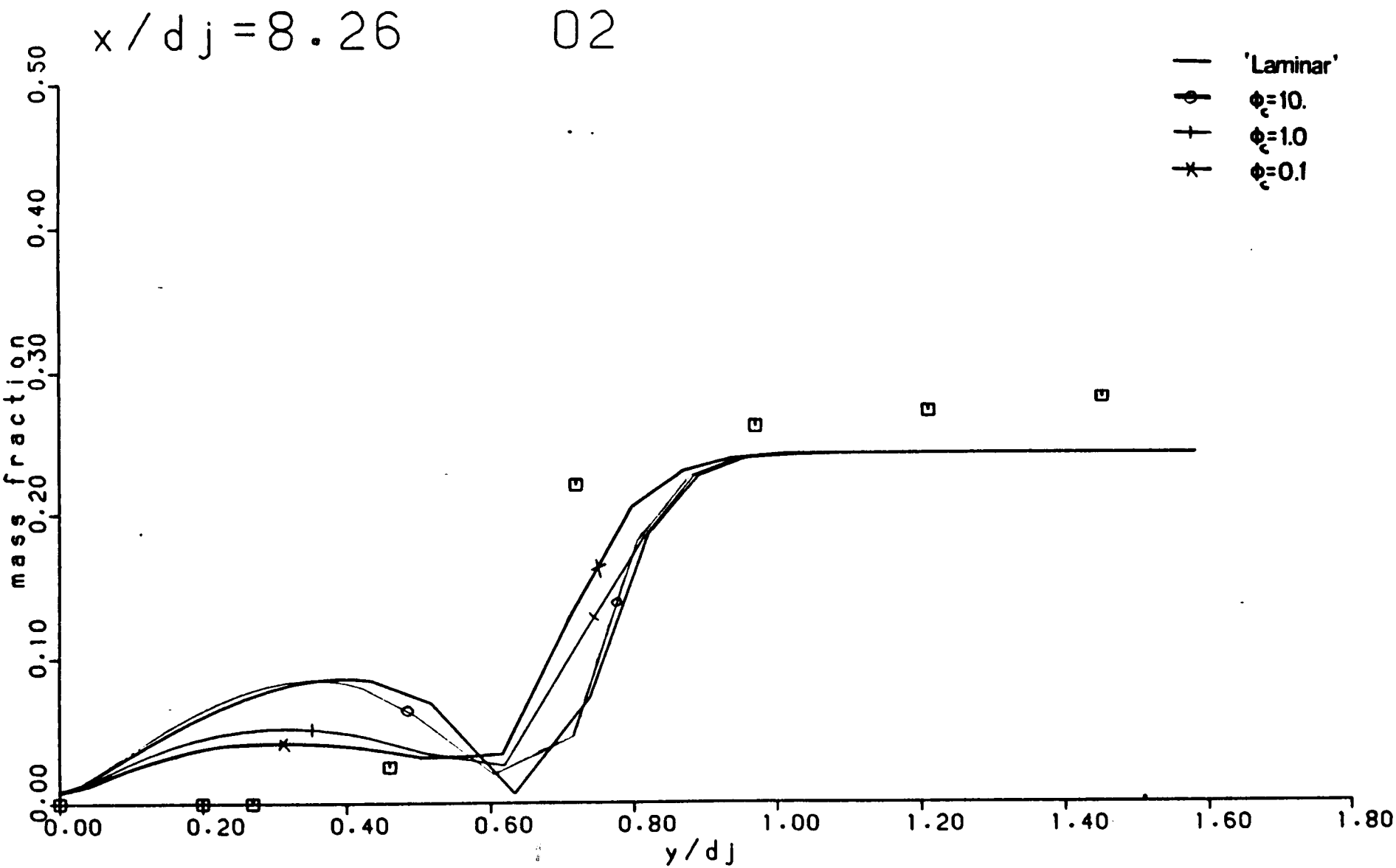

Figure 6 Radial species-concentration profiles for oxygen

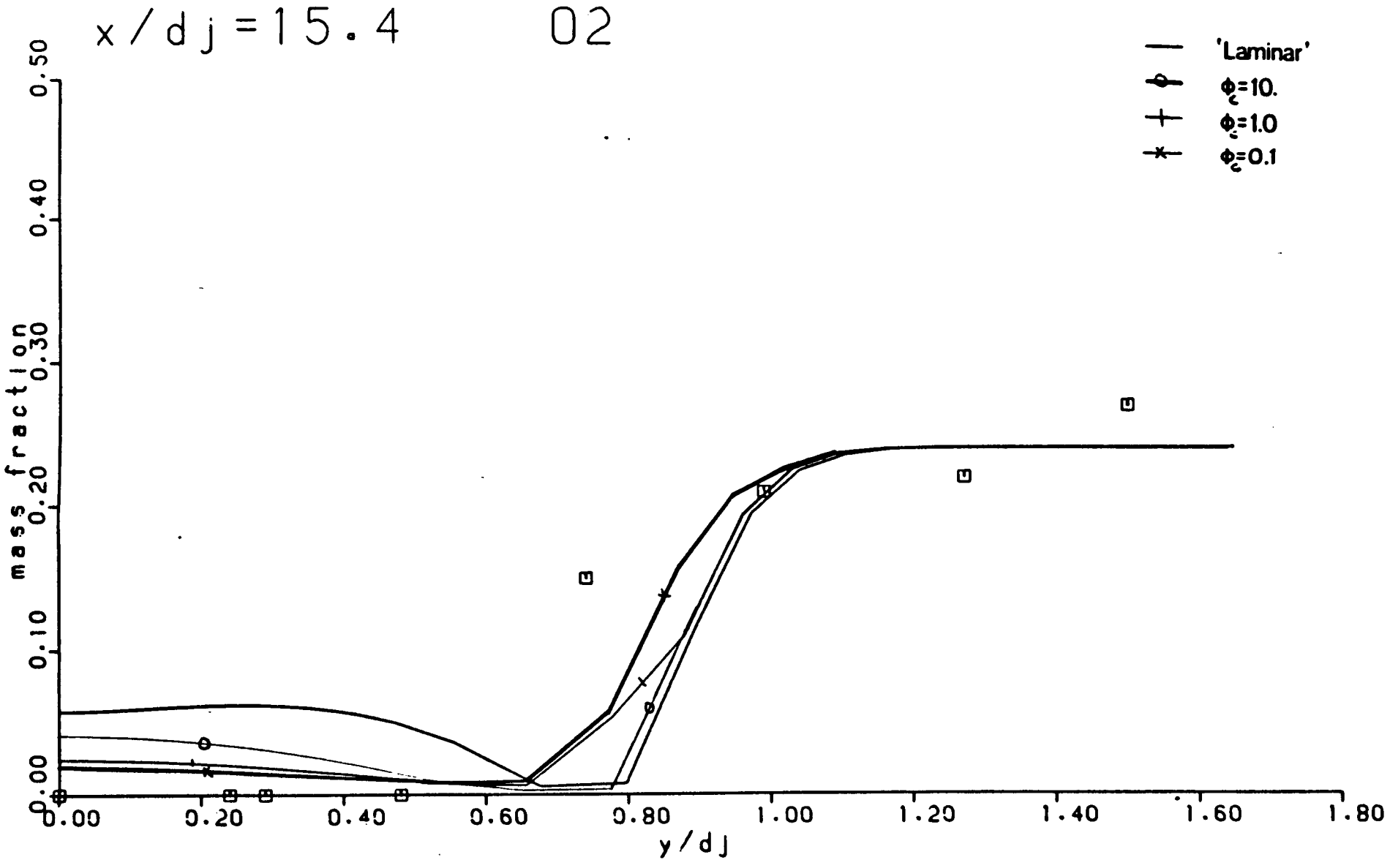

Figure 7 Radial species-concentration profiles for oxygen.

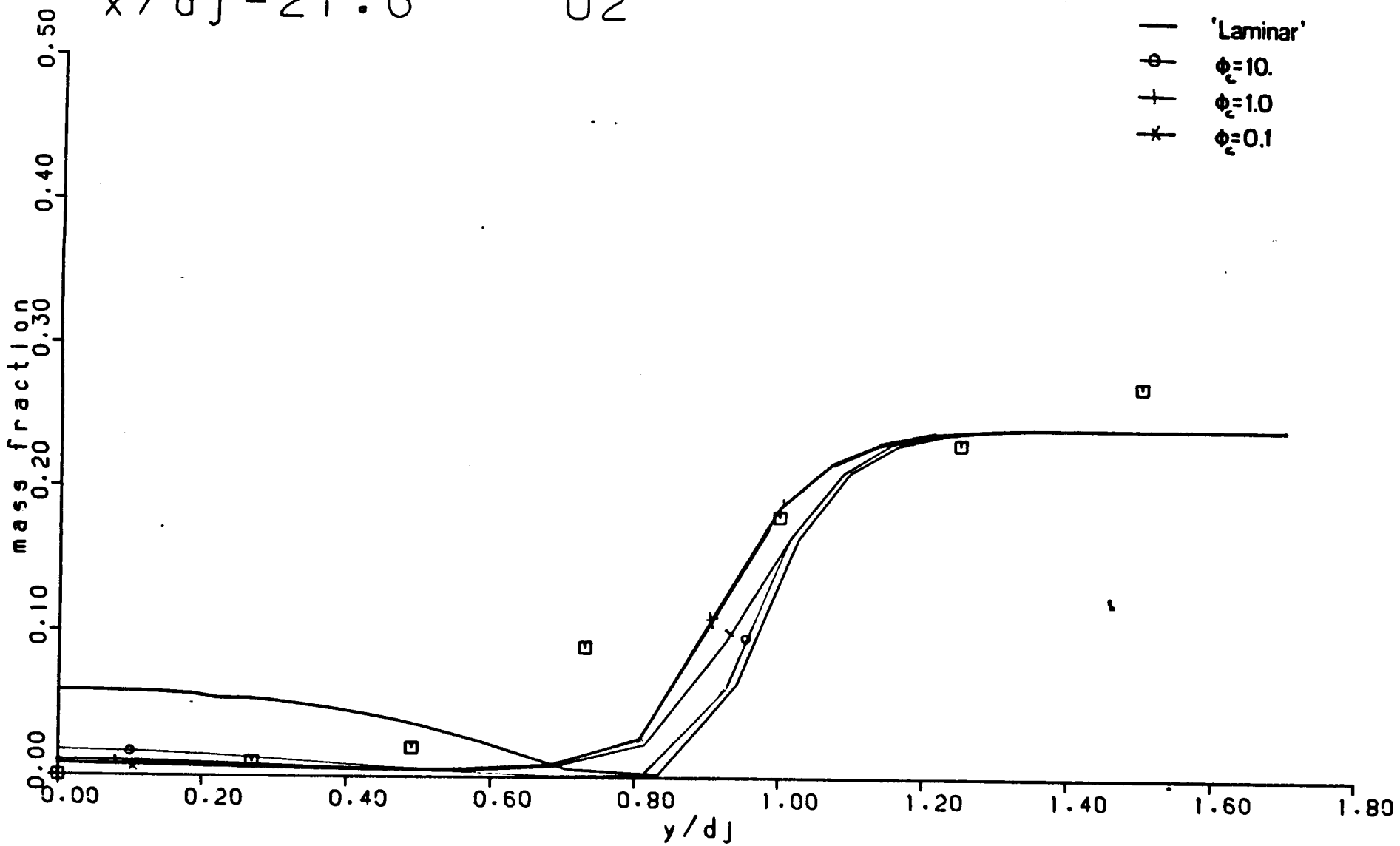

Figure 8 Radial species-concentration profiles for oxygen

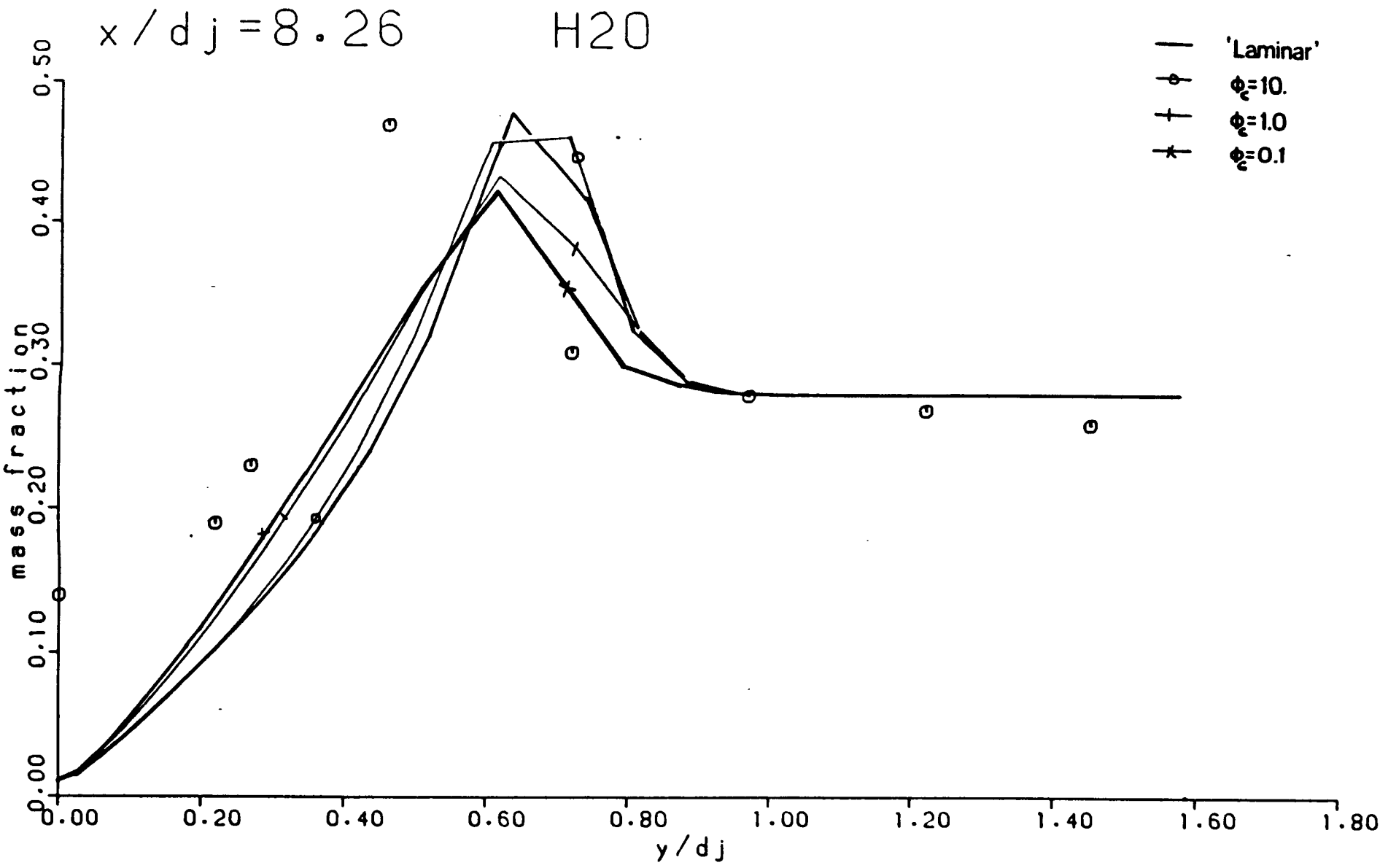

Figure 9. Radial species-concentration profiles for water.

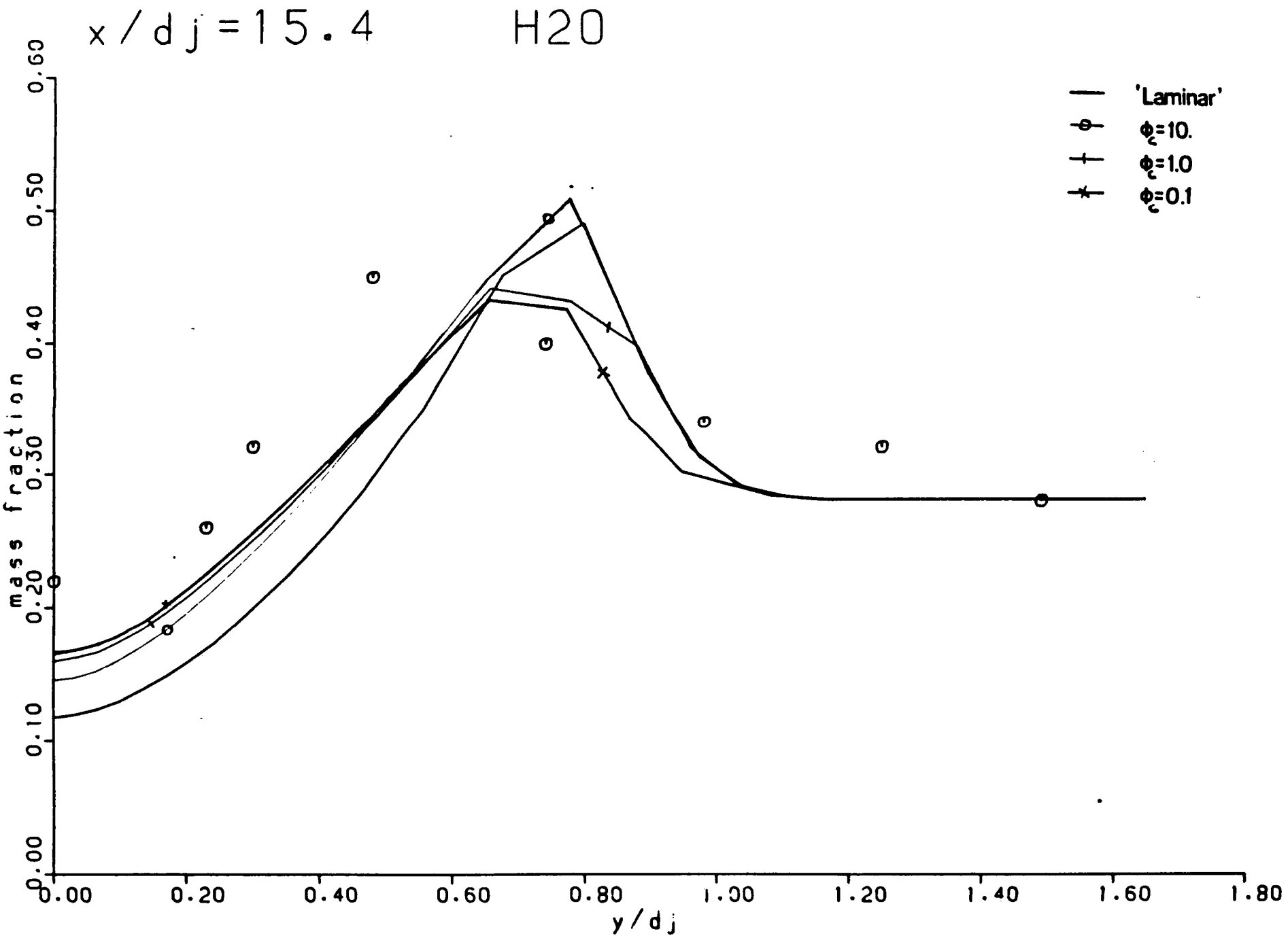

Figure 10. Radial species concentration profiles for water.

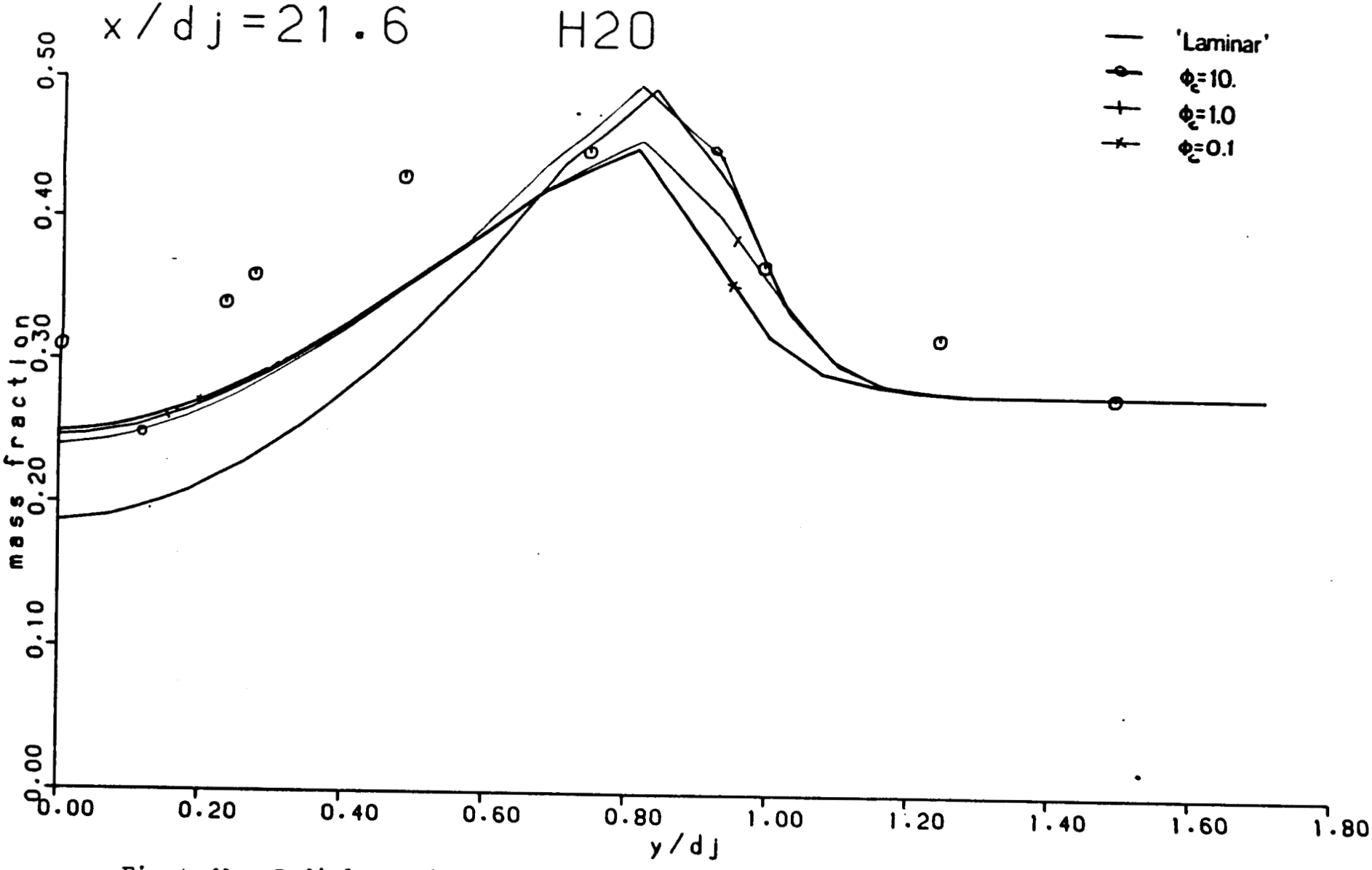

Figure 11 . Radial species-concentration profiles for water.

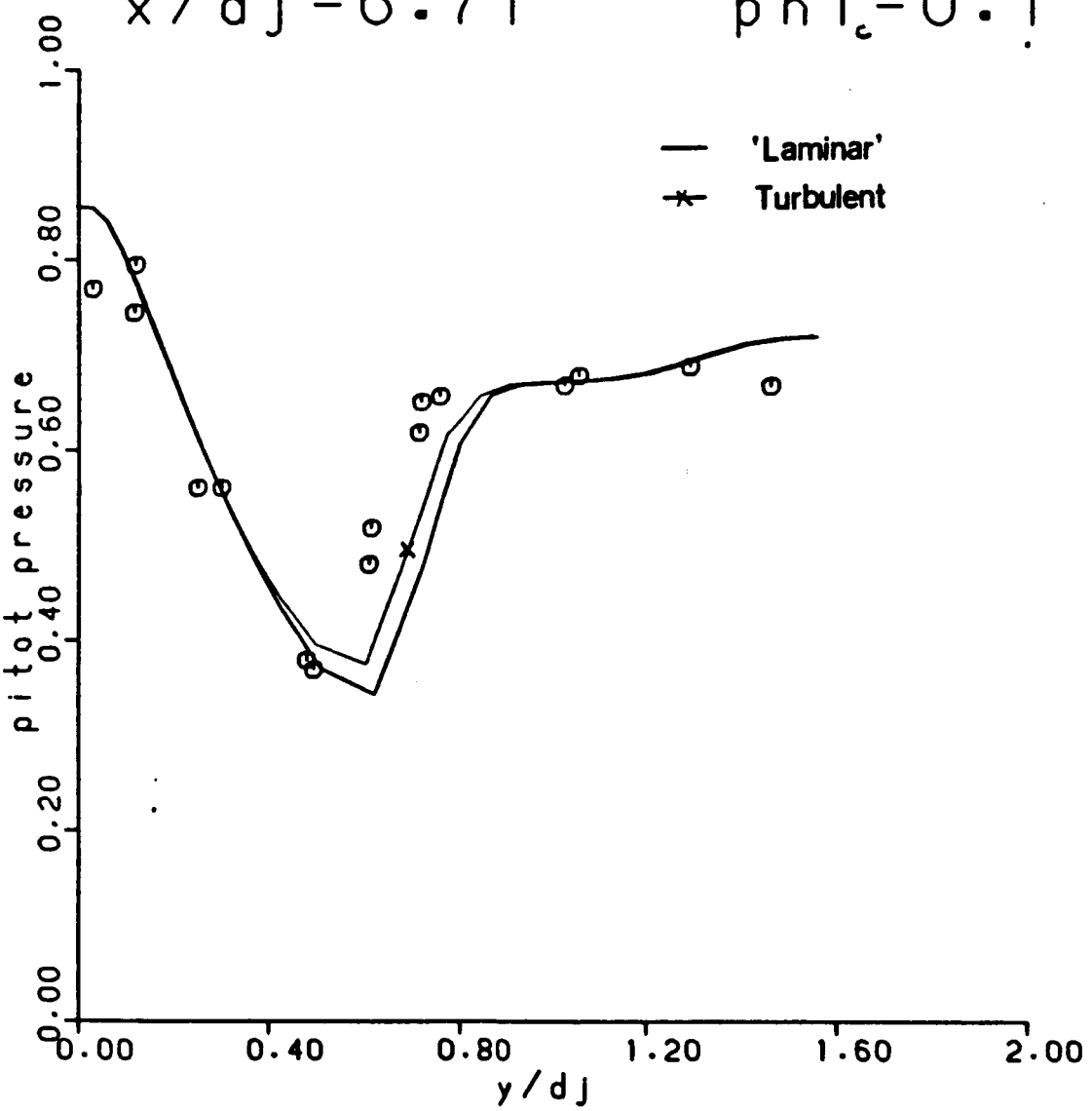

Figure 12 . Radial pitot-pressure profiles.

DR1-CUCC-RPH-1000

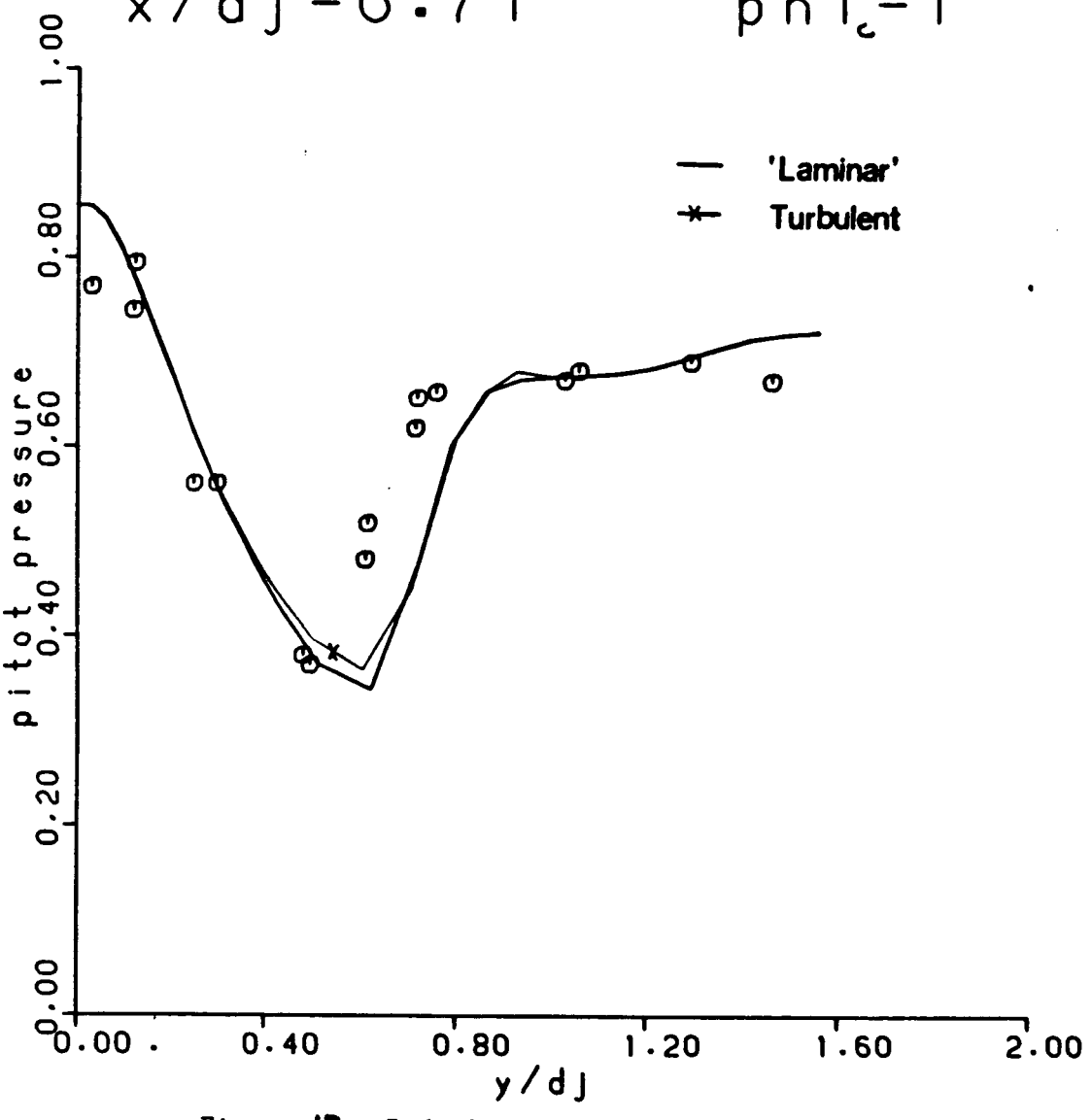

Figure 13 . Radial pitot-pressure profiles.

DRI-CUCC-RPH-1986

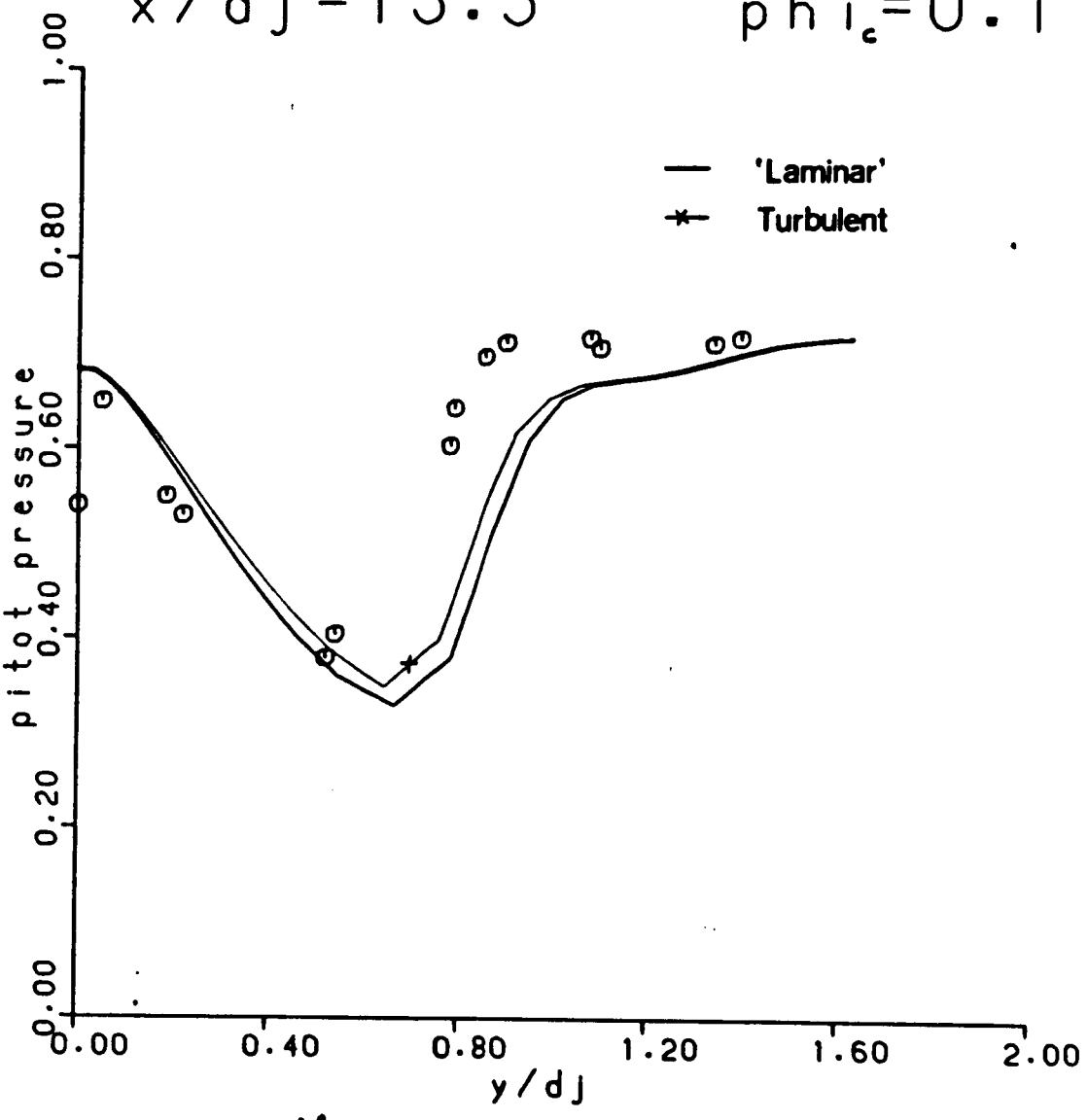

Figure 14. Radial pitot-pressure profiles.

DRI-CUCC-RPH-1980

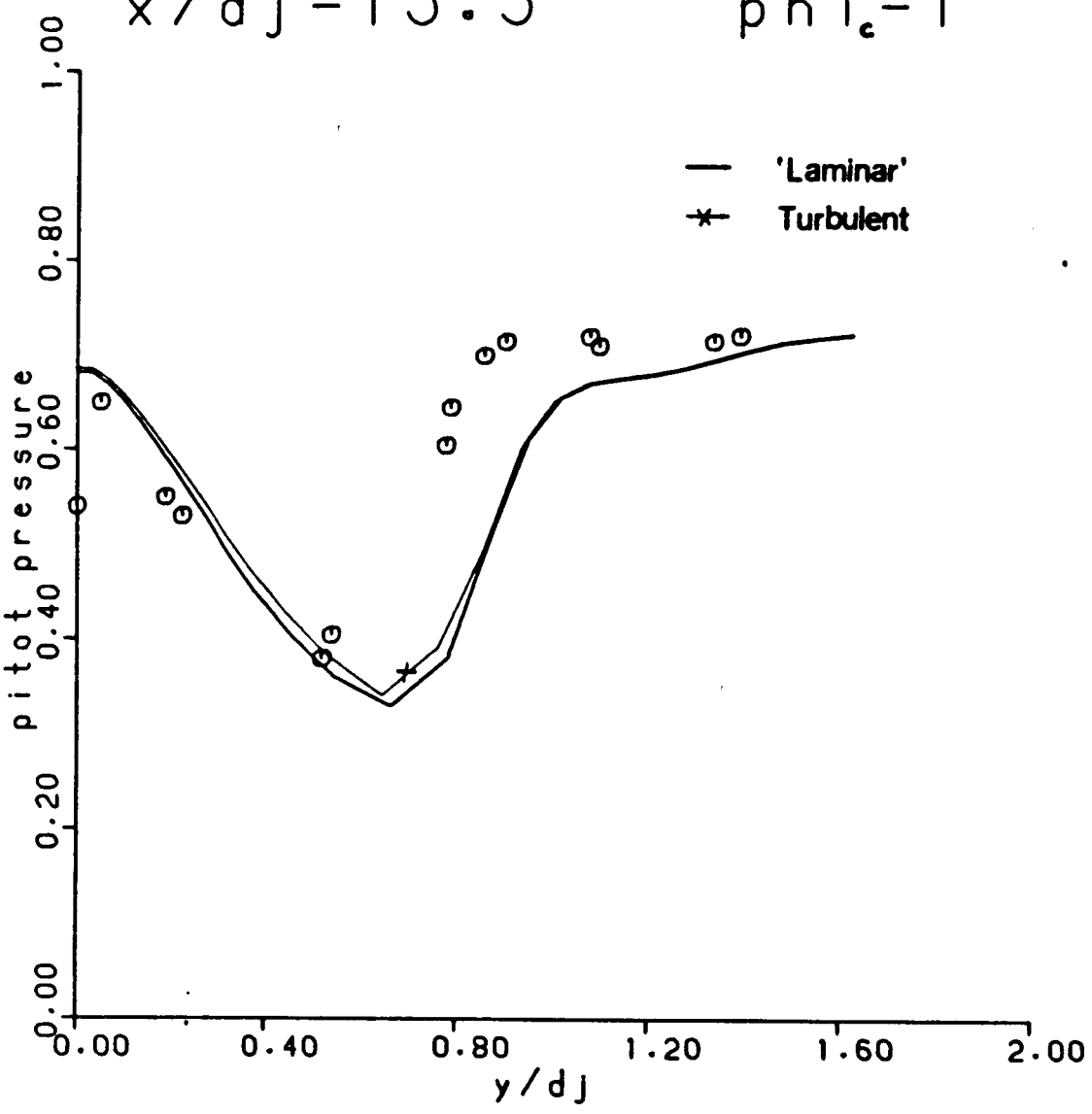

Figure 15 . Radial pitot-pressure profiles.

DRI-CUCC-RPH-1980

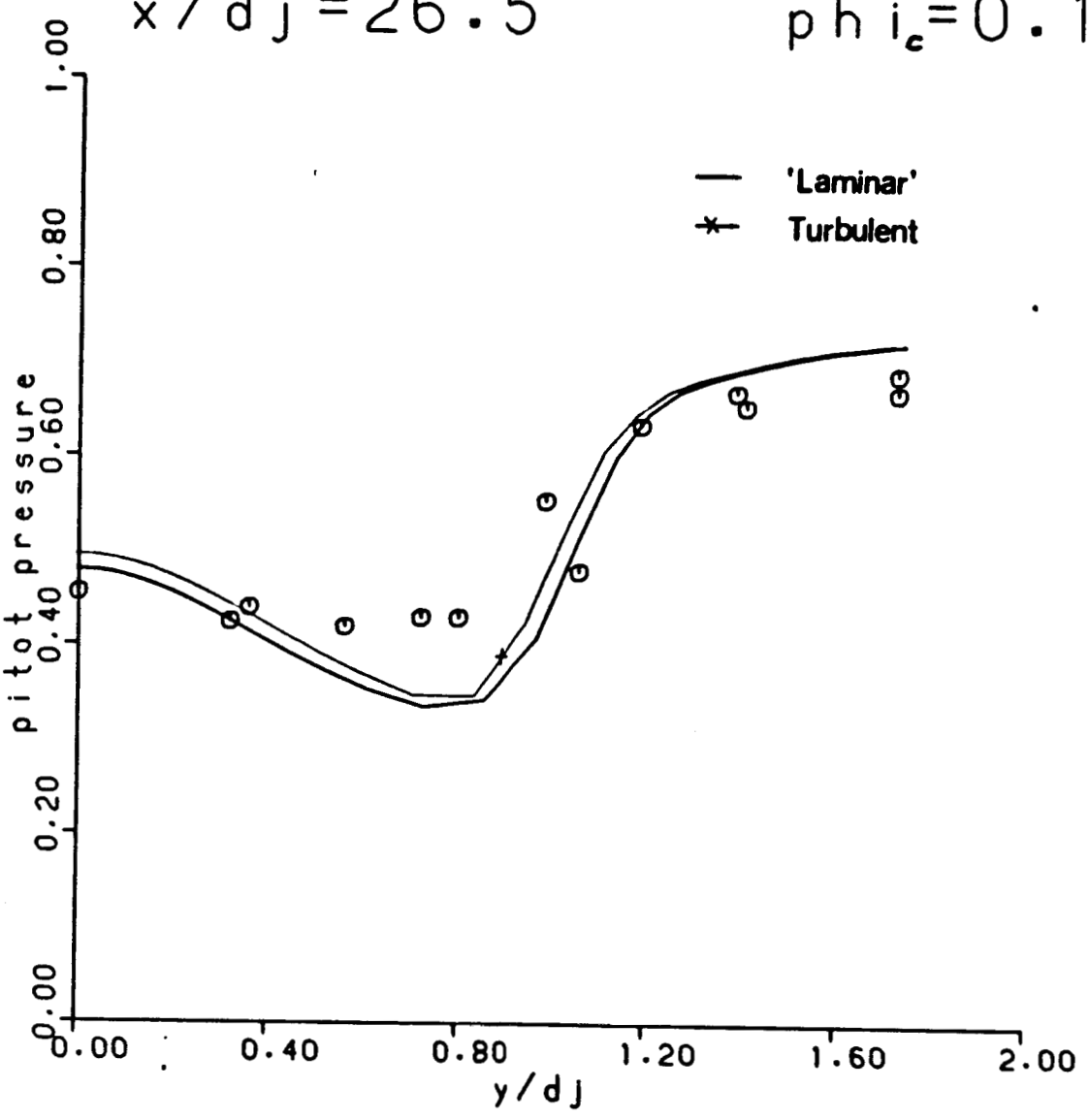

DRI-CUCC-RPH-1980

Figure 16. Radial pitot-pressure profiles.

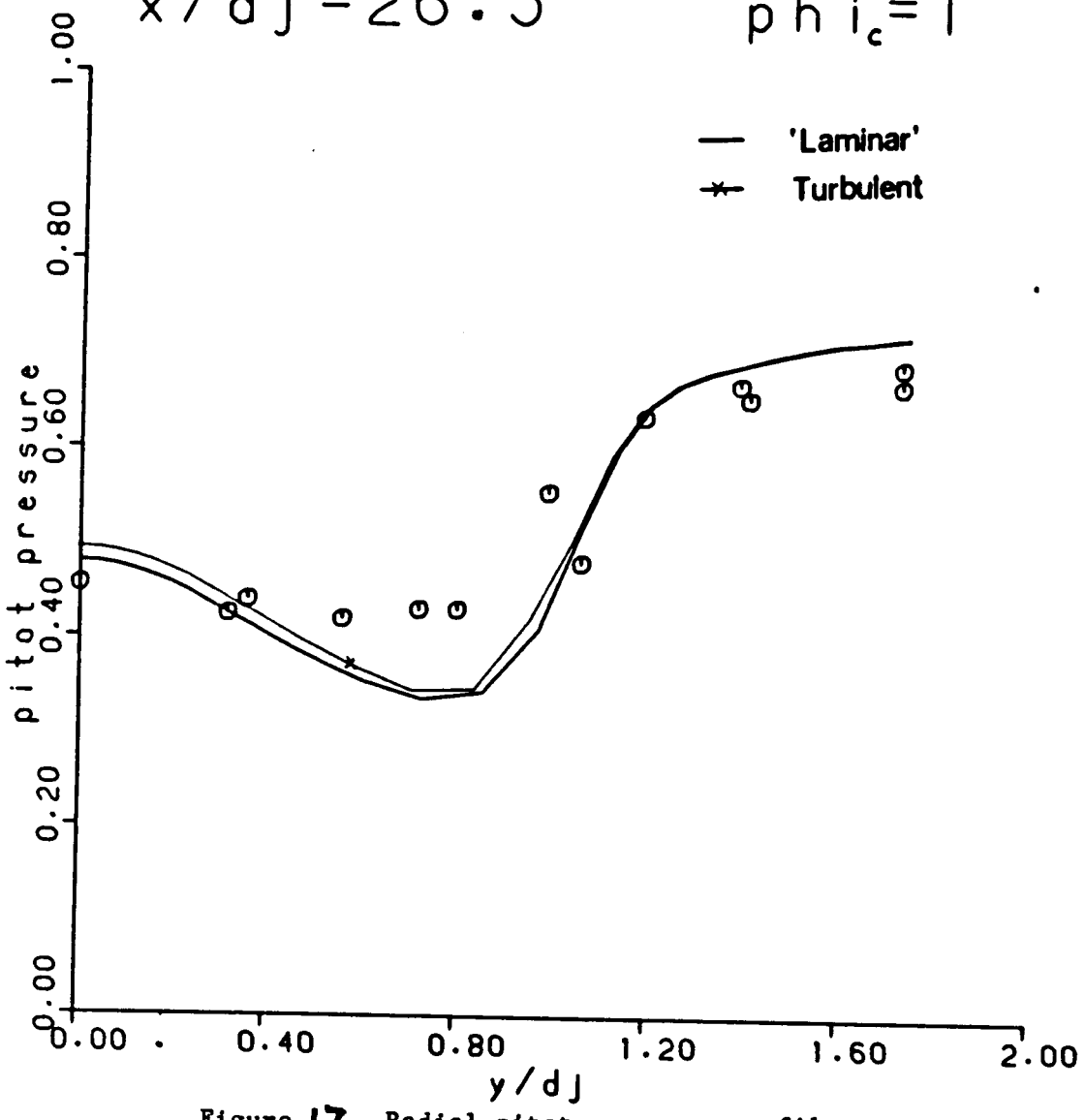

Figure 17 Radial pitot-pressure profiles.

DRI-CUCC-RPH-1980

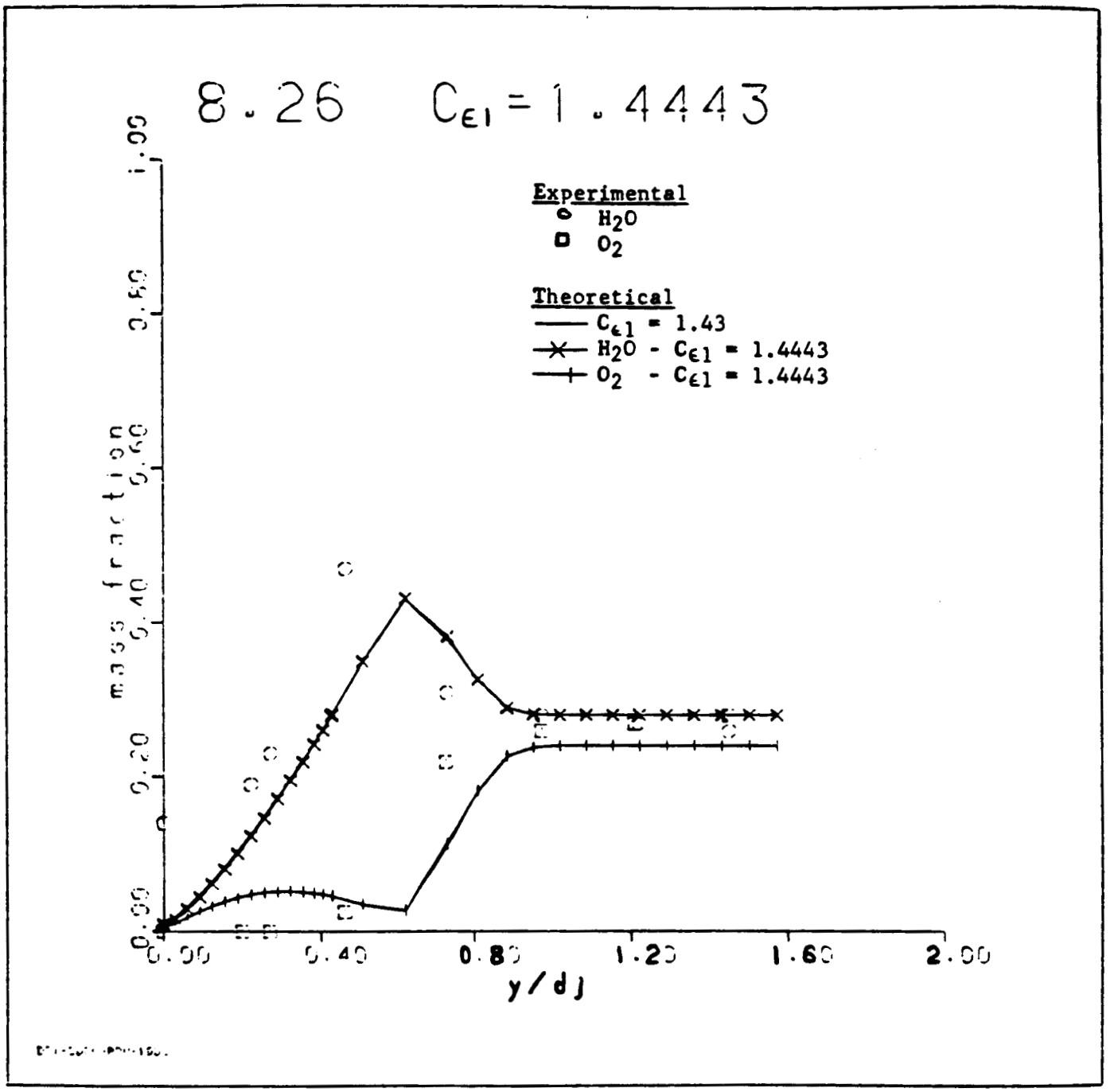

Figure 18 Species concentration profiles for a one percent increase in $C_{\epsilon 1}$.

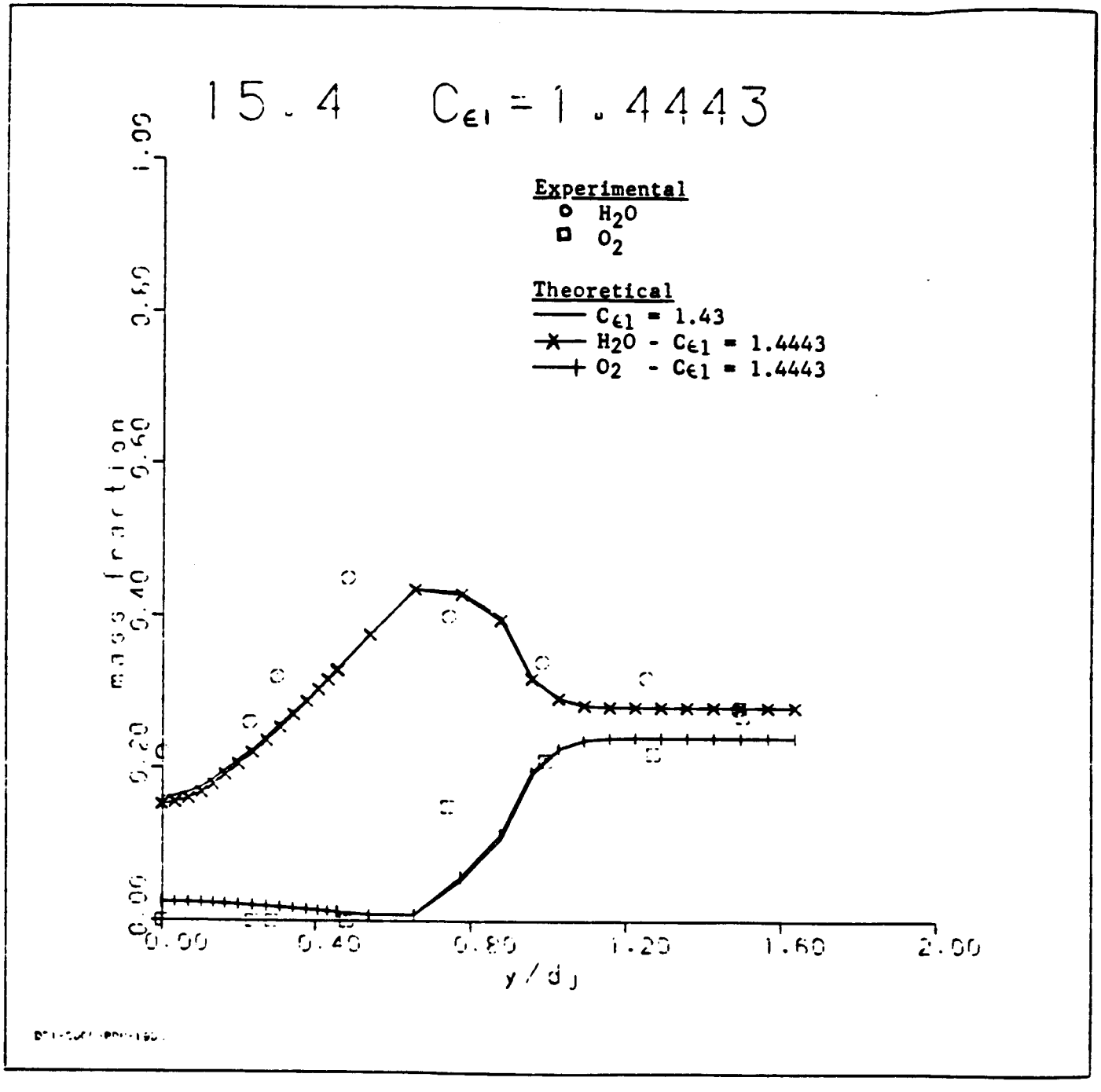

Figure 8. Continued.

18

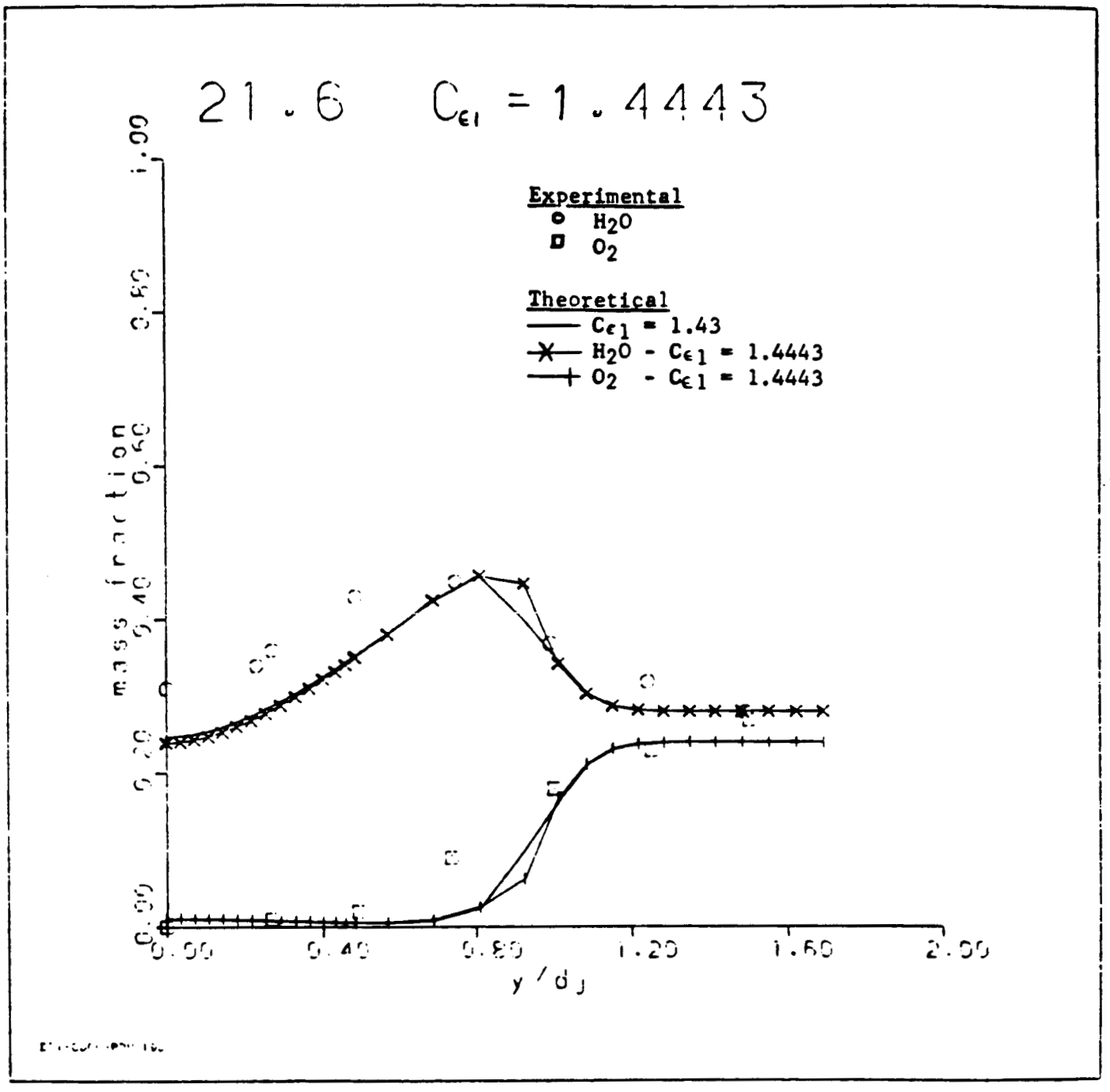

Figure 18. Concluded.

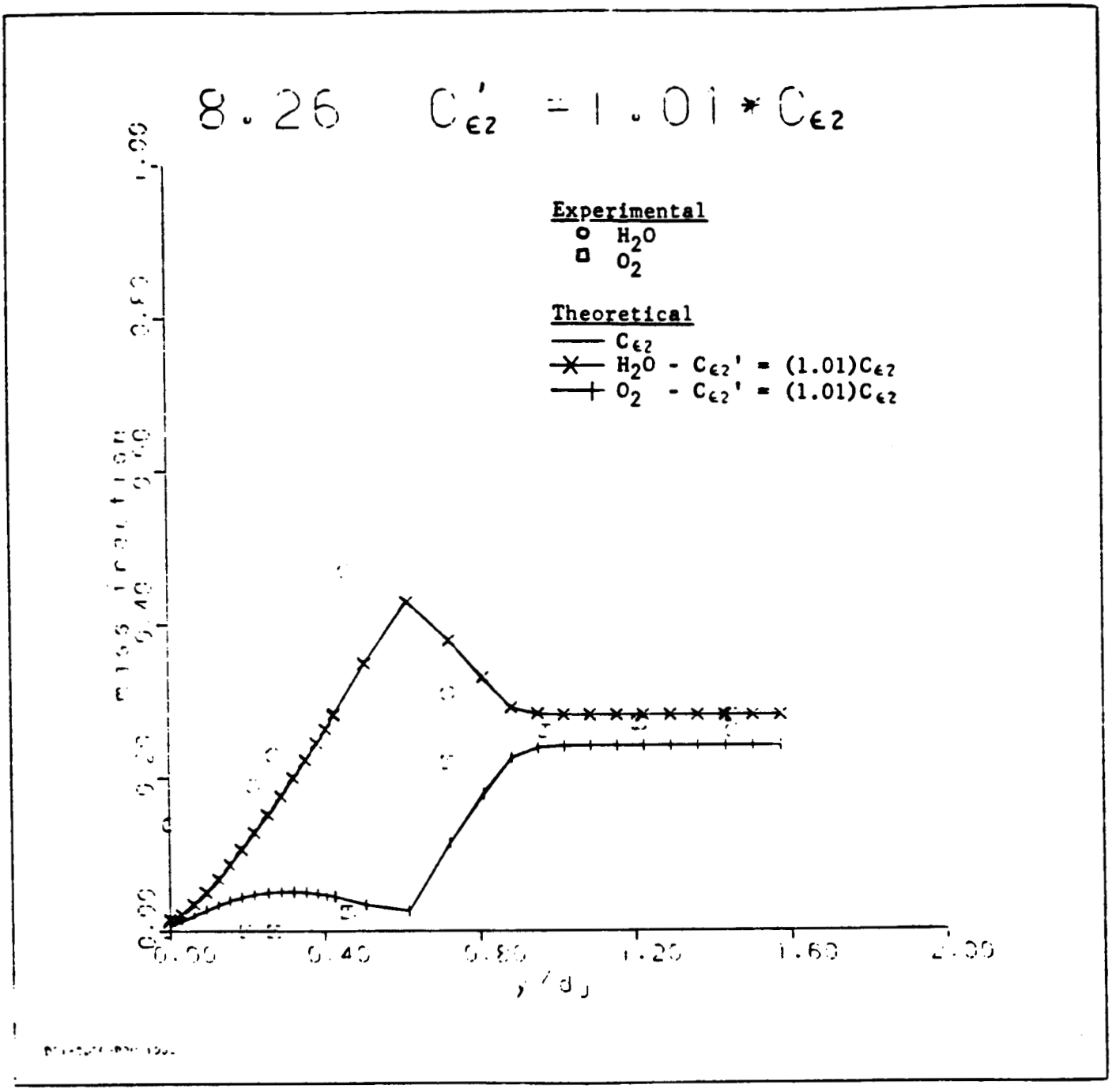

Figure 19 Species concentration profiles for a one percent increase in $C_{\epsilon 2}$.

19

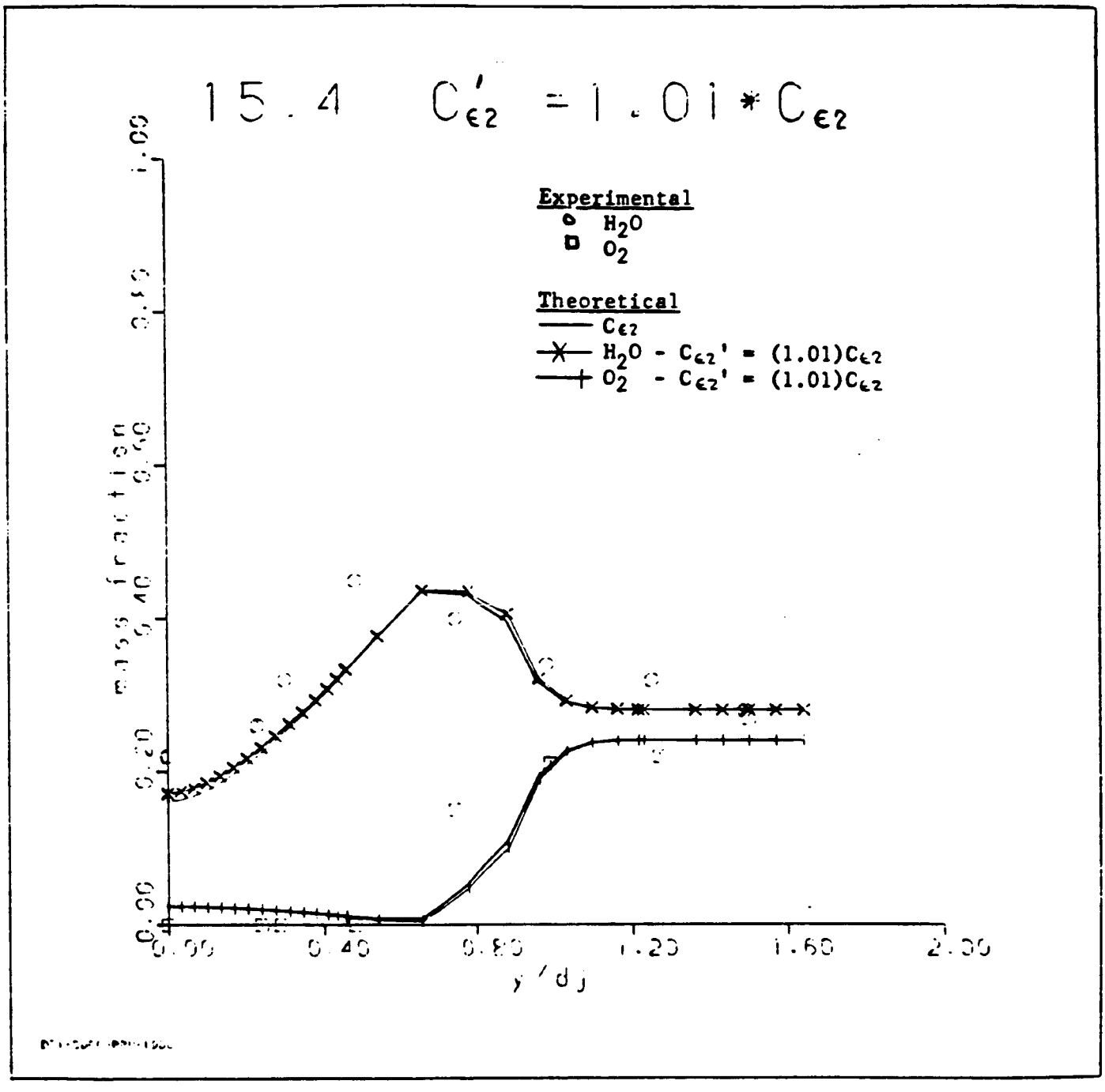

Figure 19 Continued.

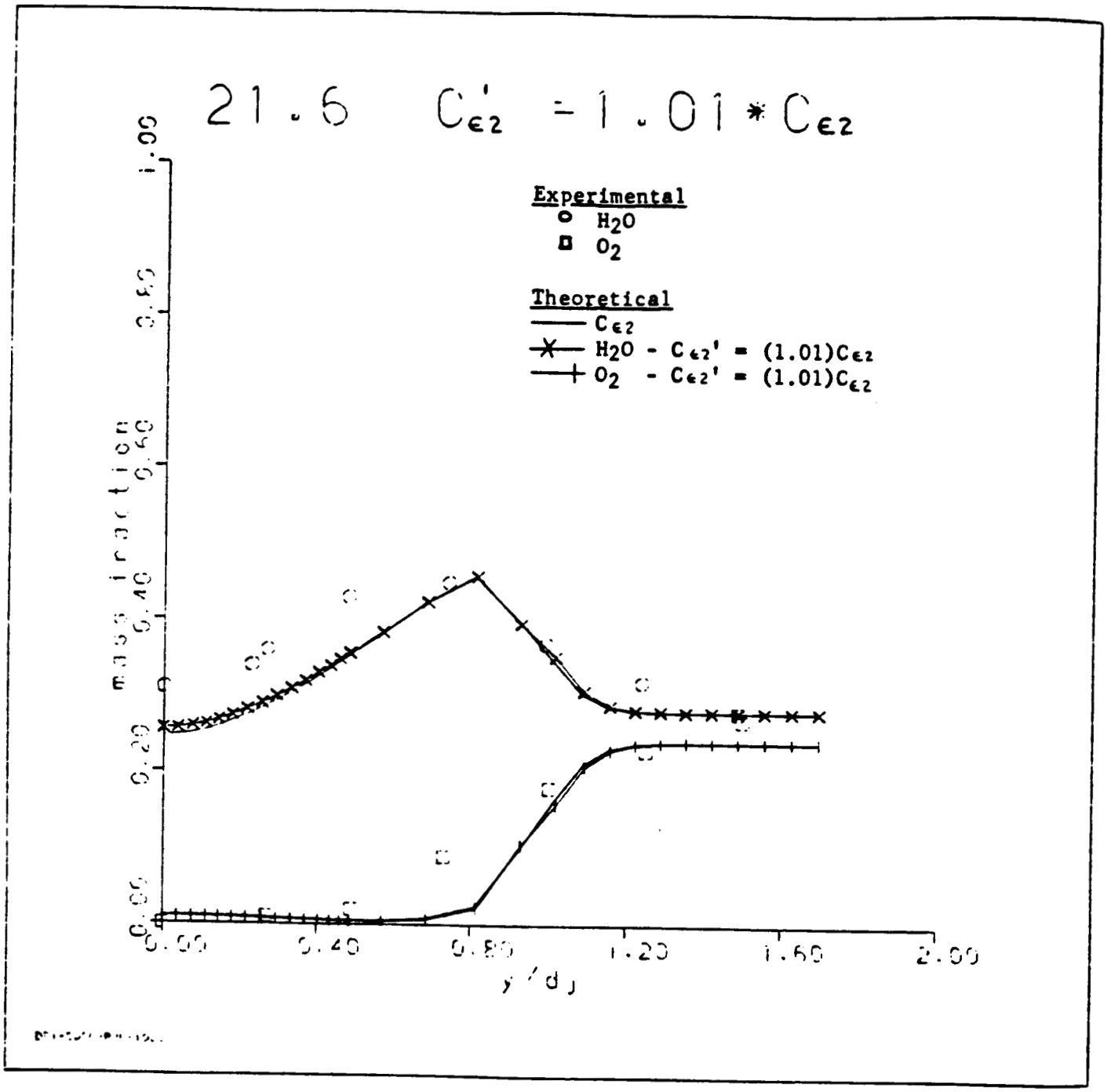

Figure 9. Concluded.

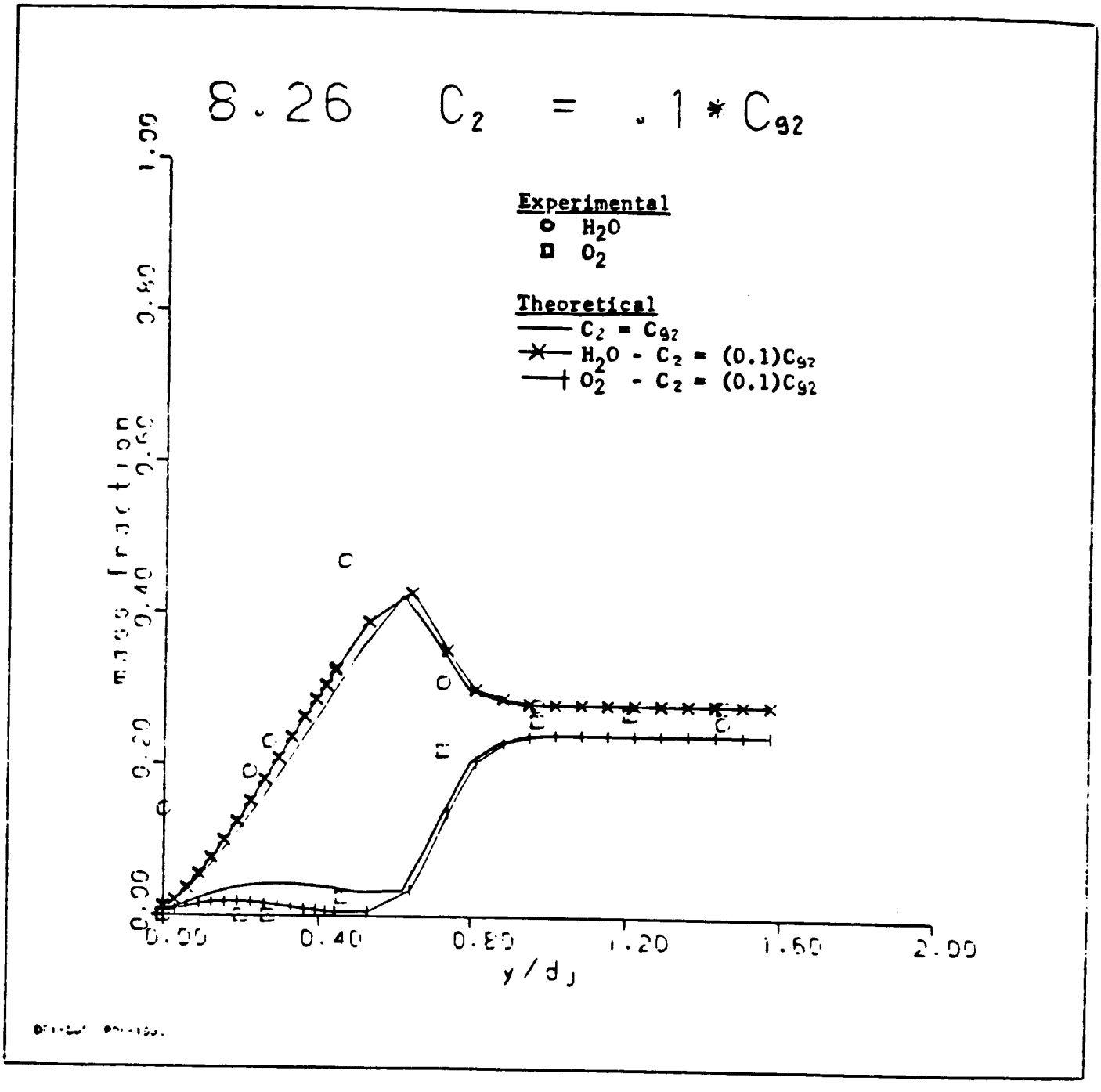

Figure 20. Species concentration profiles for a decrease in C_2 by one order of magnitude.

20

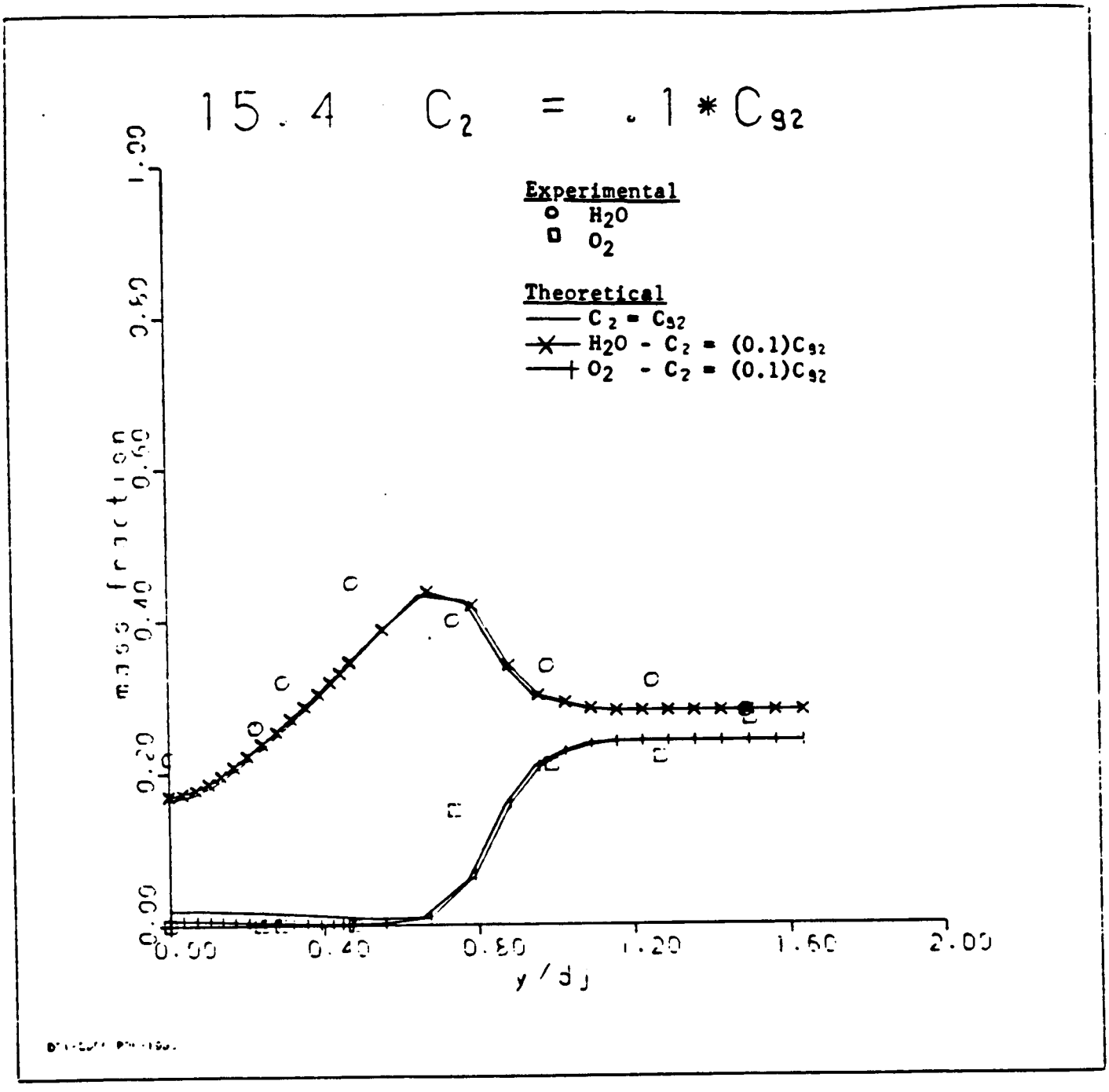

Figure 26 Continued.

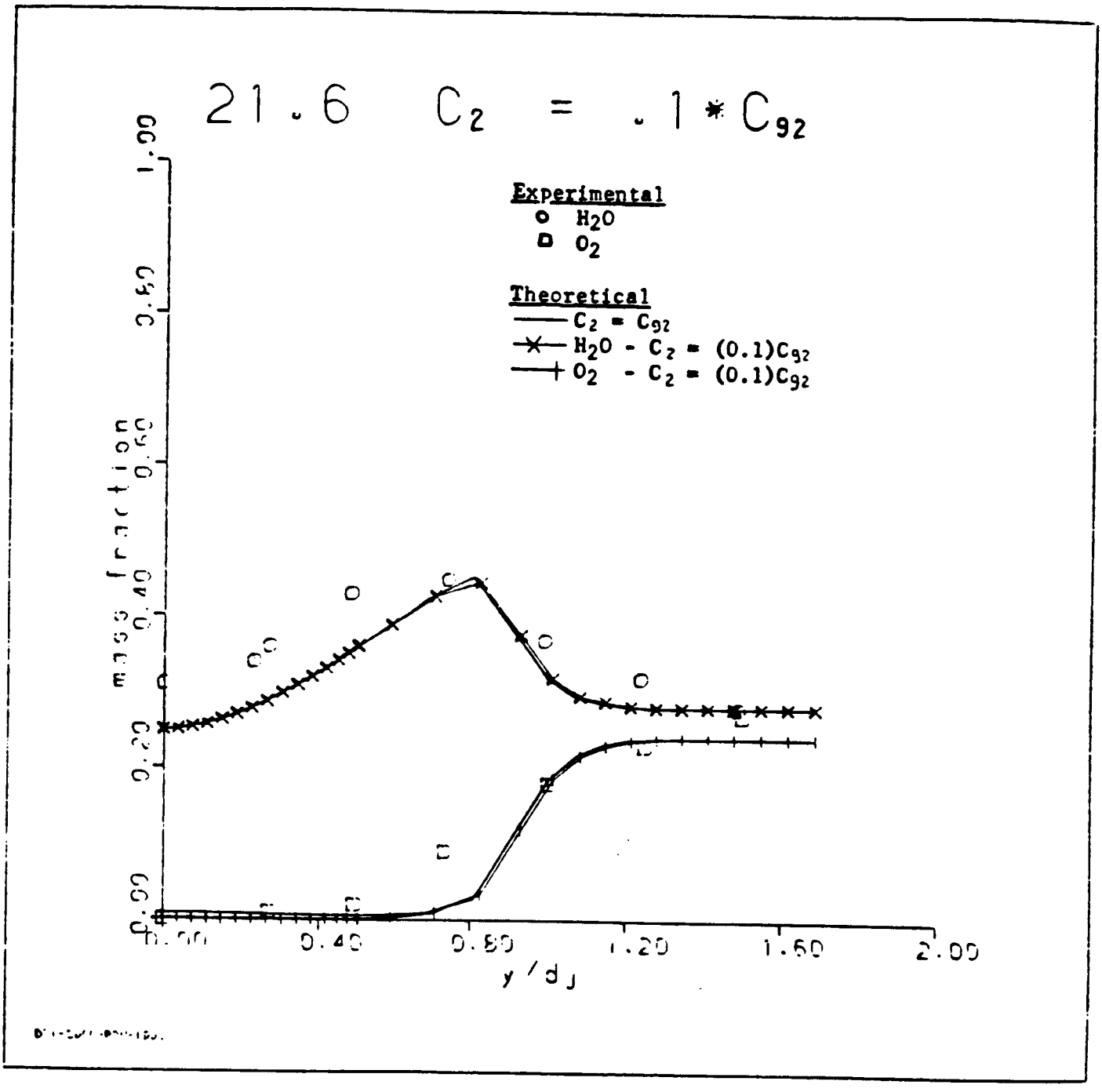

Figure 20 Concluded.

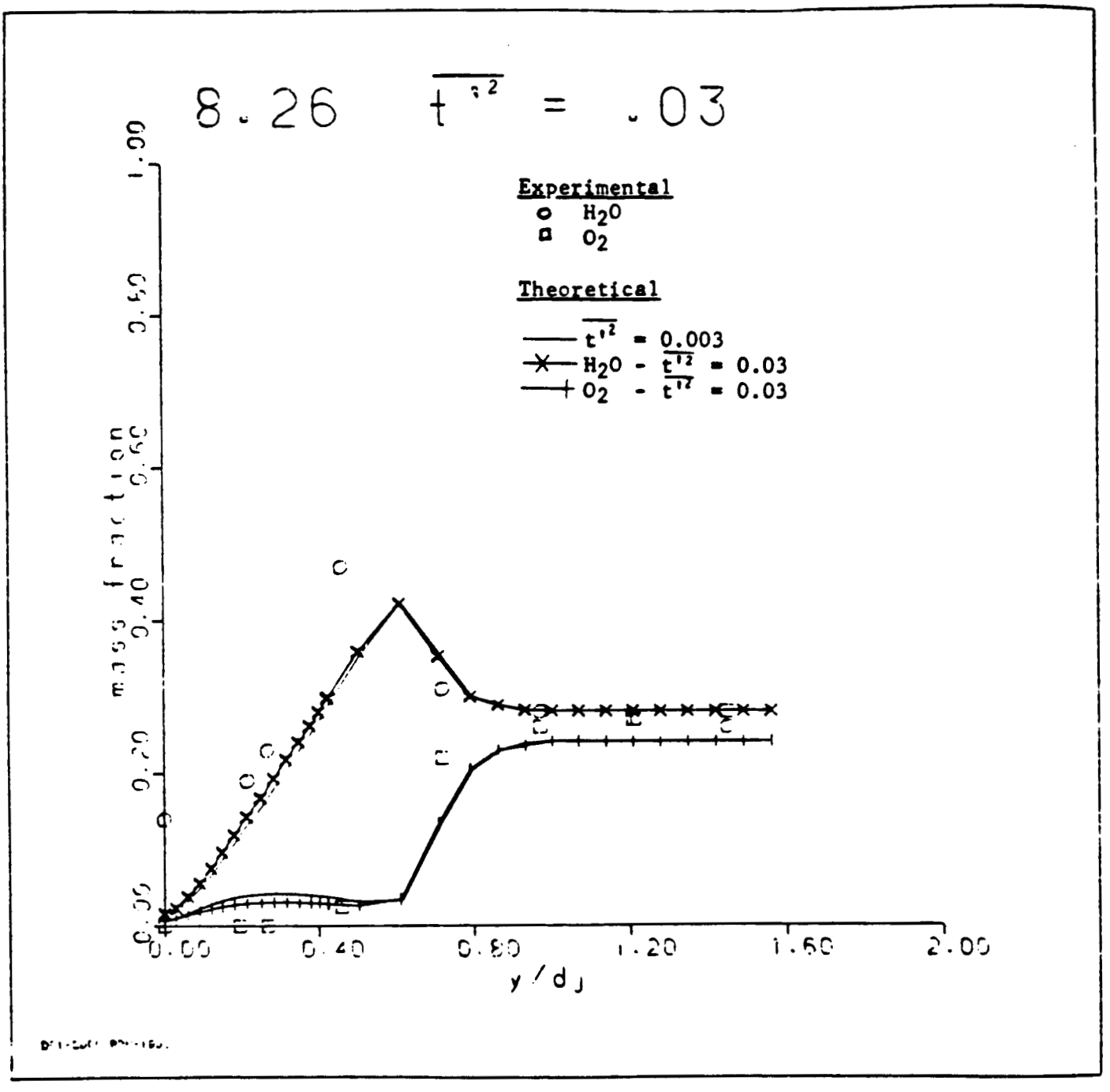

Figure 21 Species concentration profiles for an increase in initial $\overline{t'^2}$ profile by one order of magnitude.

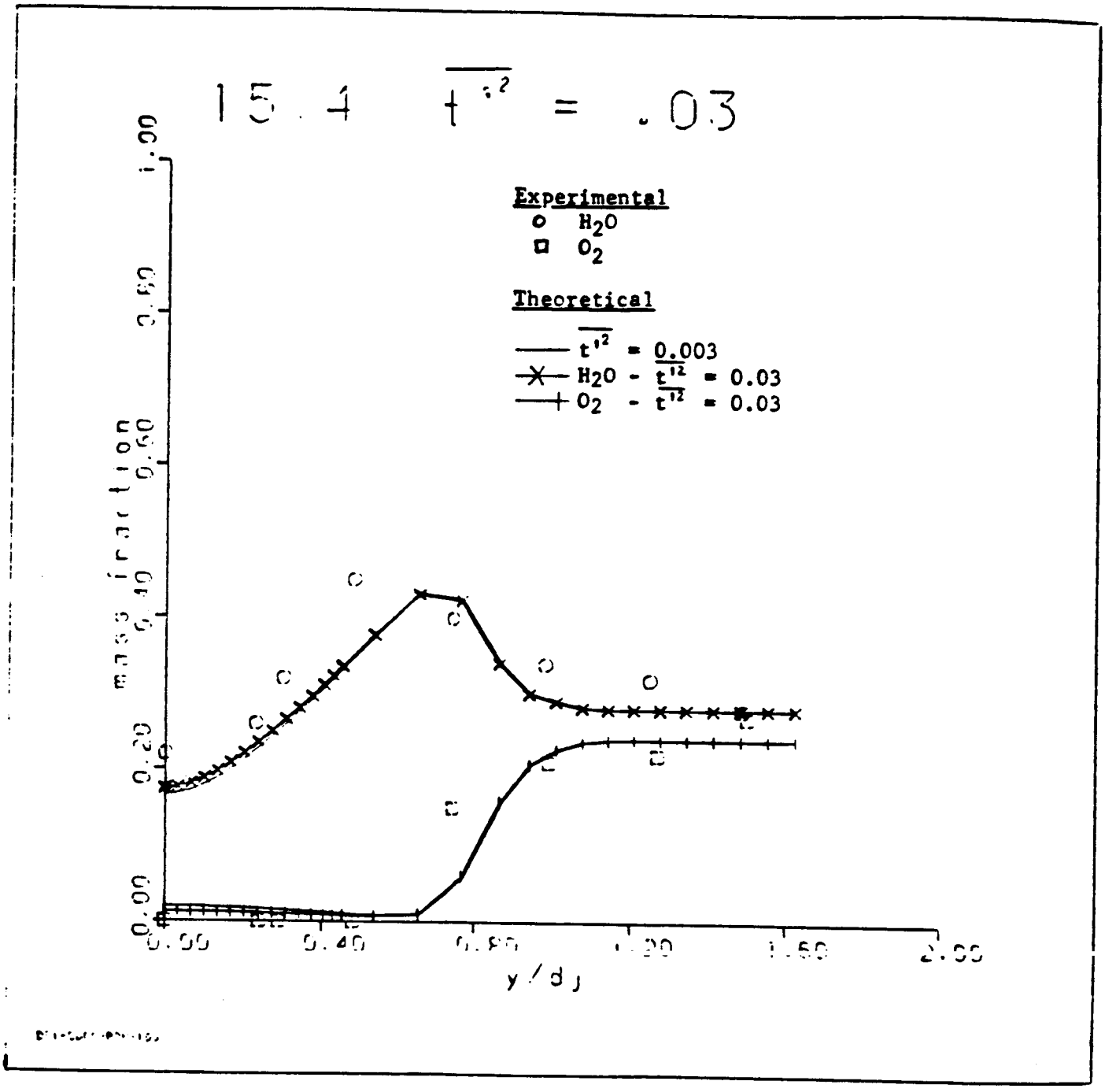

Figure 21 Continued.

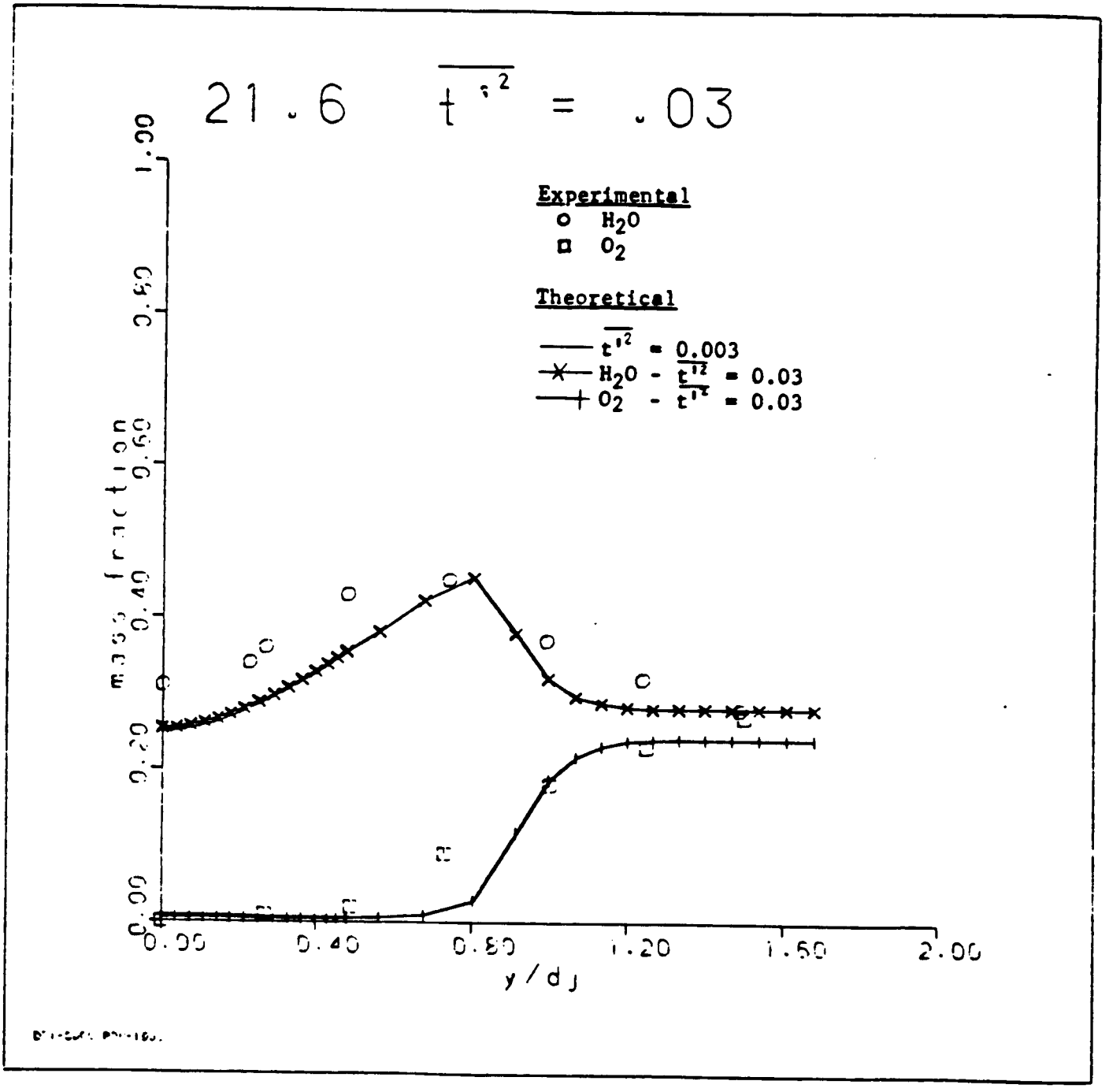

Figure 21 Concluded.

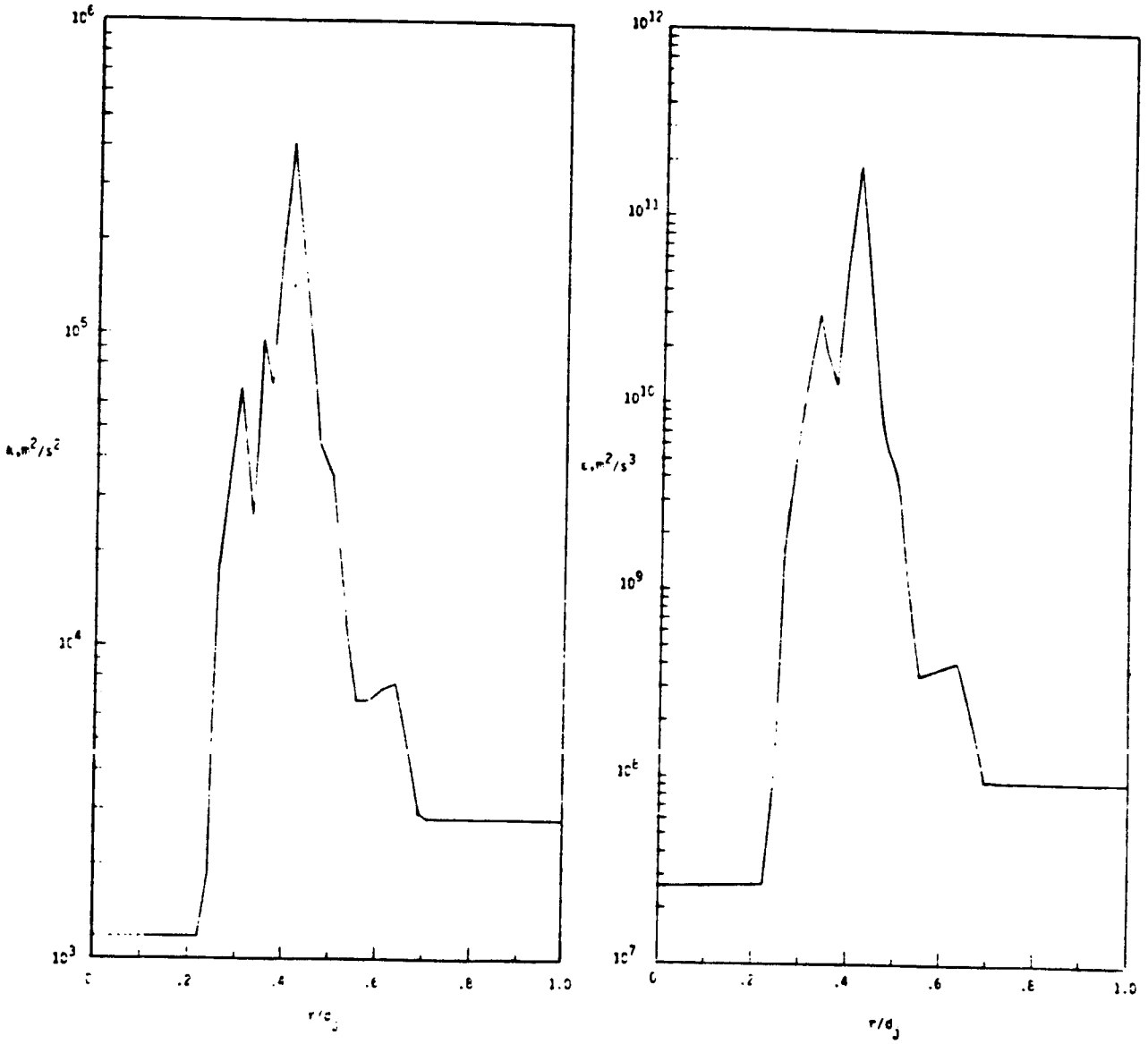

Figure 22. Experimental initial k-ε profiles.

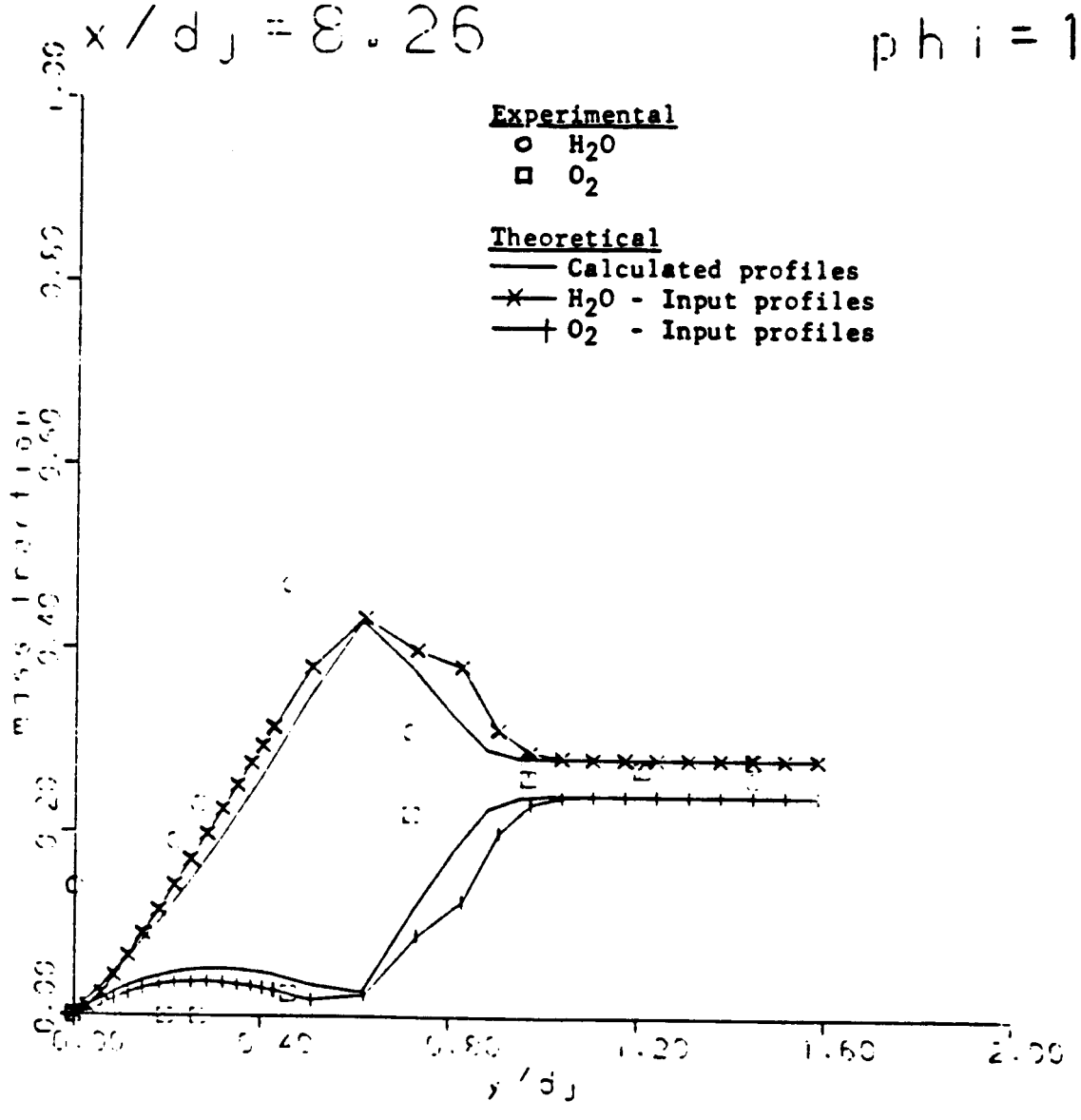

Figure 23 Species concentration profiles for input experimental k-ε profiles (Φ = 1.0).

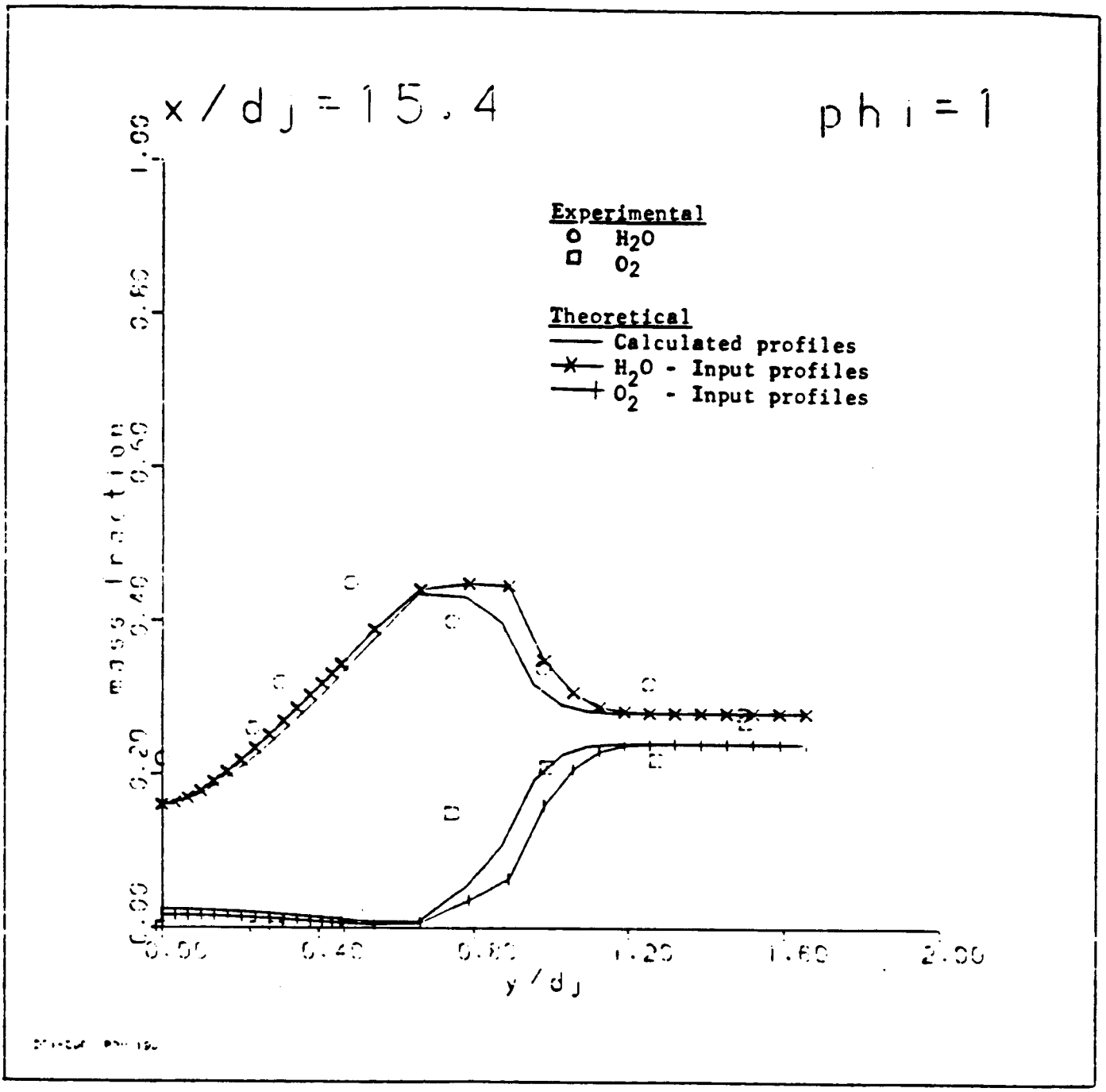

Figure 23 Continued.

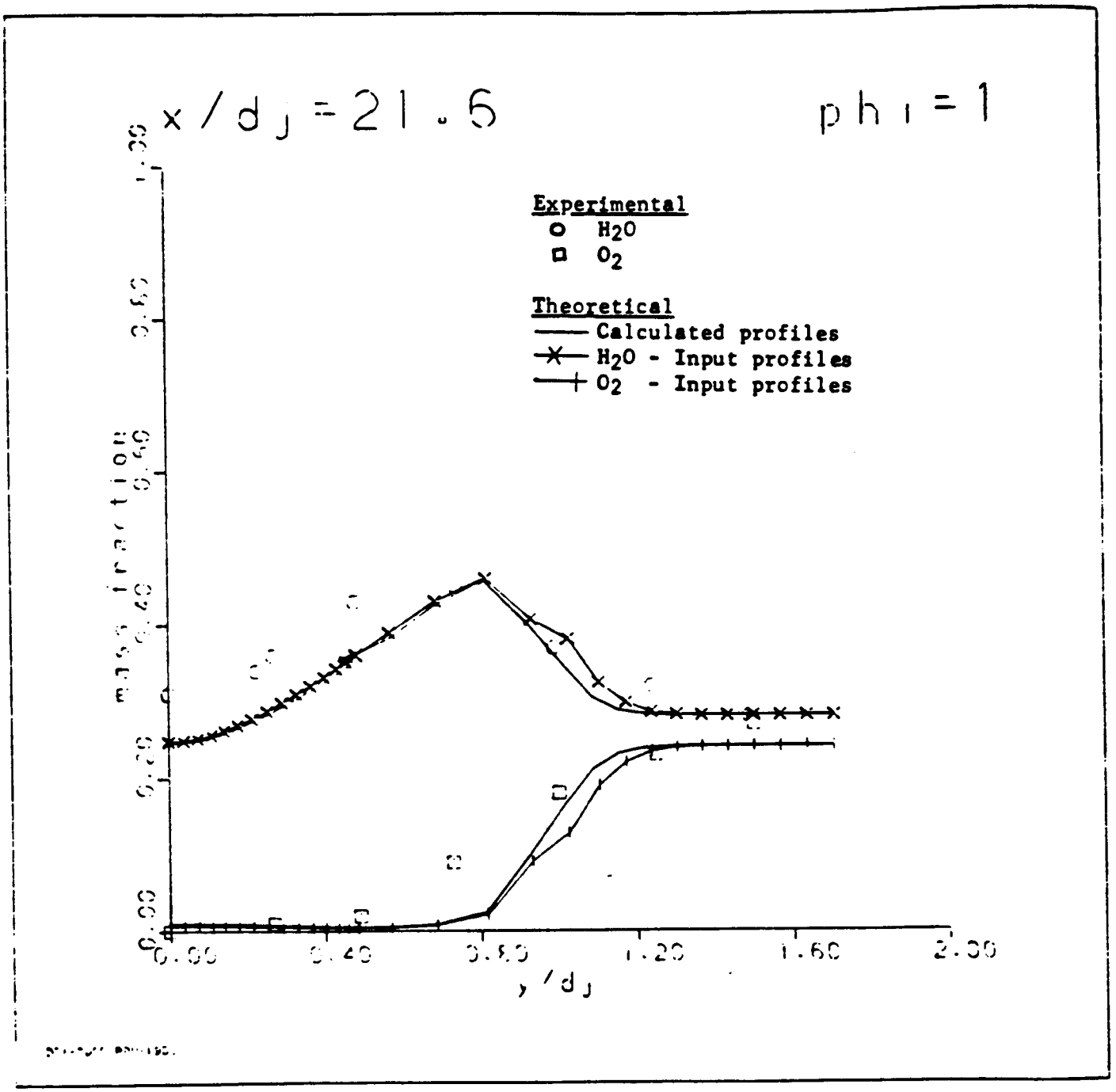

Figure 23 Concluded.

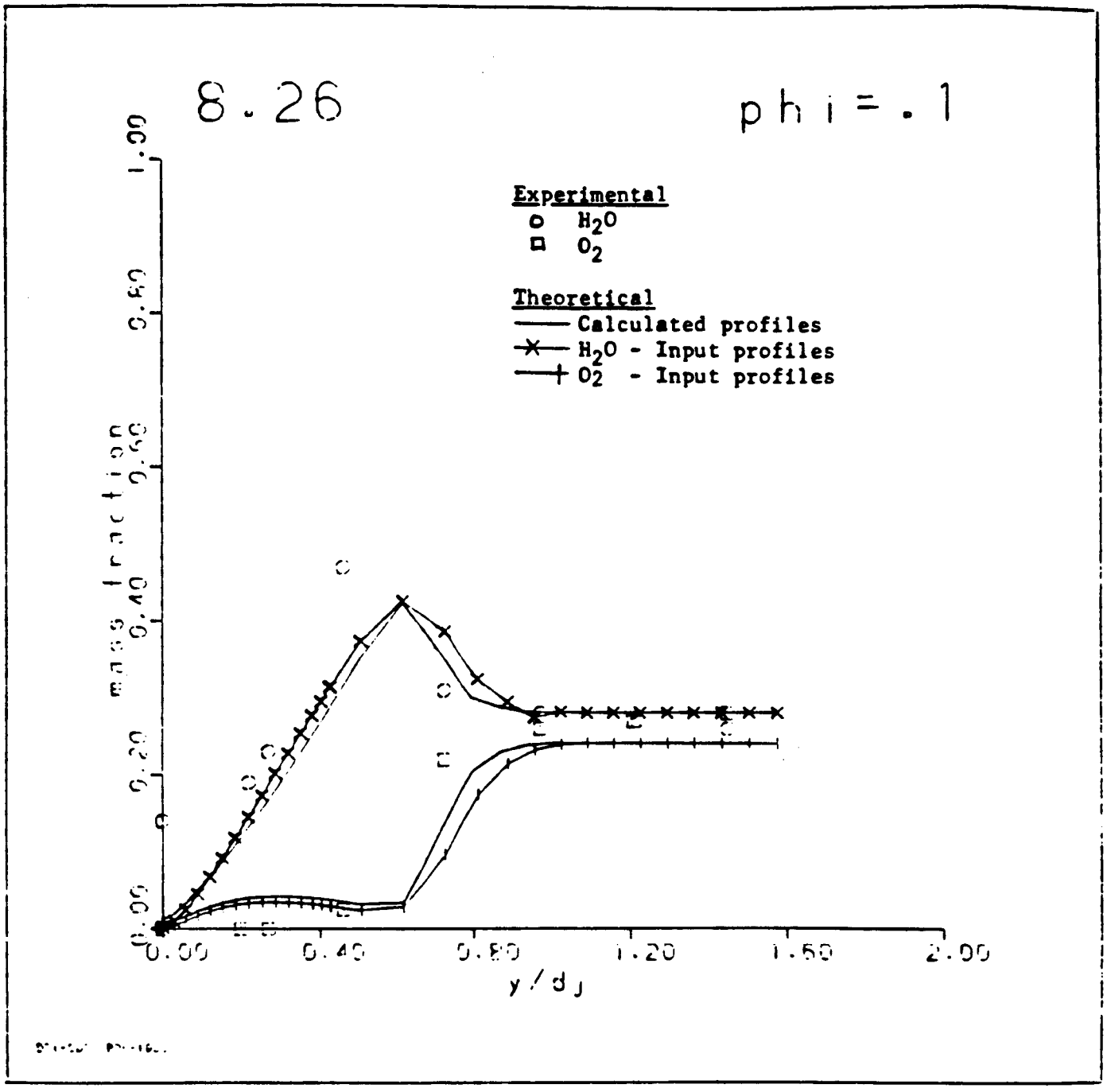

Figure 14. Species concentration profiles for input experimental k-ε profiles (ϕ = 0.1).

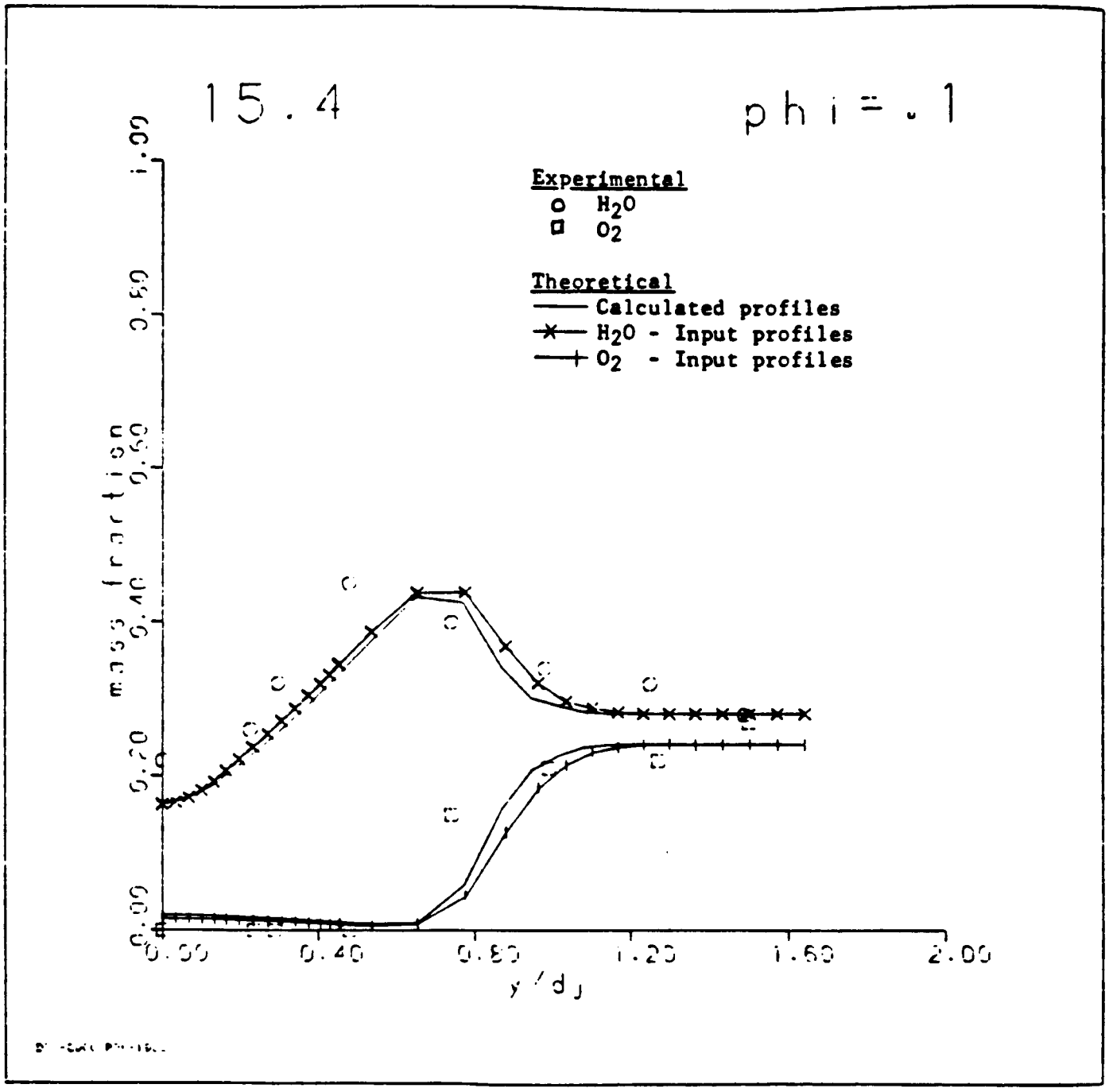

Figure 24 Continued.

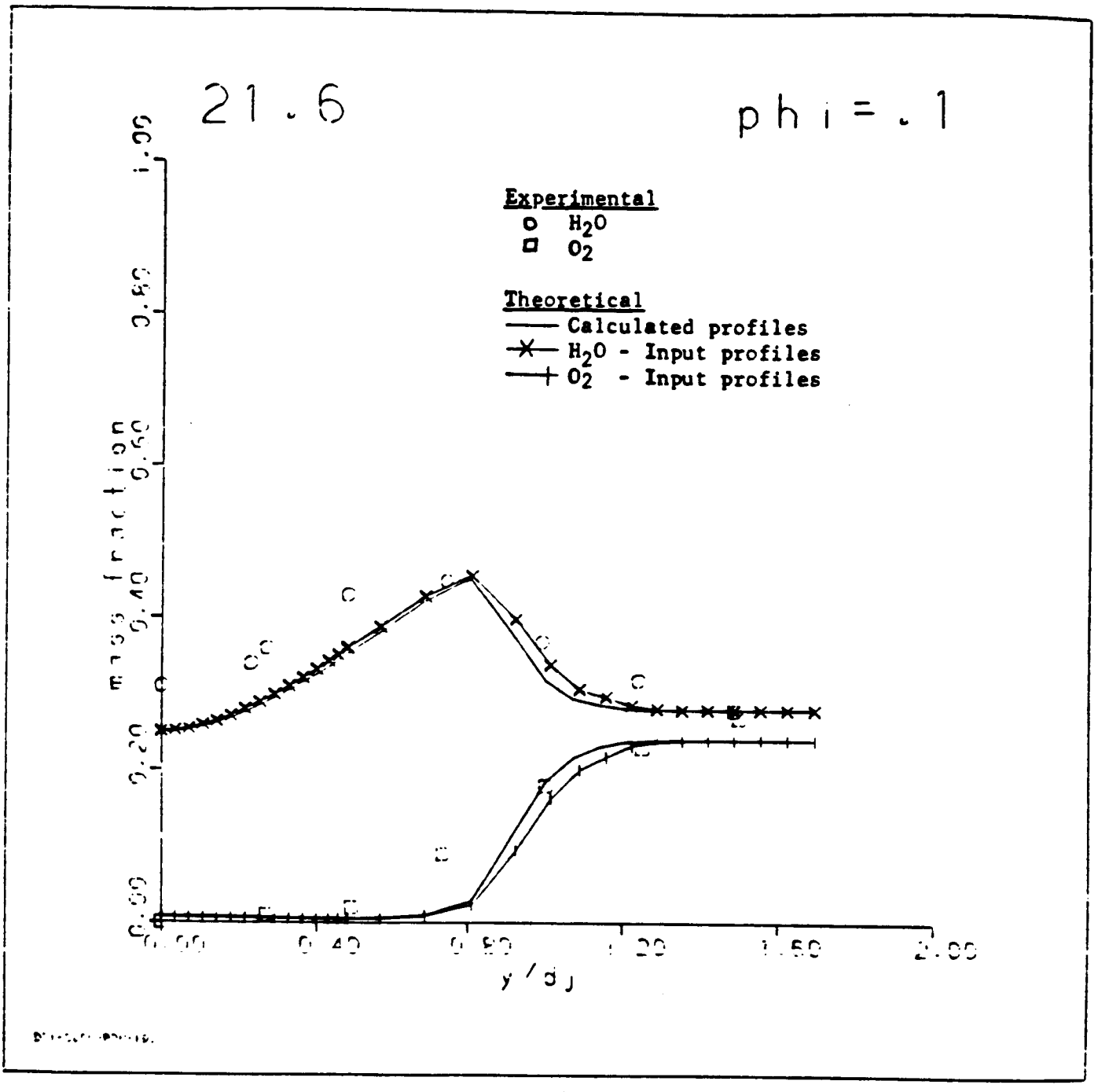

Figure 24 Concluded.

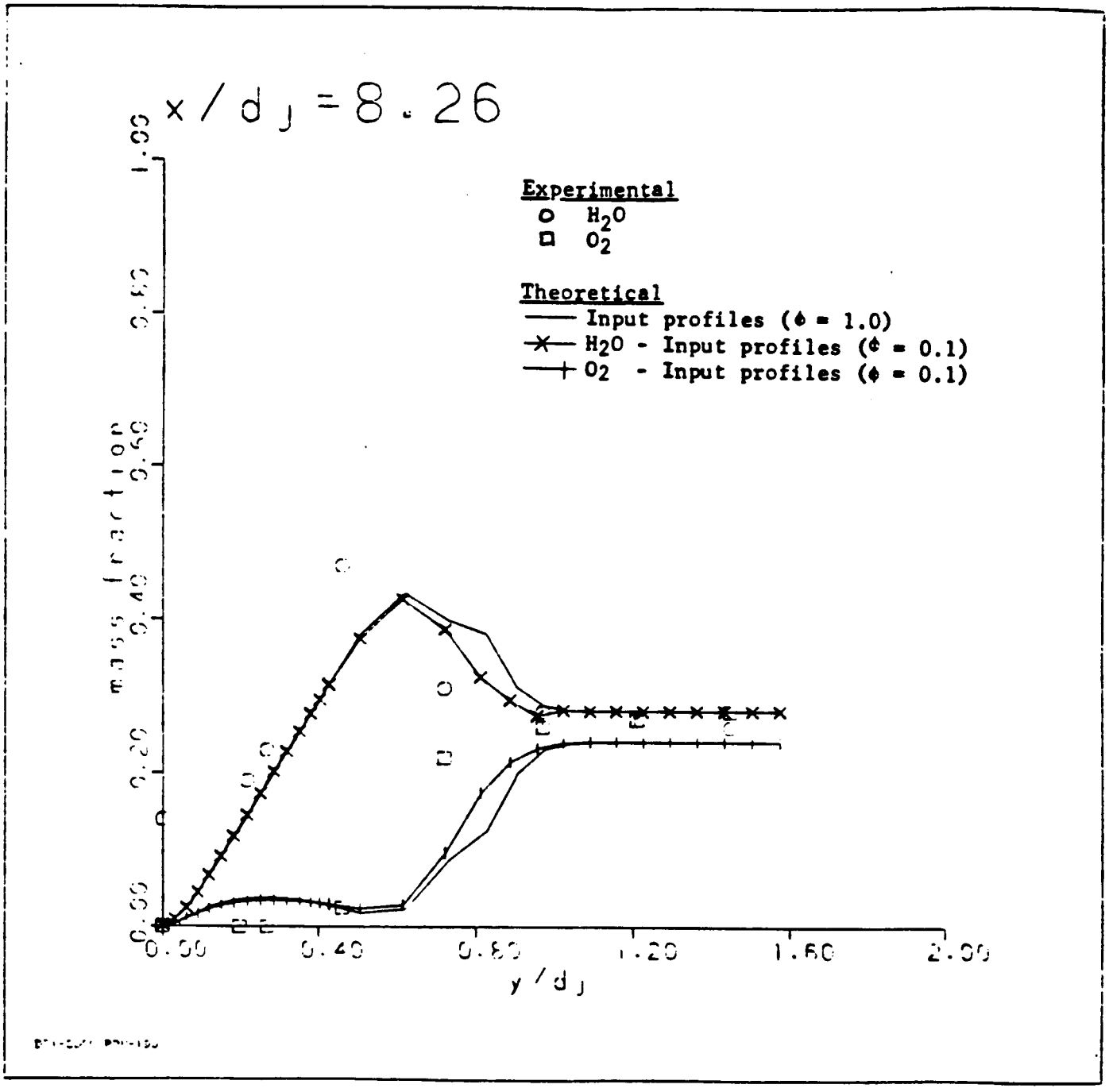

Figure 25 Species concentration profiles for input experimental k-ε profiles with ϕ= 1.0 and ϕ= 0.1.

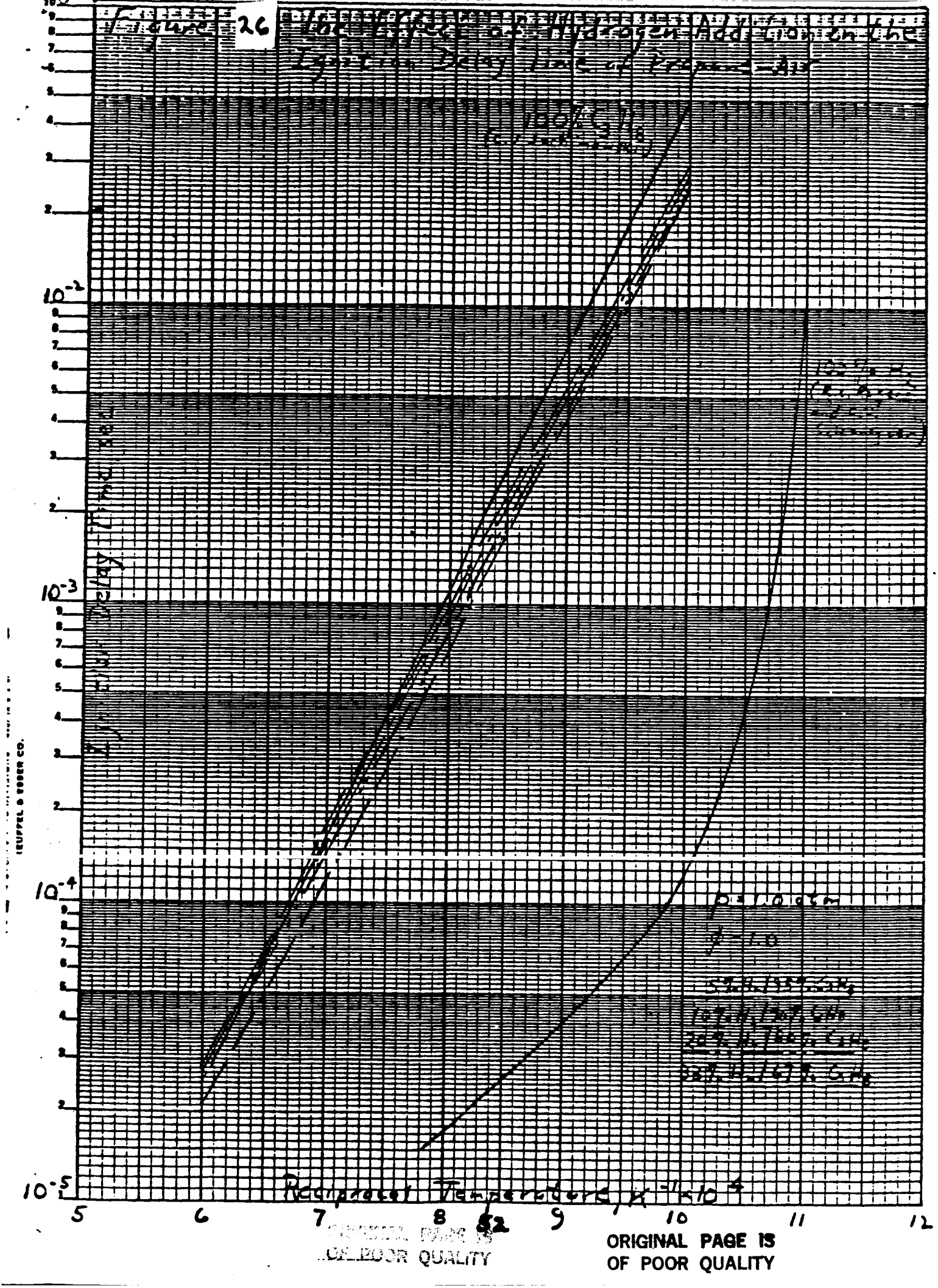

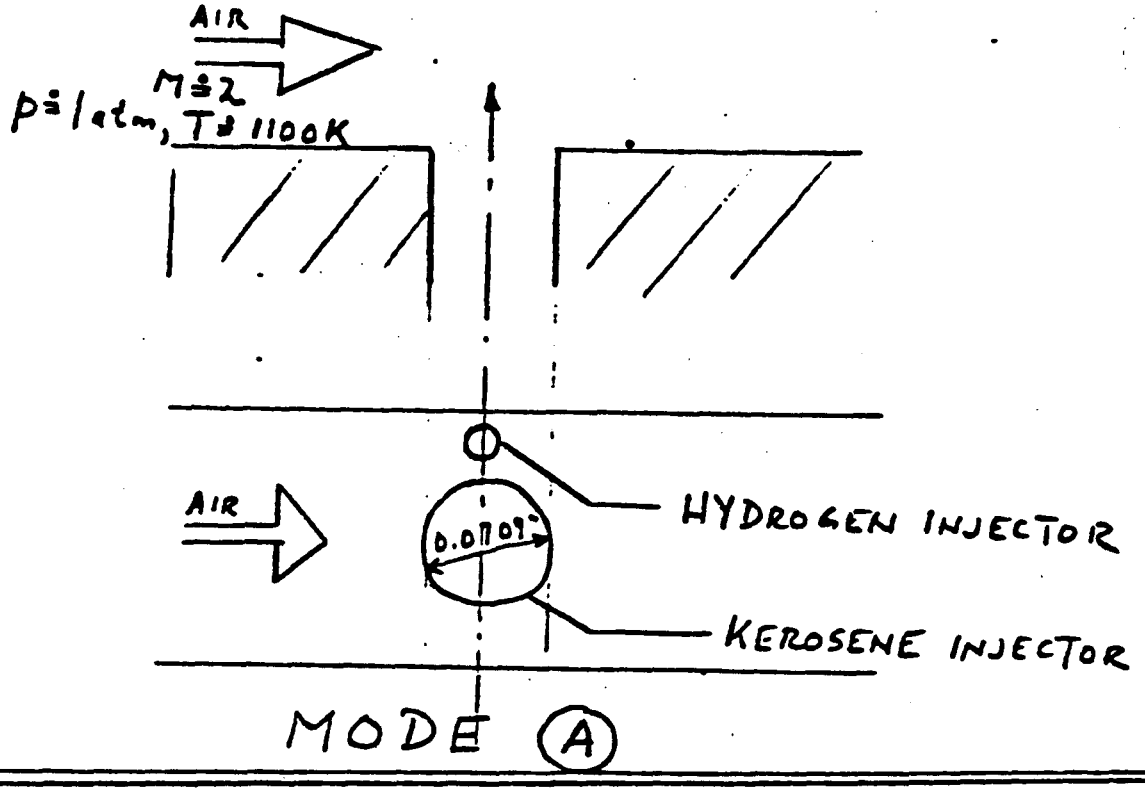

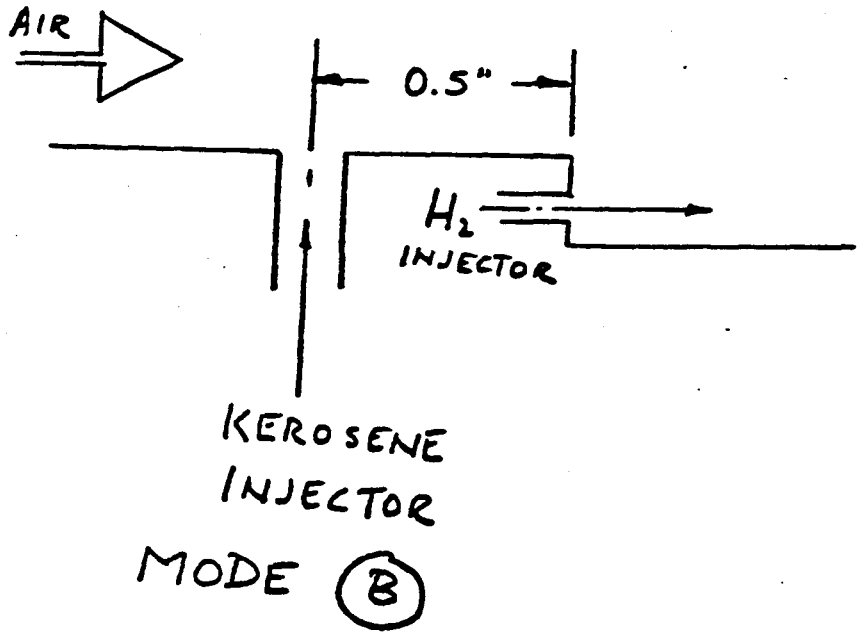

SCHEMATICS OF THE COOKSON EXPERIMENTS

FIGURE 27

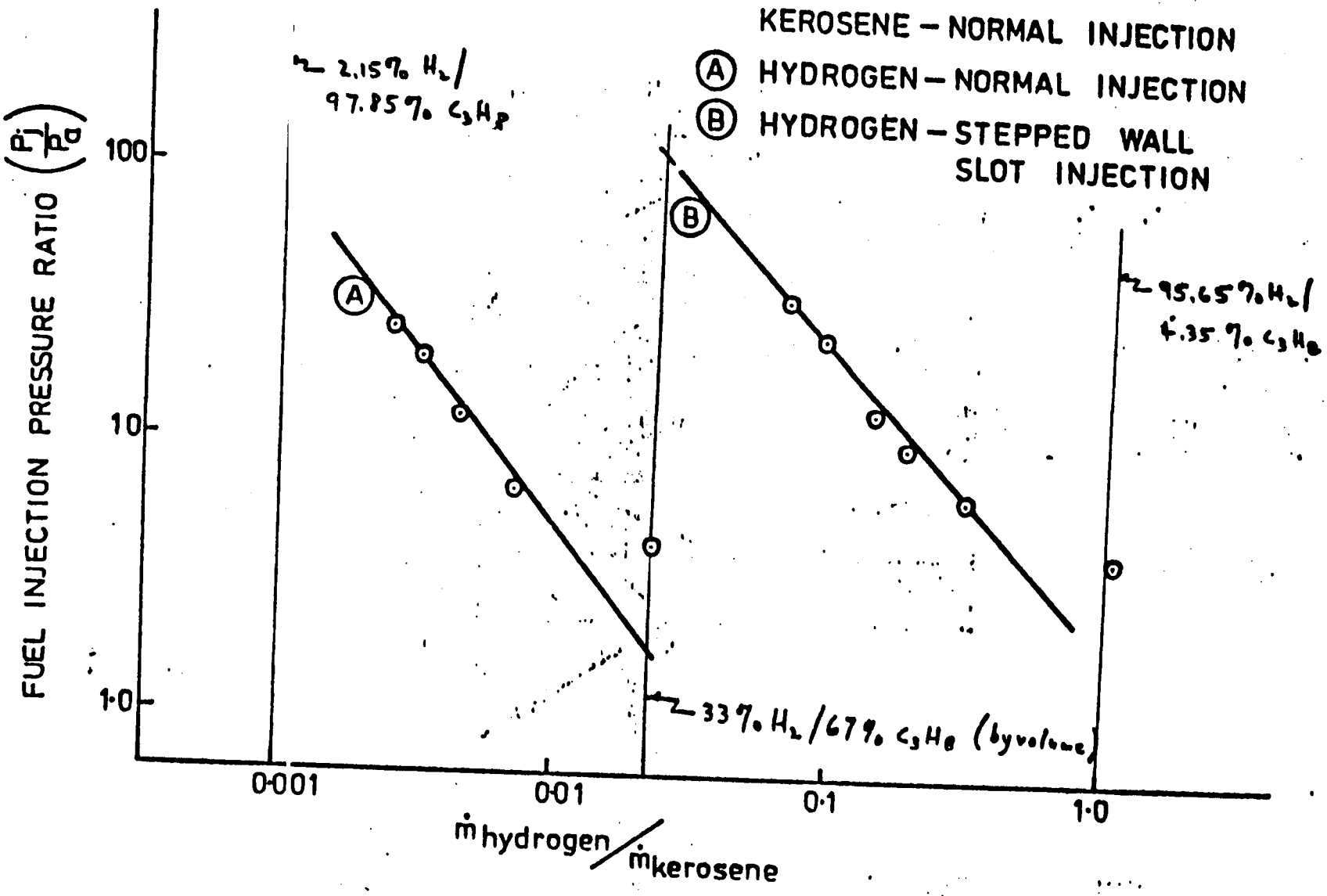

FIGURE 28 MINIMUM HYDROGEN FOR SUSTAINED COMBUSTION OF KEROSENE. (COOKSON)

THE EFFECT OF FUEL HYDROGEN CONCENTRATION ON THE IGNITION DELAY TIMES OF PROPANE-HYDROGEN FUELS

Figure 29

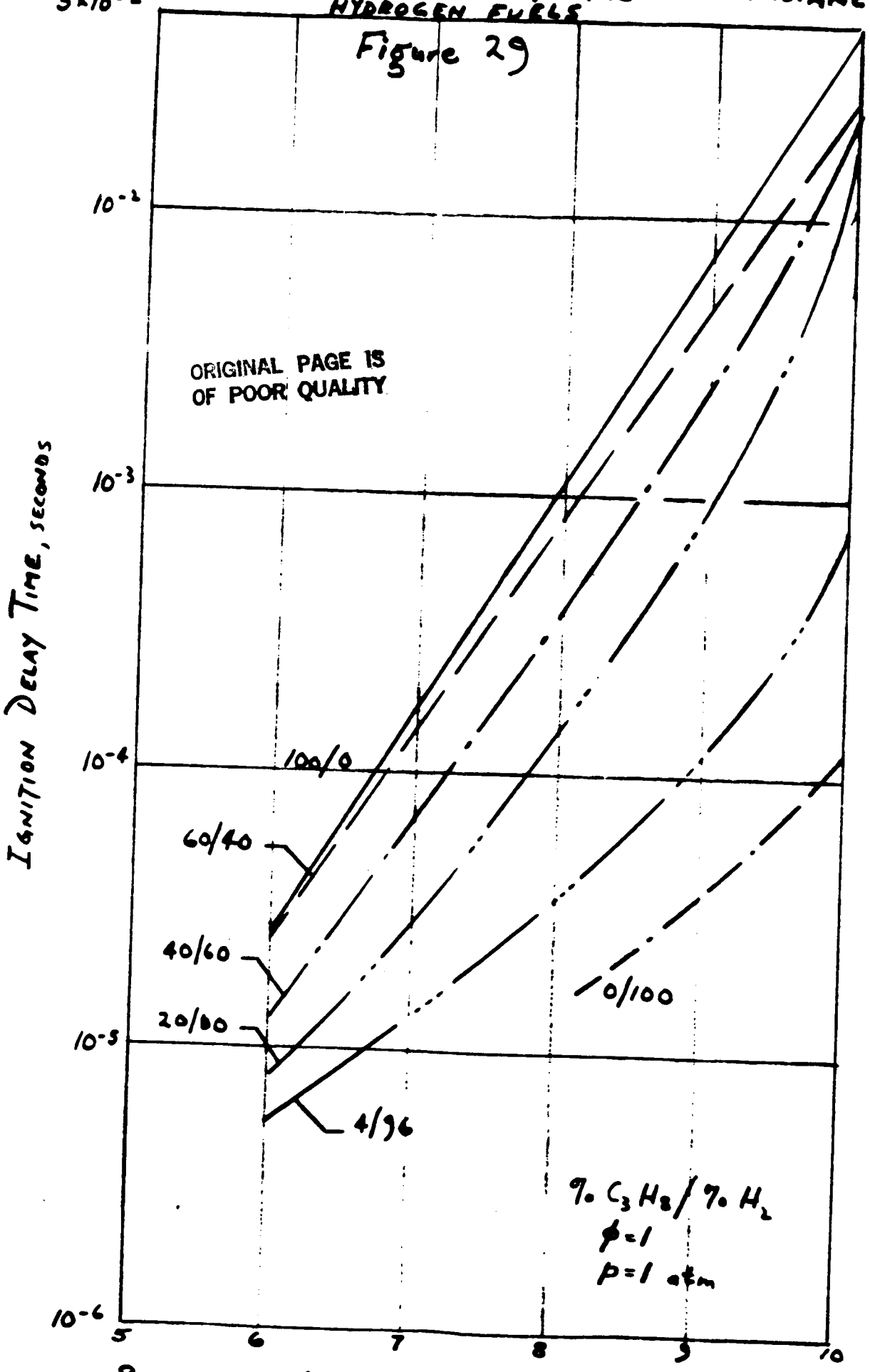

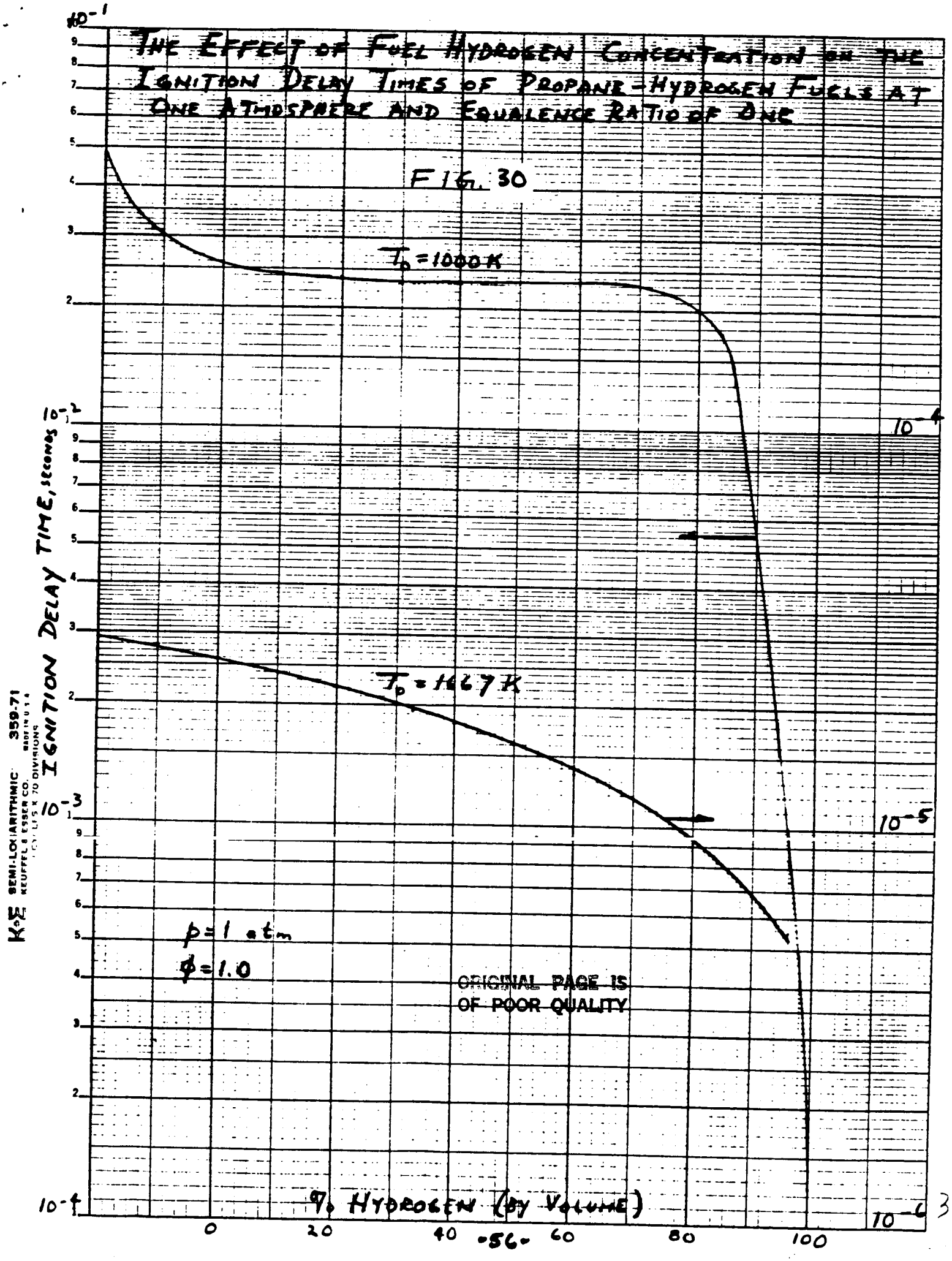
THE EFFECT OF FUEL HYDROGEN CONCENTRATION ON THE IGNITION DELAY TIMES OF PROPANE-HYDROGEN FUELS AT ONE ATMOSPHERE AND EQUALENCE RATIO OF ONE
FIG. 30
T_o = 1000 K
T_o = 1467 K
IGNITION DELAY TIME, SECONDS
10^{-1}
10^{-2}
10^{-3}
10^{-4}
10^{-5}
10^{-6}
p = 1 atm
ϕ = 1.0
% HYDROGEN (BY VOLUME)
0
20
40
60
80
100
ORIGINAL PAGE IS OF POOR QUALITY
K&E SEMI-LOGARITHMIC 359-71 KEUFFEL & ESSER CO. MADE IN U.S.A. FOLDS K 70 DIVISIONS

30

FIG. 31

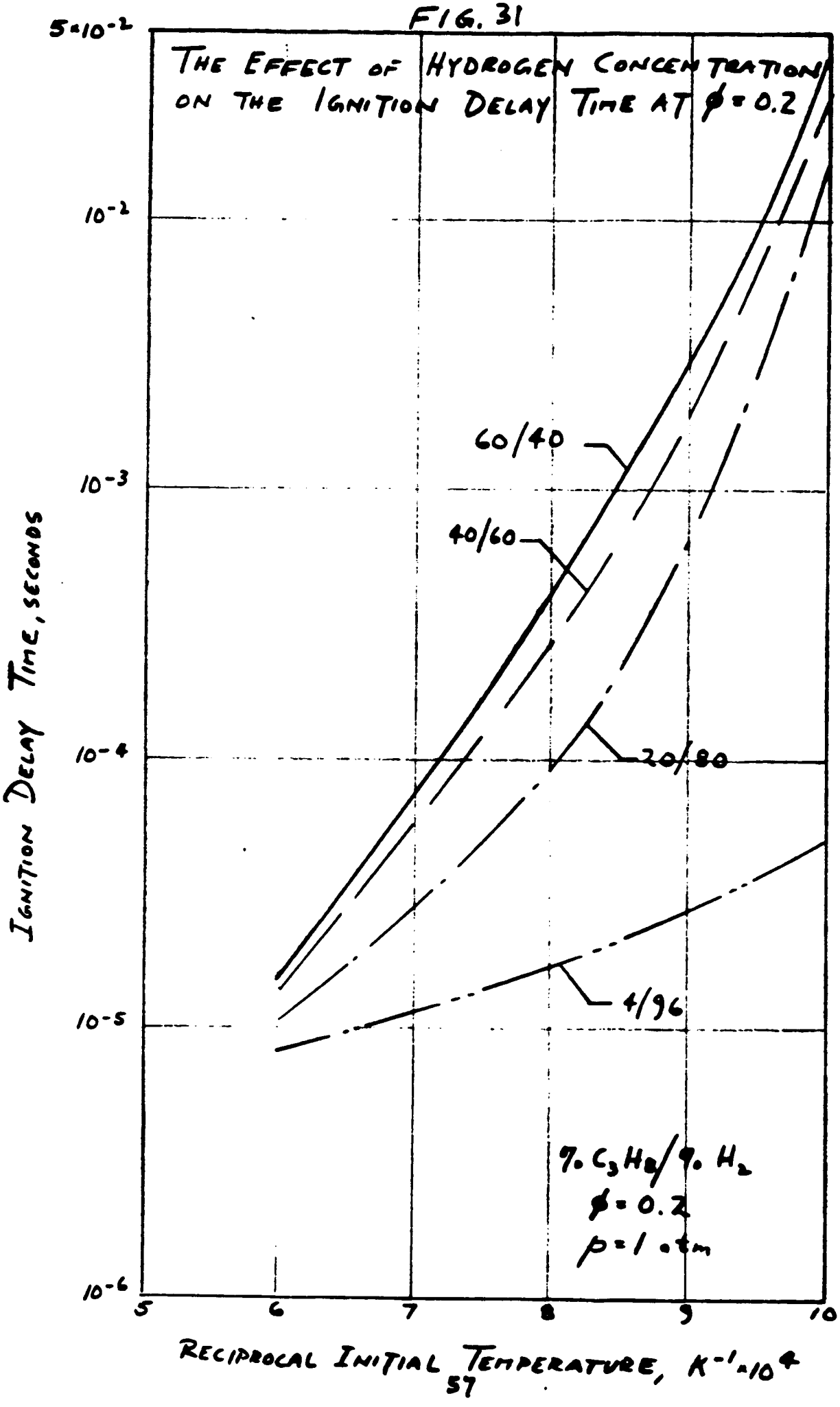
THE EFFECT OF HYDROGEN CONCENTRATION ON THE IGNITION DELAY TIME AT $\phi = 0.2$
5×10^{-2}
10^{-2}
10^{-3}
10^{-4}
10^{-5}
10^{-6}
60/40
40/60
20/80
4/96
IGNITION DELAY TIME, SECONDS
5
6
7
8
9
10
RECIPROCAL INITIAL TEMPERATURE, $K^{-1} \times 10^4$
% C_3H_8 / % H_2
$\phi = 0.2$
$p = 1$ atm

FIG. 32

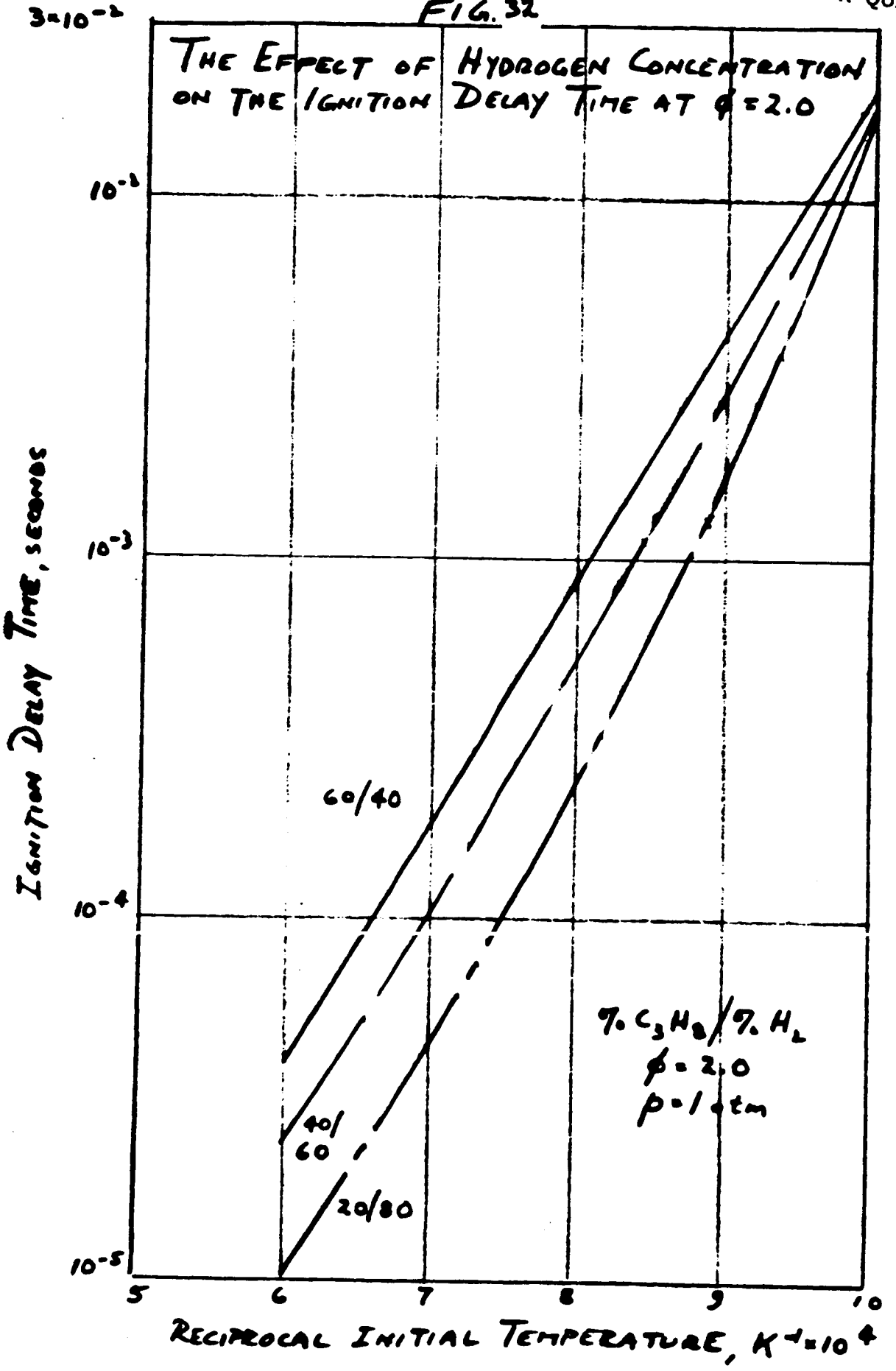

32

Reaction Times for Stoichiometric Propane-Hydrogen Fuels at One Atmosphere

FIG. 33

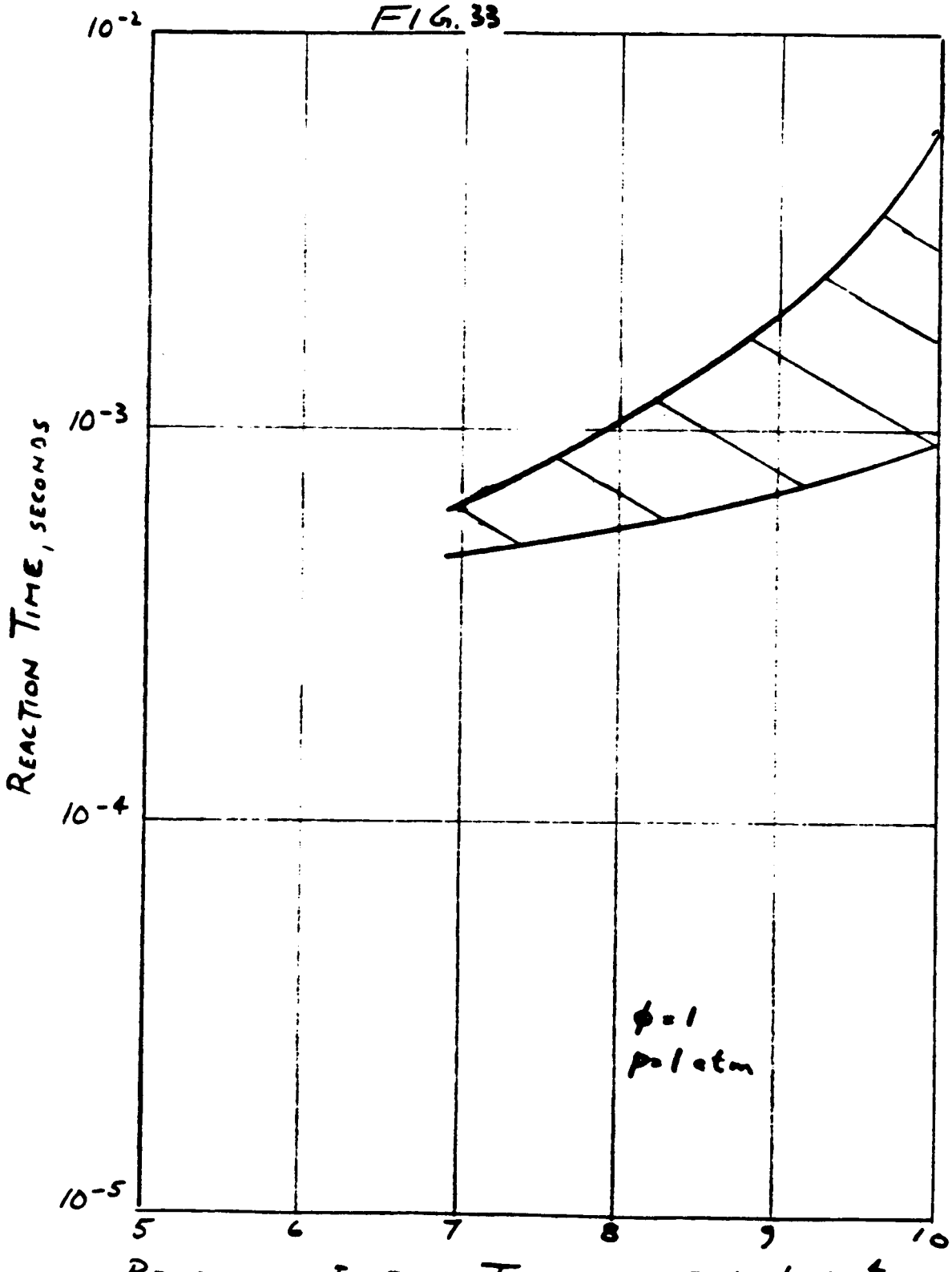

BLOWOUT LIMIT CORRELATIONS FOR PROPANE-HYDROGEN FUELS AT ONE ATMOSPHERE AND 600K INITIAL TEMPERATURE

FIG. 34

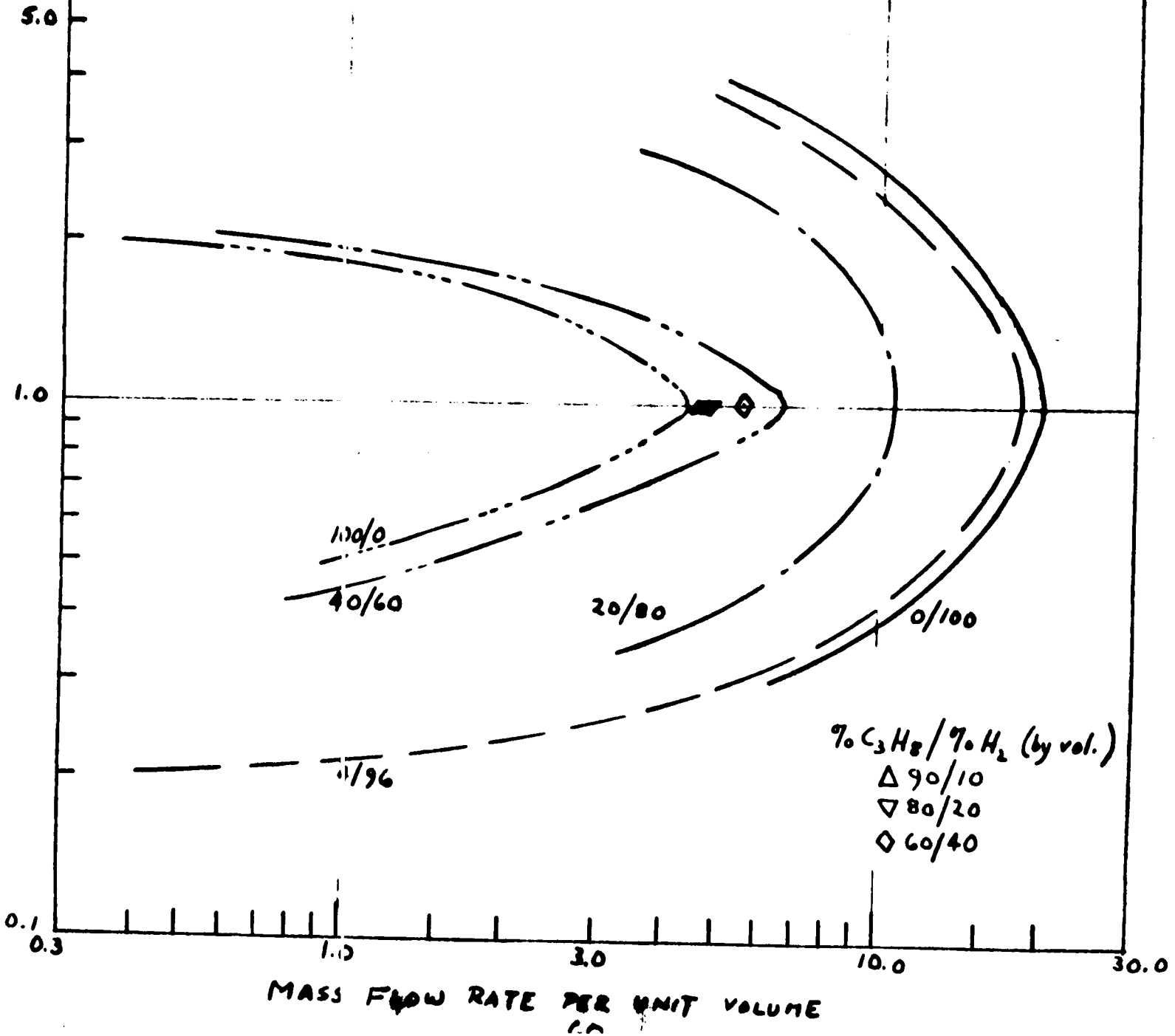

FIG. 35

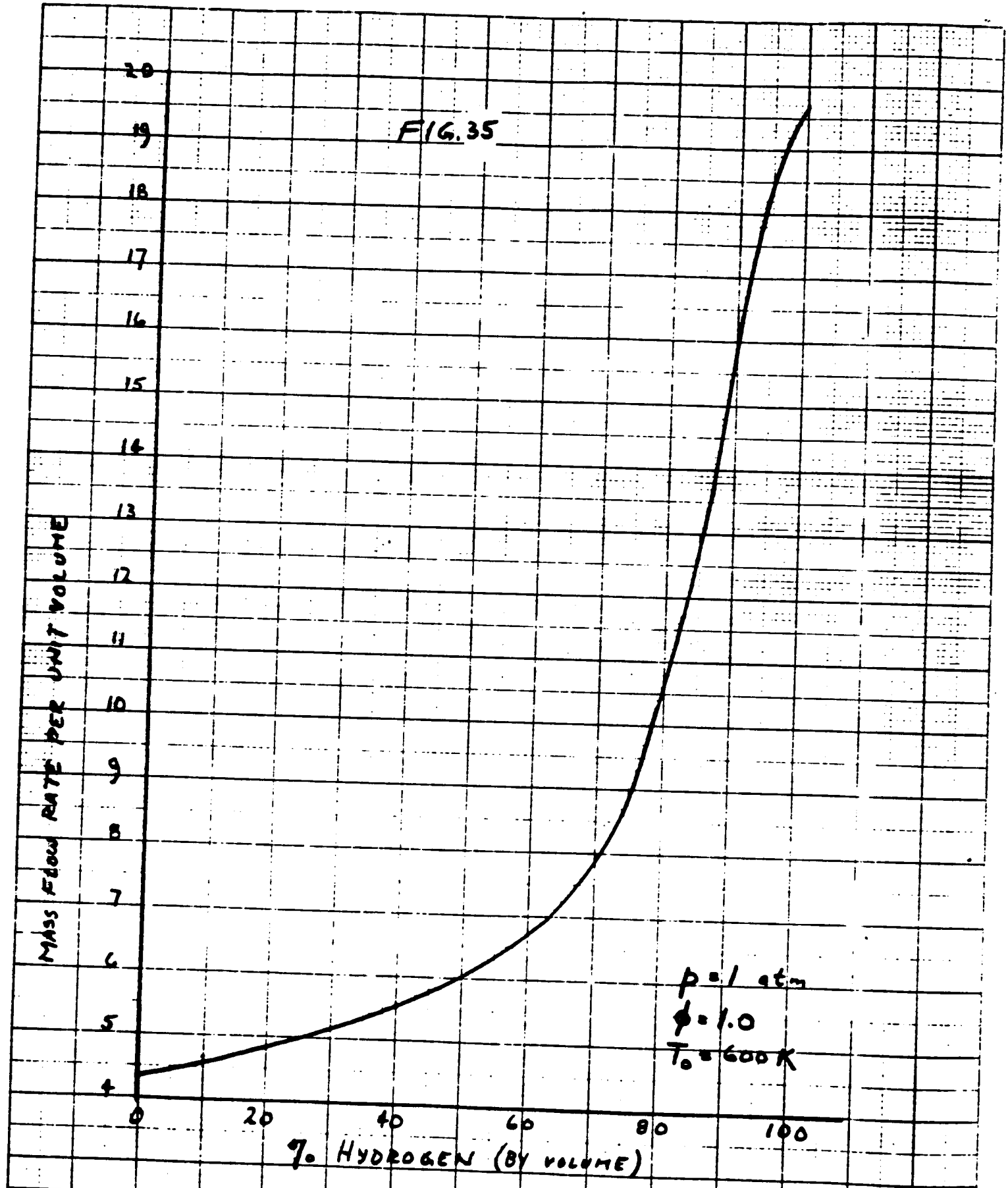

THE EFFECT OF FUEL HYDROGEN CONCENTRATION ON THE BLOWOUT LIMIT AT UNITY EQUIVALENCE RATIO, ONE ATMOSPHERE AND 600 K INITIAL TEMPERATURE

APPENDIX A. The Ranges of Applicability of Chemical Kinetic Models of Hydrogen-Air Combustion

A.1. Introduction

A.1.1 Motivation for the Present Study

The study of hydrogen-fueled supersonic combustion ramjets (scramjets) has been a major part of the research programs of the Hypersonic Propulsion Branch at the Langley Research Center. Scramjets take advantage of high flight Mach numbers (greater than 5) to achieve propulsion efficiencies greater than that of ramjet engines.[1] Propulsion efficiency is a measure of the thrust energy out divided by the combustion energy in. Due to the great flight speeds of scramjets (Mach numbers range from 4 to 7), there are time constraints for combustion within a combustor of reasonable size.

As a result of these time constraints, minimal ignition delay times are desirable. Figure 1 shows a plot of the log of the ignition time versus initial temperature for various fuels. Hydrogen fuel has a very low ignition delay time relative to hydrocarbon fuels. It is this low ignition delay time which makes hydrogen a valuable fuel for scramjets. It becomes a necessity, therefore, to study in detail hydrogen-air combustion.

Most studies, thus far, have been experimental investigations. This dependence on empirical results is due to the complexity of the flow around fuel injectors with three-dimensional geometries, which are not easily treated analytically. Numerical solutions have generally been

restricted to two- or three-dimensional parabolic flow with oversimplified chemistry models of the H_2-air system. These numerical solution schemes are applicable only in the parabolic flow region well downstream of the disturbance

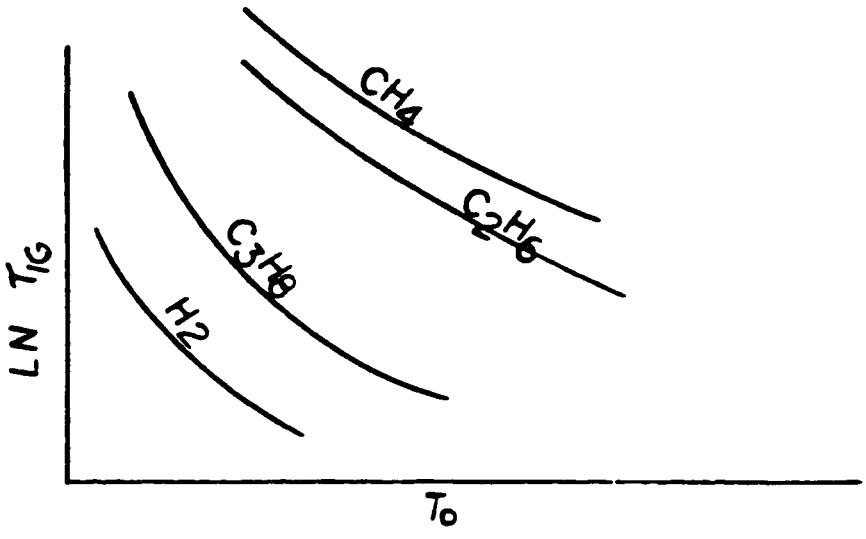

FIGURE 1 IGNITION DELAY TIME VS. INITIAL TEMPERATURE

caused by the transverse fuel injection used by scramjet combustors in order to achieve rapid mixing and reaction. A priori knowledge of the extent of fuel mixing, ignition, and reaction is required to initiate calculations.

In spite of the difficulty in obtaining quantitative information, a sufficient data base has been established to define a scramjet engine concept and to permit fabrication of subscale engine models with integrated inlet, combustor, and nozzle components. The current scramjet is designed to operate

at stagnation temperatures between 900°K and 2200°K[2] which correspond to a flight Mach number range from 4 to 7. In ground tests of subscale engine models[3], however, problems were encountered in obtaining ignition and sustaining reaction at test conditions where ignition and sustained reaction were expected.

The need to better understand the chemical mechanism of the ignition and reaction of H_2-air mixtures at conditions typical of a scramjet combustor has led to many analytical studies. Most of the analytical studies at the Langley Research Center, as well as this present study, use a computer program (references 4 and 5) to solve flowing, chemical-kinetic, isobaric, stream-tube problems involving many chemical species. It is known that the computational time requirements for any computer program employing detailed chemical kinetics is proportional to the number of species and reactions being treated. It is the purpose of this effort to develop a method which reduces these numbers in the study of H_2-air combustion and at the same time preserve the correct physical-chemical behavior. The result of this work will be to reduce computer time and computer storage requirements. Methods for reducing computational times are presented in section two of this work.

A.2. Methods to Reduce Computational Times

The method proposed in this work to reduce computer run times is an extension and refinement of the method proposed by Chintz in reference 9. This method involves the tracking of a "trigger" species which is used to determine whether the flow is in an "ignition" mode or in a "combustion" mode. Ignition and combustion are defined in the classical sense. Ignition delay time is taken to be the time required for the temperature increase to reach five percent of the overall temperature increase:

$$T_{ig} = T_o + 0.05(T_{eq} - T_o) \qquad (1)$$

When the temperature is less than the ignition temperature, the flow is in the "ignition" mode. Otherwise, the flow is in the "combustion" mode. (See Figure 2).

It will be shown that while an extensive chemical package is needed to describe the "ignition" mode, a smaller package is sufficient to deal with the "combustion" mode. Evans and Schexnayder[10] concluded that a 25-reaction scheme involving 12 species (designated 25(12) herein), was required to describe "ignition" processes, while an 8(7) sufficed to deal with the "combustion" mode. The work

discussed herein describes efforts to minimize the computational time requirements once the "combustion" process is initiated (i.e. a smaller package or one that takes less computational time than the 8(7) system might suffice to deal with the "combustion" mode).

A 37(13) system is used as the "test" chemical-kinetic package (Table 1). Any smaller system is "tested" against the 37(13) system to see if the correct physical chemical behavior is preserved. This is accomplished in the following way:

First, the full 37(13) system is run from the initial state to equilibrium. Next, the test system is run from the point where the "combustion" in the 37(13) system initiates. The test system's initial values (pressure, temperature, equivalence ratio and chemical composition) are that of the 37(13) system's values at the point of "combustion". Temperature-time profiles and chemical behavior are compared (see Figure 3). If the difference between the 37(13) system and the test system is within an acceptable

range, the test system will be sufficient to deal with the "combustion" process.

Graphs of the mass fraction of the trigger species versus time and ignition temperature versus mass fraction of the trigger species at ignition are made in accordance with reference 9. The cases from the 37(13) system serve as the data base.

An 8(7) system (Table 2) is tested to confirm the results of Evans and Schexnayder.[10]. The 8(7) system is run from the initial state to equilibrium to determine if there are any initial conditions where the 8(7) system describes the entire process (i.e. both ignition and combustion).

In order to further reduce computational times, a 2(5) global model (Table 3) developed by Rogers and Chinitz in reference 11 is tested. The method proposed in that paper must be altered to include the effects of pressure. The Arrhenius equation will have the form:

$$k_{fi} = A_i(\phi , \rho)T^{Ni}exp(-E_i/RT) \quad (2)$$

The values of the paramaters may be different from those in reference 11 because they are fixed

arbitrarily so that the 2(5) system describes the 37(13) system.

Lastly, the so-called "partial equilibrium" assumption of reference 12 is examined in connection with an 8(7) system in an effort to minimize computational times. The 8(7) mechanism consists of the following reactions:

$$H_2O + O = OH + OH \qquad (i)$$

$$H_2O + H = OH + H_2 \qquad (ii)$$

$$O_2 + H = OH + O \qquad (iii)$$

$$H_2 + O = OH + H \qquad (iv)$$

$$H_2O + M = H + OH \qquad (v)$$

$$H_2 + M = H + H + M \qquad (vi)$$

$$O_2 + M = O + O + M \qquad (vii)$$

$$OH + M = O + H + M \qquad (viii)$$

During the ignition delay period, all eight reactions play a role; however, in the "combustion" mode, the bimolecular shuffle reactions occur so rapidly in both directions that under some conditions they may be basically in equilibrium. The "partial equilibrium" assumption takes ractions (i)-(iv) to be

in equilibrium (infinitely fast reaction rates), while reactions (v)-(viii) continue to occur at a finite rate.

Infinitely fast reaction rates can be approximated by assigning very large values to the preexponential factor in the forward reaction rate constant (e.g. 10^{50}). The backward reaction rate constant is then very large to satisfy $K = k_f/k_b$ The values of the preexponential factors of reaction (i) to (iv) are determined so that the system describes the "combustion" process.

To obtain these results, 45 one-dimensional, constant pressure, H_2-air computations were performed in the ranges:

$$0.5 \leq \phi \leq 1.5$$

$$850 \leq T \leq 1200$$

$$0.5 \leq p \leq 1.0$$

where ϕ is the equivalence ratio, T is the temperature in °K, and p is the pressure in atmospheres. A listing of these individual cases is given in Table 4. Comparison of the computational times are then made and recommendations are discussed.

A.3. Results and Discussion

A.3.1 Summary

All 45 cases in Table 4, as well as the nine cases marked with an exclamation point, were performed on the 37(13) and 8(7) systems, respectively, in both the ignition and combustion modes. In addition, the 15 cases marked with an asterisk were tested on the 8(7) system, the global model, and the "partial equilibrium" model starting at the ignition point. These 15 cases were selected to encompass the entire range of interest.

What follows are the results of these test cases. First, the results from the 37(13) system including the "trigger" concept are presented. Next, the 8(7) system in its entirety and in the combustion mode alone is discussed. Global and partial equilibrium results in the combustion mode follow. Lastly, temperature-time profiles and computational times are compared for all four systems.

A.3.2 The 37(13) System

A.3.2.1 Temperature-Time Profiles

45 cases were run to serve as a basis of comparison for the test systems described

previously. Sufficient data points were obtained for all cases and each case yielded a characteristic S-shaped curve for the temperature versus time profile. For each case, it was necessary to obtain a data point at the ignition temperature, defined in the classical sense as 5% of the temperature rise from the initial state to the final equilibrium state, in order to set initial conditions for the test cases. Problems arose, however, when trying to pinpoint the ignition temperature. As a result, satisfactory ignition conditions could not be calculated for nine cases due to time constraints. These cases were omitted from data base and the remaining 36 cases are given in Table 5 with corresponding ignition temperature, time, and mass fraction of OH.

Tables 4 and 5 show that the ignition delay time is a function of initial temperature, pressure, and equivalence ratio. This function is complicated since it is inversely proportional to initial temperature, nearly independent of equivalence ratio except at low temperatures (850°K and 900°K), proportional to pressure at temperatures of 850°K and 900°K, and is inversely proportional to pressure at temperatures greater than or equal to 1000°K in the ranges studied. These results are similar to the

results reported by Rogers and Schexnayder (reference 2) in their extensive study which included 60 reactions and 20 species. Since the results are similar to those of Rogers and Schexnayder, the 37(13) system serves as a good basis for the remaining systems to be compared with.

A.3.2.2 The "Trigger" Concept

In order to test systems in the "combustion" mode it is necessary to determine when the transition to the "combustion" mode takes place. It was to this end that the concept of a "trigger" species was first proposed by Chinitz in reference 9. The concept involes the tracking of the mass fraction of one of the species. When its value becomes greater than a preset value, the system is said to be in the "combustion" mode.

There are several requirements for a species to serve as an effective trigger from ignition to combustion. The concentration of an effective trigger species must be single-valued (the value of the mass fraction at the ignition point is not again obtained) and undergo a sufficiently large change during the ignition process that its crossover into the combustion mode is unmistakeable. It was

believed that the hydroxyl radical, OH, would serve that purpose.

Results here confirm the work of reference 9. Table 6 and Figure 4 show how the mass fraction of OH varies with time for a representative case (case number 23). It is easily seen that OH has all the requirements to serve as the trigger species. The ignition point is well-defined and is single-valued.

It is of interest to estimate the trigger point for all values of equivalence ratio, pressure, and temperature studied. A plot of the ignition temperature vs the mass fraction for OH at the ignition point is shown in Figure 5. A least-squares linear fit of ln T_{ig} is $Y_{OH_{ig}}$ was determined to be

$$\ln T_{ig} = 0.085 \ln Y_{OH_{ig}} + 7.65 \quad (3)$$

This linear relationship predicts values within a factor of 2.5 (generally well within) for all pressures and equivalence ratios examined. This provides a large advantage over the non-linear relationship developed in reference 9 which was limited to an equivalence ratio of 1. With the selection of a trigger species whose value can be estimated, the test systems can now be examined.

A.3.3 The 8(7) System

A.3.3.1 Ignition and Combustion

The 8(7) sytstem was run from time zero to equilibrium for the nine cases marked with an exclamation point in Table 4. Five of these cases (3, 6, 9, 12, 15) represent a set of constant pressure, constant equivalence ratio conditions with varying initial temperature. These were selected to determine how the initial temperature affects the ignition delay time when compared to the 37(13) system. The remaining four cases (13, 22, 25, 29) were arbitrarily picked in an attempt to see the effects of pressure and equivalence ratio.

Figures 6-10 show a comparison of temperature-time histories for the 37(13) and 8(7) systems for cases 3, 6, 9, 12, 15, respectively, in both the ignition and combustion modes. Figures 6 and 7 show the delay time to be more than an order of magnitude lower for the 8(7) system at low temperature. Figures 8-10, however, show that the delay time for the 8(7) system is greater than the 37(13) system at higher temperatures. It is therefore concluded that a transition takes place between an initial temperature of 900°K and 1000°K. (It should be noted that a ten percent mixture of hydrogen in air has an ignition temperature of between 893°K and 1020°K[13]).

Figure 11 shows a plot of ignition delay time vs. $1000T_o^{-1}$ for the 8(7) and 37(13) systems at a pressure of one atmosphere and an equivalence ratio of 0.5. The two curves cross at a temperature of 970°K where their ignition delay times are equal.

These results imply that for any constant pressure and constant ϕ there is a T_o for which the two systems have the same ignition delay time. At these conditions, the 8(7) system can describe the 37(13) system in both the ignition and combustion modes. It also might be expected that at temperatures away from this particular initial temperature, the 8(7) system might lag behind or proceed ahead of the 37(13) system when tested at ignition conditions in the "combustion" mode.

The remaining four cases all had initial temperatures at or above 1000°K. The results of these cases were again that the delay time was higher for the 8(7) system than that of the 37(13) system. No significant effects of pressure or equivalence ratio were found in these limited case. The 8(7) system was now tested in the "combustion" mode with a focus on the effect of initial temperature.

A.3.3.2 The "Combustion" Mode

The 15 cases marked with an asterisk in Table 4 were run for the 8(7) system in the "combustion mode." For all pressures, temperatures, and equivalence ratios studied, the 8(7) system had a higher equilibrium temperature than that of the 37(13) system. This result was expected in that the 8(7) system neglects nitrogen dissociation. It was also found that for all conditions, the 8(7) system lagged behind the 37(13) system after the ignition point then equaled and surpassed the 37(13) curve (see Figure 12). This result was contrary to the expectations of section 4.3.2.1. It was thought that for some initial temperatures the 8(7) system would reach equilibrium more equickly than the 37(13) system. This, however, was not the case.

The amount of lag, however, was found to be a function of the relationship between the actual ignition temperature and the ignition temperature calculated from equation 1 (designated herein as "classical" ignition temperature). If the ignition temperature used (and also all other initial conditions) was between the initial temperature and the classical ignition temperature, then the 8(7) system described the 37(13) system very well. If the temperature used was greater than the classical

ignition temperature, there was an appreciable lag (see Figure 12). Therefore, as the difference between the initial temperature and ignition temperature used increased, the lag became greater. No cases were found where the 8(7) system reached equilibrium more quickly than the 37(13) system. It is concluded, therefore, that ignition temperatures lower than the classical ignition temperature should be used. It was not determined what percent below five percent should be used.

A.3.4 The Global Model

The global model in Table 3 was first proposed in reference 11. The reaction rate constant for each reaction is adjusted so that the global model describes the 37(13) system in the combustion mode.

Before determining these adjusted rate constants, it was useful to observe how varying each rate constant affected the temperature-time profile. It was observed that increasing k_{f4} (the subscript 4 refers to the first reaction; subscript 5 refers to the second reaction using the notation in reference 11) slows down the reaction. This was referred to as a "lagging" system in the previous section. Increasing k_{f5} speeds up the reaction. The system is very sensitive to an increase or

decrease in k_{f5} while being rather insensitive to a variation in k_{f4}. It was decided to fix Ni and Ei at the same values as in reference 10; namely,

$$E_4 = 4865 \text{ cal/mol}$$
$$N_4 = -10$$
$$E_5 = 42{,}500 \text{ cal/mol}$$
$$N_5 = -13$$

Due to the insensitivity of the system to k_{f4}, it was also decided that A_4 could be retained as in reference 11:

$$A_4(\phi) = (8.917\phi + 31.433)\phi - 28.950) \times 10^{47}, \text{ cm}^3/\text{mol-s} \qquad (4)$$

It should be noted that A_4 is a function of ϕ only.

The effect of pressure, which was neglected in reference 11, was included in the determination of A_5. As a result, A_5 is a function of pressure and equivalence ratio and has the form $A_5(\phi, p)$. The sensitivity of the system to k_{f5} permitted substantial changes to be made to the temperature profiles produced by the global system.

Table 8 shows the values of A_4 and A_5 determined in order to describe the temperature-time profile required. Figure 13 shows a plot of A_4 (which is independent of pressure) vs. ϕ. Figure 14 shows plots of A_5 vs. pressure for various ϕ's.

As other authors have reported, large discrepancies exist between results for equivalence ratios less than or greater than one. The relationship between A_5 and pressure and equivalence ratio must be broken up into two equations for the ranges studied:

For $\phi \geq 1$

$$A_5 = \left(8.80 + 5.85/\phi - 3.67\phi - 4.80p - 3.20p/\phi + 2.00p\phi\right) \times 10^{64}$$

For $\phi < 1$

$$A_5 = 0.67\phi^{-1.5}p^{-0.7}\,(8.80 + 5.85/\phi - 4.80p - 3.20p/\phi + 2.00p\phi) \times 10^{64}$$

These equations predict values of A_5 to within 10% for the ϕ's studied..

In all cases, the global mode lags behind the 37(13) system for a short period following ignition. Then the global model equals and exceeds the 37(13) system and reaches equilibrium (see Figure 15). The equilibrium temperature of the global model should be higher than that of the 37(13) system due to dissociation.

This again, however, is controlled by the ignition temperature used by the global model. If the ignition temperature used is greater than the classical ignition temperature, then the equilibrium temperature is less than the classical ignition temperature. If the ignition temperature is less

than the classical, then the equilibrium temperature reached is greater than the 37(13) system as expected.

Initial temperature also has an effect on the accuracy of the global model. As the initial temperature increases, the difference between the global model and the 37(13) system increases. No effect on pressure or equivalence ratio was found.

The global model predicts very well the temperature-time profile of the 37(13) system. These results, however, show the importance of the ignition temperature used. It is suggested that ignition temperature be a variable to be tested in future work. Nonetheless, the global model shows promise in accurately reproducing temperature-time profiles with a minimum of computational time and computer storage requirements.

A.3.5 The "Partial Equilibrium" Assumption

The "partial equilibrium" assumption is already in use in combustion analysis; however its applicability to this present study in the ranges of interest has not been determined. This assumption states that the bimolecular shuffling reactions occur

so rapidly that the are basically in equilibrium. If this is the case, the kinetics equations can be replaced by the algebraic laws of mass action as discussed in reference 12. Therefore, a number of partial differential equations are replaced by algebraic equations and the remaining partial differential equations are simplified. If appropriate criteria are specified as to when this assumption is applicable, computer running times will be greatly reduced.

It was to this end that an approximation to tne "partial equilibrium" assumption was tried. Instead of incorporating algebraic equations into the computer program, infinitely fast reaction rates would be approximated by using extremely large numbers (on the order of 10^{50}) for the preexponential factor. It was anticipated that this would sufficiently approximate the "partial equilibrium" assumption.

Substantial numerical difficulties arose in trying the approximation. First, the largest preexponential factors that could be used were of the order of 10^{24}. Still, this was at least 5 orders of magnitude greater than any other preexponential factors, Next, the precision of the program needed to be upgraded two orders of magnitude by adjusting the

EMAX parameter. Finally, this approach produced erroneous results such as temperatures exceeding the equilibrium temperature when the Gear integration procedure was used. The slower Adams method was then used which gave results which were physically plausible. Due to these problems, running times were very long. This was not the main concern, however. Rather, the primary goal was to test the partial equilibrium assumption against the 37(13) system in the ranges studied.

Figures 16-30 show how the approximation to the "partial equilibrium" assumption compared to the 37(13) system. For low temperatures (850°K, 900°K) and for all cases with an equivalence ratio of 0.5, the partial equilibrium assumption reproduced the 37(13) curve well. In the remaining cases, however, the assumption did not approximate the profile accurately. The shape of the curve was not even preserved.

It appears that the approach to approximating the "partial equilibrium" assumption has a narrow region of validity; namely, low initial temperatures and low equivalence ratios. As stated before, no conclusion can be drawn about the assumption itself. It is suggested that future work include the

incorporation of algebraic laws of mass action into the computer program to more precisely determine the validity of the assumption.

A.3.6 Comparison of the Four Systems

A.3.6.1 Temperature-Time Profiles

Figures 16-30 show a comparison of the 37(13) systems for the 15 cases marked with an asterisk in Table 4. The ignition mode of all 15 cases is that of the 37(13) system which continues in the combustion mode. The test systems start at the ignition point and reach an equilibrium temperature different from the 37(13) system.

The lag of the 8(7) system is shown in these figures. The lag is more a function of the relationship between the ignition temperature used and the classical ignition temperature than the initial temperature, pressure, or equivalence ratio. The 8(7) system reproduces the temperature-time curve very well, as expected.

The inital lag and eventual higher equilibrium temperature of the global model is shown in all 15 cases. Initial temperature has a substantial effect on the accuracy of the global mode. As the initial temperature increases, the temperature differences

between the global model and the 37(13) curves become large. These perhaps could be corrected by starting the global model at a different ignition temperature.

Partial equilibrium curves accurately reproduced the temperature-time curves for cases 2, 4, 9, 11, 15, 18, 20 and 31. This suggests that the partial equilibrium assumption might suffice at lower initial temperatures and equivalence ratios. The numerical difficulty in obtaining these results sheds uncertainty on this conclusion.

Figures 31 and 32 represent the results of using an ignition temperature higher than the classical one to cases 11 and 15, respectively. The 8(7) system is observed to lag behind the 37(13) system to a greater extent than usual. The global model, in fact, has an equilibrium temperature which is 200 degrees below normal. These figures reinforce the importance in the selection of initial conditions for any test system.

A.3.6.2 Computational Time

Results of the average computational times for the various systems are shown in Table 9. The global model has the lowest computational time as expected, with an average time

of approximatley 1/8 that of the 37(13) system. Excessive computational time of the partial equilibrium system was related to the relatively high reaction rate constants employed, the use of the Adams method rather than the Gear method, and the precision which was required to perform "partial equilibrium" calculations.

A.4. Conclusions and Recommendations

A.4.1 Summary

A data base, in the ranges of initial temperature between 850°K and 1200°K, pressure between 0.5 and 1.00 atmospheres and equivalence ratio between 0.5 and 1.5, was established with the 37(13) system serving as the basis. Due to the large amount of data produced, it is necessary to clarify these results. First, these results are summarized. Next, conclusions are enumerated. Finally, recommendations for future work are given.

The first part of the work was selecting a good trigger species. It was concluded that the hydroxyl radical, OH, serves as an effective trigger. The value of the mass fraction of OH at ignition can be estimated in the ranges studied within a factor of 2.5 (generally well within) according to equation 32.

Next the 8(7) system was studied in the "ignition" and "combustion" modes together and then in the "combustion" mode alone. It was concluded that a transition takes place between an initial temperature of 900°K and 1000°K (at a pressure of one atmosphere and an equivalence ratio of 0.5) where the ignition delay time of the 8(7) system switches from less than to

greater than the 37(13) system. It was further concluded that at an equivalence ratio of 0.5, pressure of 1.0 atmosphere and initial temperature of 970±30°K the 8(7) system can approximate the temperature-time profiles of the 37(13) system in both the ignition and combustion modes. It is recommended that future work include the investigation of conditions where the 8(7) system can describe the 37(13) system in both modes.

In the combustion mode alone, the 8(7) system reproduces the temperature-time profiles very well for all cases studied. The variables which were major factors in the accuracy of these profiles were the temperatures and species' concentrations used at ignition. If the temperature used was less than, but close to, the classical ignition temperature, then the profiles were very accurate. If, however, the temperature used was greater than the classical ignition temperatures, then the 8(7) system lagged behind the 37(13) system somewhat. Future work, should include the investigation of this phenomenon.

Next, the global model was studied in the combustion mode. Preexponential factors were determined with a rather large discrepancy between results for an equivalence ratio less than or greater than one. For all cases, the global model lags

behind the 37(13) system initially then exceeds it at equilibrium. Two variables had an effect on the accuracy of this model. First, the conditions used at ignition had a substantial effect on accuracy again. A lag was produced by using a temperature greater than the classical ignition temperature. Secondly, as the initial temperature increases the accuracy of the global model decreases.

Finally, an approximation to the "partial equilibrium" assumption was tried. Numerical difficulties arose in the execution of this approximation. Nonetheless, it was concluded that at low temperatures and low equivalence ratios the approach to approximating the partial equilibrium assumption is valid. No conclusions could be drawn about the "partial equilibrium" assumption itself.

Results for the various systems show the global model to have the lowest average computational time followed by the 8(7) system, the 37(13) system, and the "partial equilibrium" model. The two-step global model has a computational time of approximatley 1/8 that of the 37(13) system.

A.4.2 Conclusions

The following conclusions can be drawn based on the results of this study:

(1) The hydroxyl radical, OH, serves as an effective trigger species.

(2) A transition takes place between 900°K and 1000°K (at a pressure of 1 atmosphere and an equivalence ratio of 0.5) where the ignition delay time of the 8(7) system switches from less than to greater than the 37(13) system.

(3) At a pressure of one atmosphere, an equivalence ratio of 0.5 and an initial temperature of 970 ± 30°K the 8(7) system can accurately approximate the temperature-time profile of the 37(13) system in both the ignition and combustion modes.

(4) For all cases, the 8(7) system describes the 37(13) system very well in the combustion mode.

(5) A lag is produced in the 8(7) and global models when using ignition temperatures greater than the classical ignition temperature.

(6) The global model satisfactorily reproduces the temperature-time profiles of the 37(13) system with a minimum of computational time and computer storage requirements.

(7) As the initial temperature increases, the accuracy of the global model decreases.

(8) No conclusions can be drawn concerning the "partial equilibrium" assumption.

(9) The approach to approximating the "partial equilibrium" assumption has a narrow region of validity; namely, low initial temperatures and low equivalence ratios.

(10) The global model can approximate the 37(13) system with an average of 1/8 the computational time.

A.4.3 Recommendations

Based on the results of this study, the following recommendations are made for future work:

(1) Investigate conditions where the 8(7) system can accurately describe both the ignition and combustion processes.

(2) Study the effects of varying ignition conditions; namely, above and below the classicial ignition temperature. This will show the relationship between ignition conditions and the lag of the system.

(3) Continue to investigate the two-step global model as it seems to have the most promise in reproducing temperature-time profiles with a minimum of computational time.

(4) Incorporate the algebraic laws of mass action into the computer program to more precisely determine the validity of the "partial equilibrium" assumption.

Table 1 - 37(13) System

REACTION NUMBER								
1	M	+	1*O2	=	1*O	+	1*O	
2	M	+	1*H2	=	1*H	+	1*H	
3	M	+	1*H2O	=	1*H	+	1*OH	
4	1*H	+	1*O2	=	1*HO2	+	M	
5	M	+	1*NO2	=	1*NO	+	1*O	
6	M	+	1*NO	=	1*N	+	1*O	
7	M	+	1*H2O2	=	1*OH	+	1*OH	
8	M	+	1*O3	=	1*O2	+	1*O	
9	1*O	+	1*H	=	1*OH	+	M	
10	1*H2O	+	1*O	=	1*OH	+	1*OH	
11	1*H2	+	1*OH	=	1*H2O	+	1*H	
12	1*O2	+	1*H	=	1*OH	+	1*O	
13	1*H2	+	1*O	=	1*OH	+	1*H	
14	1*H2	+	1*O2	=	1*OH	+	1*OH	
15	1*H	+	1*HO2	=	1*H2	+	1*O2	
16	1*H2	+	1*O2	=	1*H2O	+	1*O	
17	1*H	+	1*HO2	=	1*OH	+	1*OH	
18	1*H2O	+	1*O	=	1*H	+	1*HO2	
19	1*O	+	1*HO2	=	1*OH	+	1*O2	
20	1*OH	+	1*HO2	=	1*O2	+	1*H2O	
21	1*H2	+	1*HO2	=	1*H2O	+	1*OH	
22	1*HO2	+	1*H2	=	1*H	+	1*H2O2	
23	1*H2O2	+	1*H	=	1*OH	+	1*H2O	
24	1*HO2	+	1*OH	=	1*O	+	1*H2O2	
25	1*HO2	+	1*H2O	=	1*OH	+	1*H2O2	
26	1*HO2	+	1*HO2	=	1*H2O2	+	1*O2	
27	1*O	+	1*O3	=	1*O2	+	1*O2	
28	1*O3	+	1*NO	=	1*NO2	+	1*O2	
29	1*O3	+	1*H	=	1*OH	+	1*O2	
30	1*O3	+	1*OH	=	1*O2	+	1*HO2	
31	1*O	+	1*N2	=	1*NO	+	1*N	
32	1*H	+	1*NO	=	1*OH	+	1*N	
33	1*O	+	1*NO	=	1*O2	+	1*N	
34	1*NO2	+	1*H	=	1*NO	+	1*OH	
35	1*NO2	+	1*O	=	1*NO	+	1*O2	
36	1*HO2	+	1*NO	=	1*2O	+	1*OH	
37	1*O3	+	1*HO2	=	2*O2	+	1*OH	

N_2 is an inert species

TABLE 2 - 8(7) SYSTEM

REACTION NUMBER	REACTION						
1	M	+	O2	=	O	+	O+M
2	M	+	H2	=	H	+	H+M
3	M	+	H2O	=	H	+	OH+M
4	M+O	+	H	=	OH	+	M
5	H2O	+	O	=	OH	+	H
6	H2	+	OH	=	H2O	+	H
7	O2	+	H	=	OH	+	O
8	H2	+	O	=	OH	+	H

N_2 is an inert species

TABLE 3 - 2 STEP GLOBAL MODEL

$$H2 + O2 \xrightarrow{k_{f4}} 2*OH \qquad (1)$$

$$2*OH + H2 \xrightarrow{k_{f5}} 2*H2O \qquad (2)$$

N_2 is an inert species

TABLE 4 - 45 CASES

CASES	ϕ	p, atm	T, K
1	0.5	0.5	850
* 2	0.5	0.75	850
! 3	0.5	1.0	850
* 4	0.5	0.5	900
5	0.5	0.75	900
! 6	0.5	1.0	900
7	0.5	0.5	1000
8	0.5	0.75	1000
!* 9	0.5	1.0	1000
10	0.5	0.5	1100
*11	0.5	0.75	1100
!12	0.5	1.0	1100
!13	0.5	0.5	1200
14	0.5	0.75	1200
*!15	0.5	1.0	1200
16	1.0	0.5	850
17	1.0	0.75	850
*18	1.0	1.0	850
19	1.0	0.5	900
*20	1.0	0.75	900
21	1.0	1.0	900
!22	1.0	0.5	1000
*23	1.0	0.75	1000
24	1.0	1.0	1000
•!25	1.0	0.5	1100
26	1.0	0.75	1100
27	1.0	1.0	1100
*28	1.0	0.5	1200
!29	1.0	0.75	1200
30	1.0	1.0	1200
*31	1.5	0.5	850
32	1.5	0.75	850
33	1.5	1.0	850
34	1.5	0.5	900
35	1.5	0.75	900
*36	1.5	1.0	900
37	1.5	0.5	1000

TABLE 4 (Cont.)

CASES	ϕ	p, atm	T, K
38	1.5	0.75	1000
*39	1.5	1.0	1000
40	1.5	0.5	1100
*41	1.5	0.75	1100
42	1.5	1.0	1100
*43	1.5	0.5	1200
44	1.5	0.75	1200
45	1.5	1.0	1200

TABLE 5 - 37(13) DATA

CASE	T_{ig}	τ_{ig}	$Y_{OH,ig}$
2	918	0.48E0	0.66E-4
4	961	0.80E-3	0.10E-3
5	960	0.13E-2	0.13E-3
6	974	0.11E-1	0.16E-3
7	1045	0.21E-3	0.51E-3
8	1063	0.15E-3	0.60E-3
9	1024	0.12E-3	0.15E-3
-11	1160	0.69E-4	0.90E-3
13	1260	0.60E-4	0.34E-2
15	1260	0.29E-4	0.22E-2
18	935	0.46E0	0.19E-3
19	970	0.76E-3	0.40E-3
20	985	0.12E-2	0.19E-3
21	966	0.48E-2	0.10E-3
22	1027	0.20E-3	0.20E-3
23	1012	0.14E-3	0.11E-3
24	1039	0.12E-3	0.19E-3
25	1170	0.10E-3	0.16E-3
26	1117	0.60E-4	0.27E-3
27	1170	0.45E-4	0.90E-3
28	1275	0.55E-4	0.30E-2
29	1275	0.38E-4	0.30E-2
30	1270	0.36E-4	0.30E-2
31	926	0.11E-1	0.80E-4
32	892	0.27E0	0.17E-4
34	934	0.80E-3	0.57E-4
35	968	0.11E-2	0.11E-3
36	954	0.35E-2	0.61E-4
37	1012	0.20E-3	0.67E-4
38	1024	0.15E-3	0.11E-3
39	1062	0.13E-3	0.28E-3
40	1160	0.10E-3	0.91E-3
41	1163	0.70E-4	0.91E-3
42	1160	0.45E-4	0.90E-3
43	1275	0.59E-4	0.17E-2
45	1303	0.30E-4	0.29E-2

TABLE 6 - TRIGGER SPECIES vs. TIME

TIME	Y_{OH}
0	0
0.1E-5	0.68E-9
0.2E-4	0.38E-8
0.3E-4	0.81E-8
0.4E-4	0.17E-7
0.6E-4	0.75E-7
0.7E-4	0.16E-6
0.8E-4	0.35E-6
0.9E-4	0.82E-6
0.1E-3	0.21E-5
0.12E-3	0.15E-4
*0.14E-3	0.11E-3
0.2E-3	0.15E-1
0.3E-3	0.19E-1
0.4E-3	0.19E-1
0.5E-3	0.18E-1
0.8E-3	0.17E-1

* ignition point

TABLE 7

COMPARISON OF IGNITION TIMES FOR 37(13) AND 8(7) SYSTEMS

T_o	37(13) τ_{ig} (sec)	8(7) τ_{ig} (sec)
850	6.7×10^{-1}	1.1×10^{-3}
900	1.1×10^{-2}	6.6×10^{-4}
1000	1.3×10^{-4}	2.6×10^{-4}
1100	0.5×10^{-4}	1.5×10^{-4}
1200	0.3×10^{-4}	0.7×10^{-4}

TABLE 8

PREEXPONENTIAL FACTORS FOR GLOBAL MODEL

CASE	A_4	A_5
2	3.8E48	4.1E65
4	3.8E48	4.4E65
9	3.8E48	2.3E65
11	3.8E48	2.3E65
15	3.8E48	1.1E65
18	1.2E48	5.5E64
20	1.2E48	9.0E64
23	1.2E48	6.0E64
25	1.2E48	9.0E64
28	1.2E48	8.0E64
31	5.0E47	6.3E64
36	5.0E47	3.7E64
39	5.0E47	4.0E64
41	5.0E47	4.6E64
43	5.0E47	5.1E64

TABLE 9

COMPARISON OF COMPUTATIONAL TIMES

SYSTEM	AVERAGE COMPUTIONAL TIME (seconds)
37(13)	87.5
8.(7)	12.3
Global	11.4
Partial	1258

REFERENCES
FOR APPENDIX A

1) Chinitz, W., Personal Communication, Cooper Union, New York, Apr., 1983.

2) Rogers, R.C., and Schexnayder, C.J., Jr., "Chemical Kinetic Analysis of Hydrogen-Air and Reaction Times", NASA TP-1856, July, 1981.

3) Guy, Robert W., and Mackley, Ernest A., "Initial Wind Tunnel Tests at Mach 4 and 7 of a Hydrogen-Burning, Airframe-Integrated Scramjet," NASA paper presented at the 4th International symposium on Air Breathing Engines (Lake Buena Vista, Fla.), Apr. 1-6, 1979.

4) Bittker, David A., and Scullio, Vincent J., "General Chemical Kinetics Computer Program for Static and Flow Reactions, with application to Combustion and Shock-Tube Kinetics," Nasa TN D-6586, 1972.

5) McLain, Allen G., and Rao, C.S.R., "A Hybrid Computer Program for Rapidly Solving Flowing or Static Chemical Kinetic Problems Involving Many Chemical Species," NASA TM X-3403, 1976.

6) Yee, Barbara, "The Chemical Kinetic Modeling of Silane-Hydrogen-Air Reactions", M.E. Thesis, Cooper Union, School of Engineering, April, 1982.

7) Hindmarsh, A.C., "Gear: Ordinary Differential Equation System Solveer," UCID-30001, Rev.1, Computer Documentation, Lawrence Livermore Lab, Univ. California, Aug. 20, 1972.

8) Gear, C. William, "Numerical Value Problems in Ordinary Differential Equations", Prentice-Hall, Inc., C. 1971.

9) Chinitz, W., "Simplifying Chemical Kinetic Analyses of Reacting Flows Using an Ignition-Combustion Model, "Report Submited to the Hypersonic Propulsion branch (HSAD), NASA LaRC, August, 1979.

10) Evans, J.S., and Schexnayder, C.J., Jr., "Influence of Chemical Kinetics and Unmixedness on Burning in Supersonic Hydrogen Flames", AIAA J., 21, 4, April, 1983, pp. 586-592.

11) Rogers, R.C., and Chinitz, W., "Using a Global Hydrogen-Air Combustion Model in Turbulen Reacting Flow Calculations", AIAA J. 21, 4, April, 1983, pp. 586-592.

12) Chinitz, W., "The Application of the Partial Equilibrium Assumption to Non-Equilibrium Analyses of Reacting Flows," Hypersonic Propulsion Branch NASALangley Research Center, July-Aug., 1980.

13) Baumeister et. al., "Mark's Standard Handbook for Mechanical Engineers," McGraw-Hill Eighth Ed., 1978.

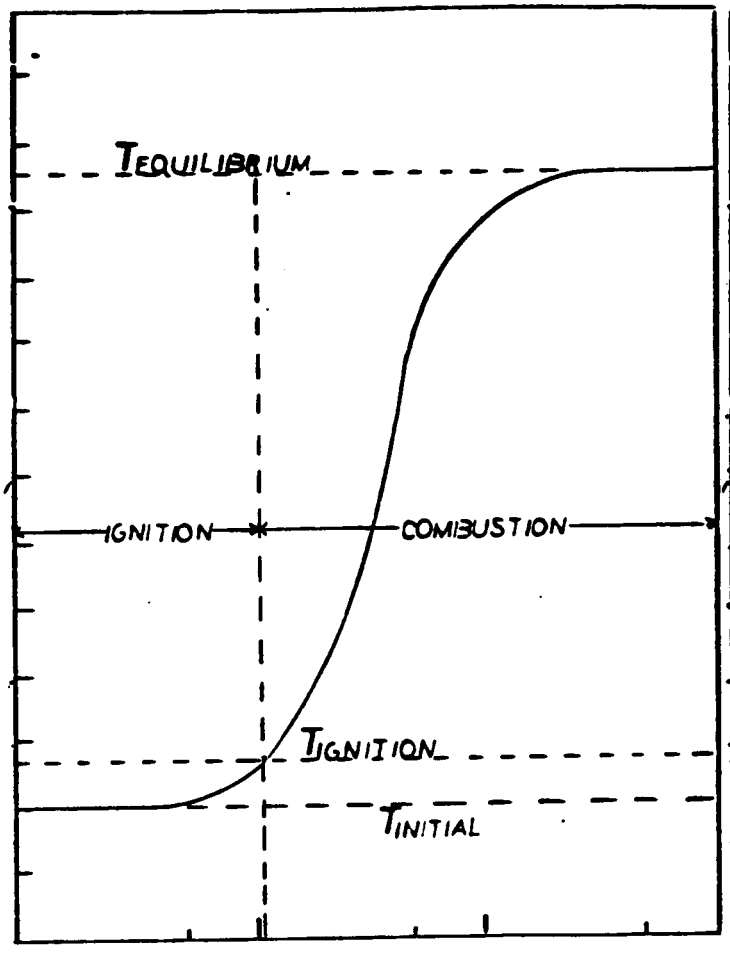

FIGURE 2 DEFINING IGNITION AND COMBUSTION

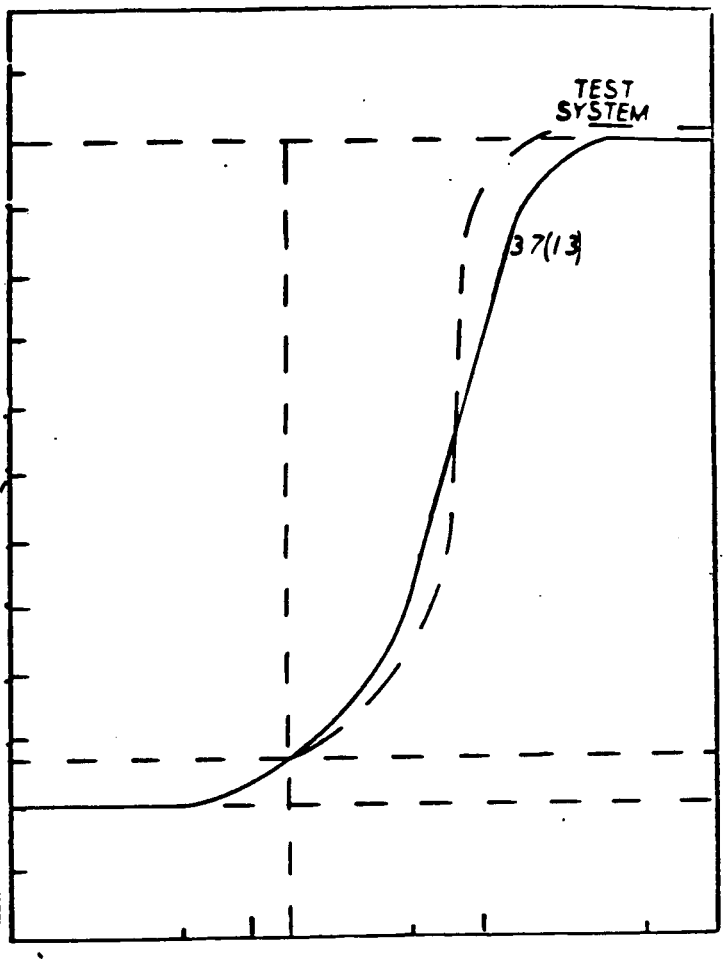

FIGURE 3 COMPARISON OF TEMPERATURE - TIME PROFILES FOR 37(13) AND TEST SYSTEMS

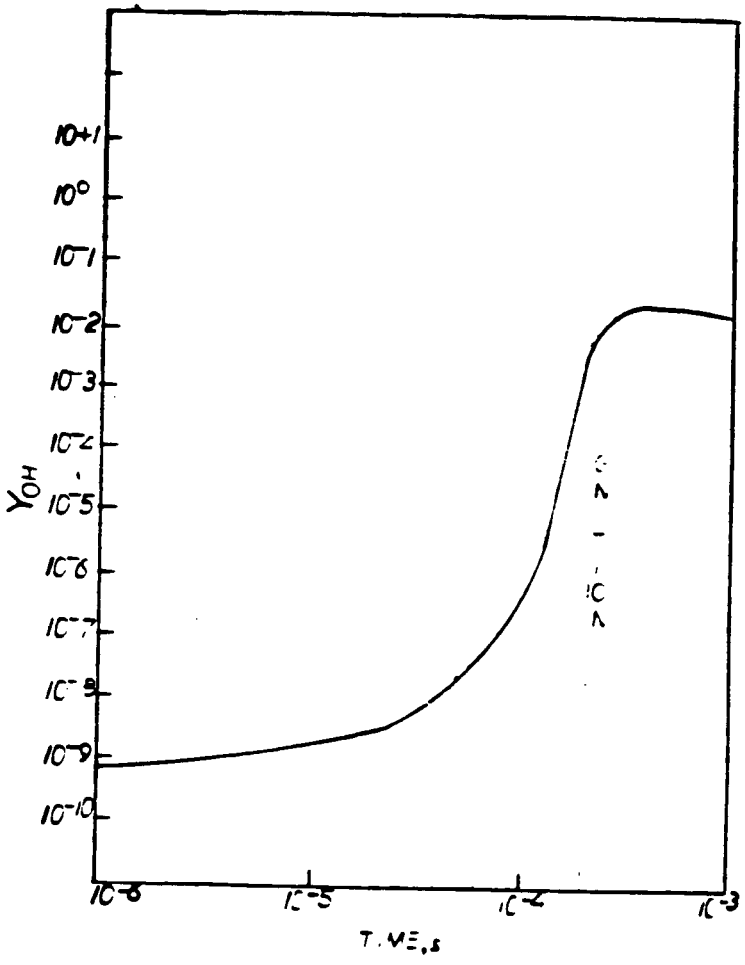

FIGURE 4 MASS FRACTION OH VS TIME

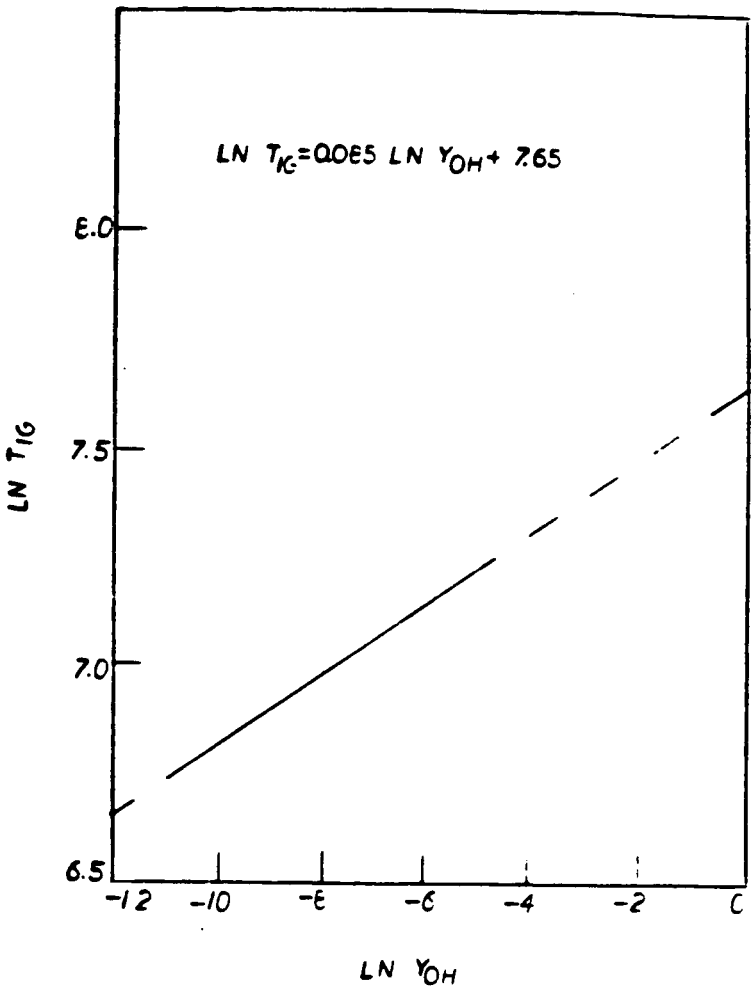

FIGURE 5 IGNITION TEMPERATURE VS. MASS FRACTION OH

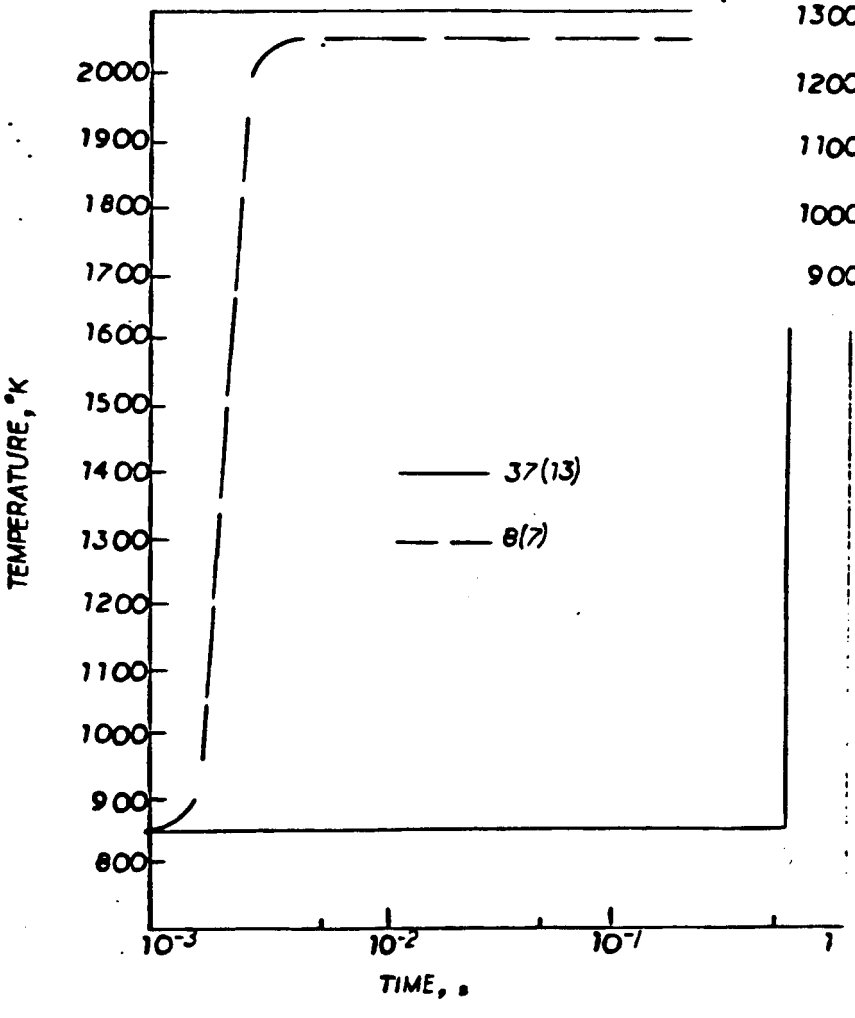

FIGURE 6 $\phi = 0.5, P = 1.0, T_0 = 850$

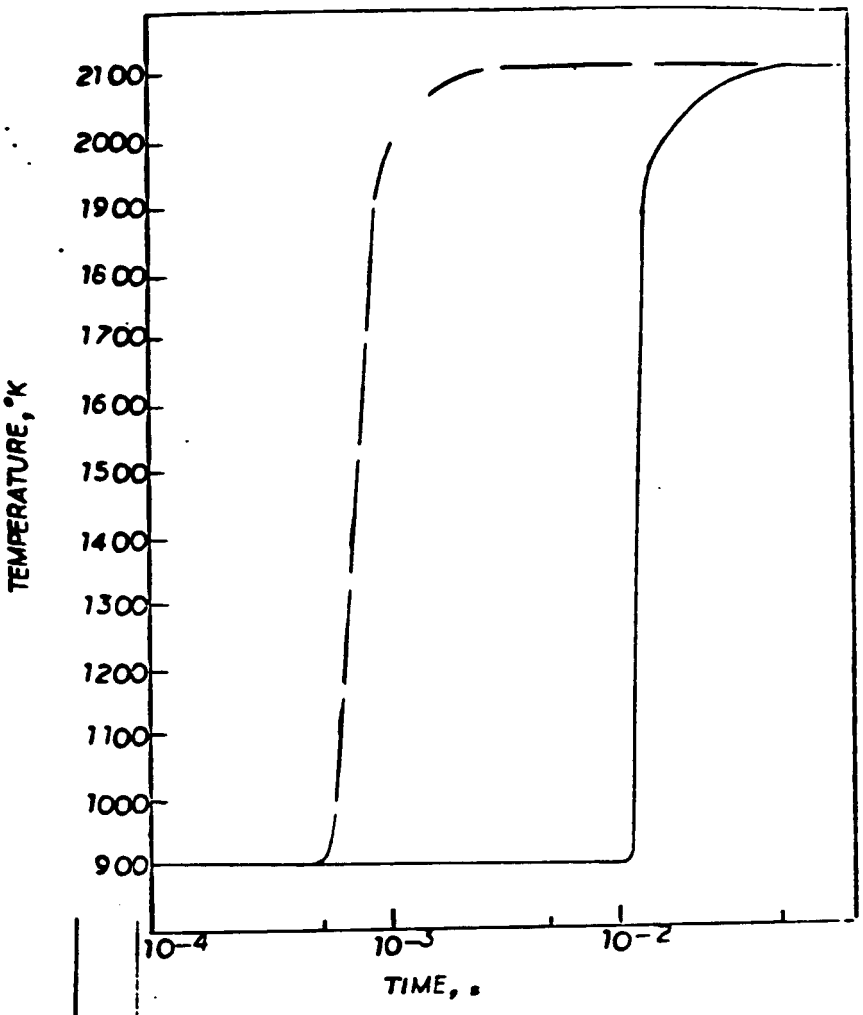

FIGURE 7 $\phi = 0.5, P = 1.0, T_0 = 900$

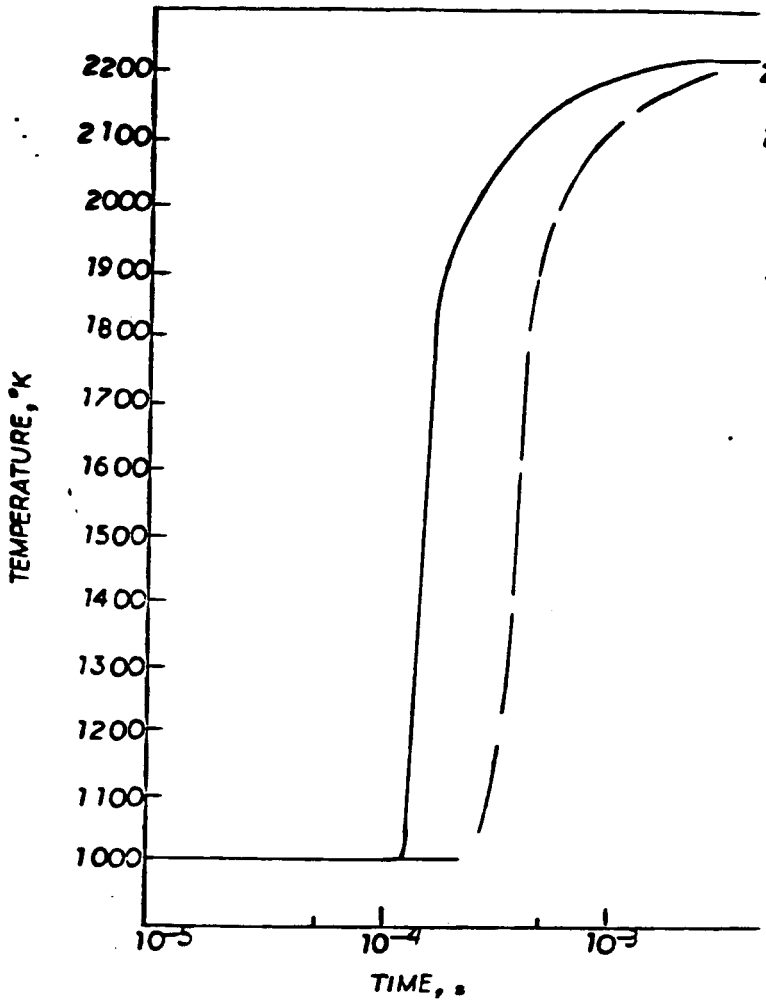

FIGURE 8 $\phi = 0.5, P = 1.0, T_0 = 1000$

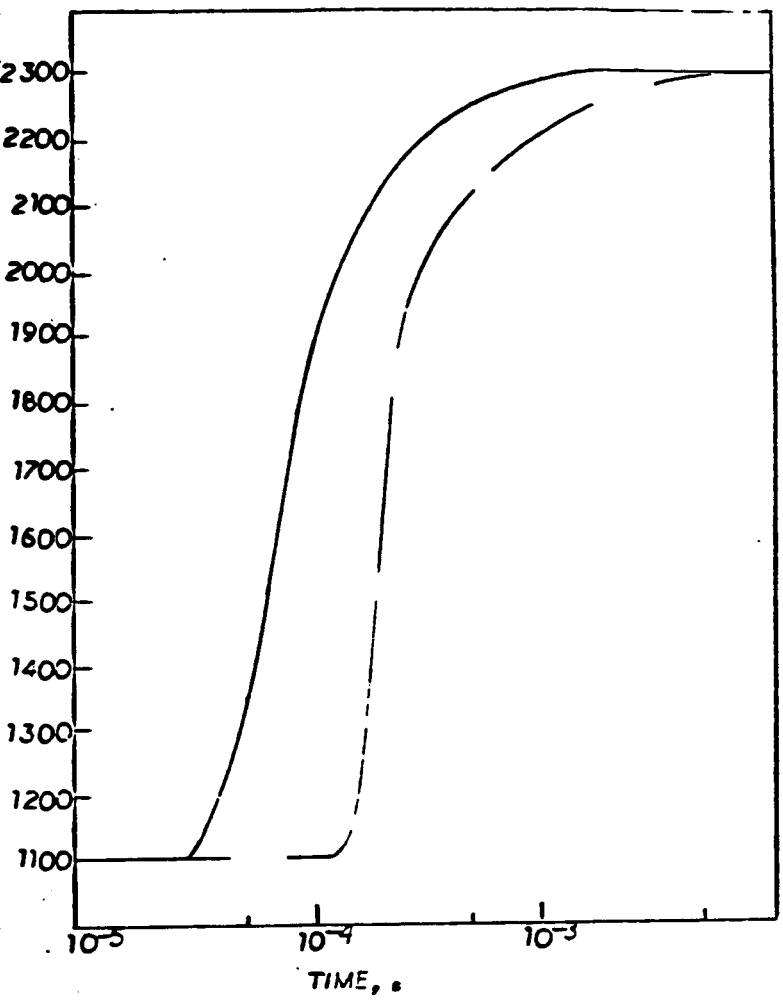

FIGURE 9 $\phi = 0.5, P = 1.0, T_0 = 1100$

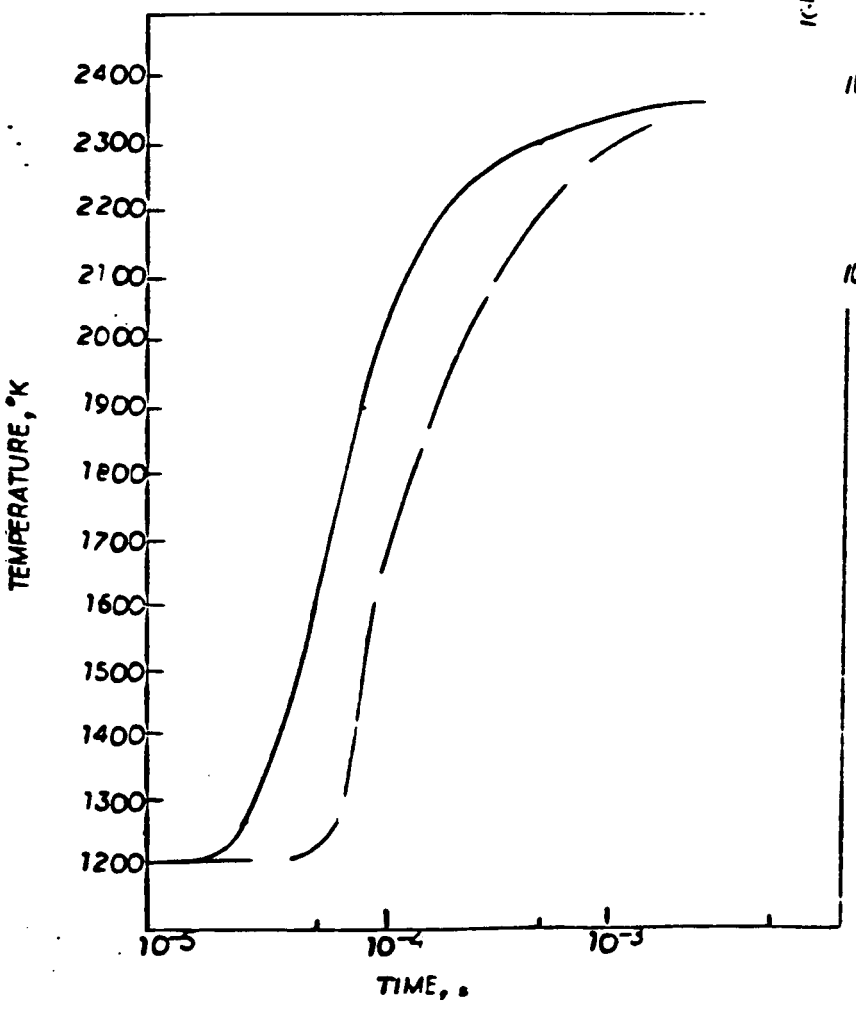

FIGURE 10 $\phi = 0.5, P = 1.0, T_0 = 1200$

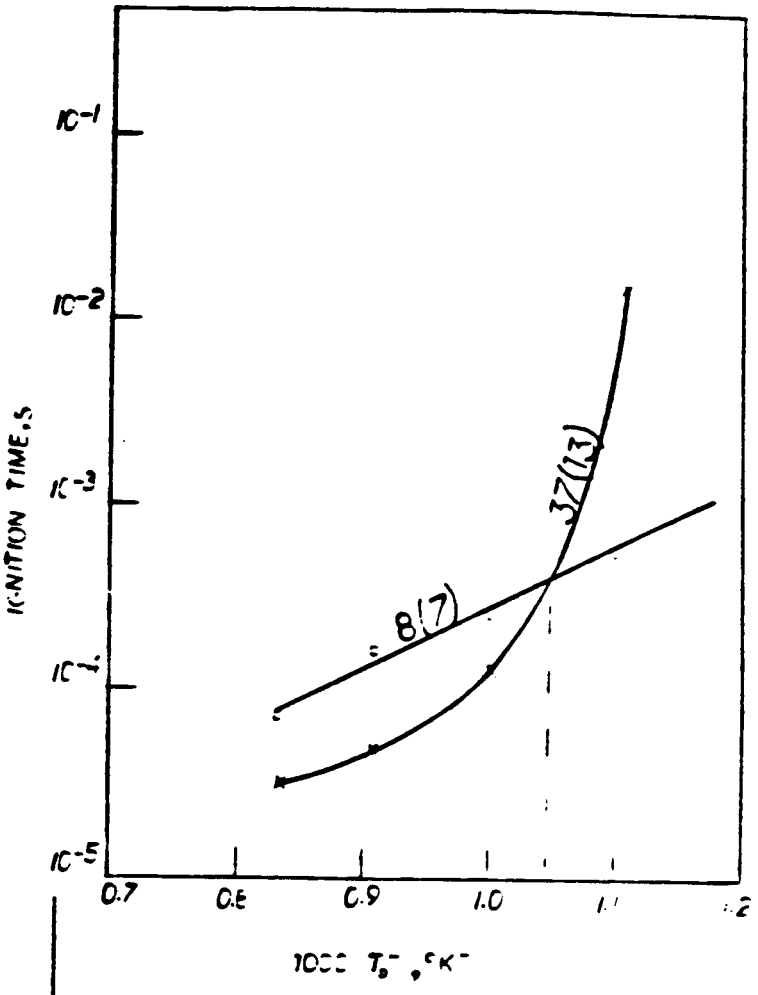

FIGURE 11 IGNITION TIME VS 1000 T_0^{-1}

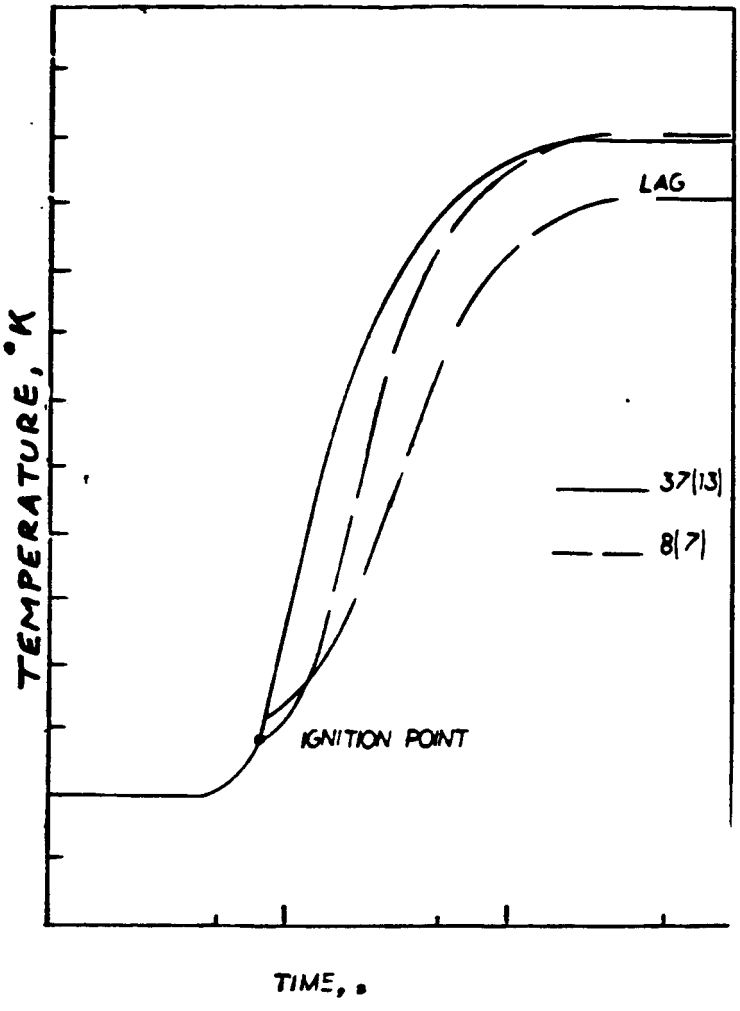

FIGURE 12 COMPARISON OF 37[13] AND 8[7] SYSTEMS IN COMBUSTION MODE

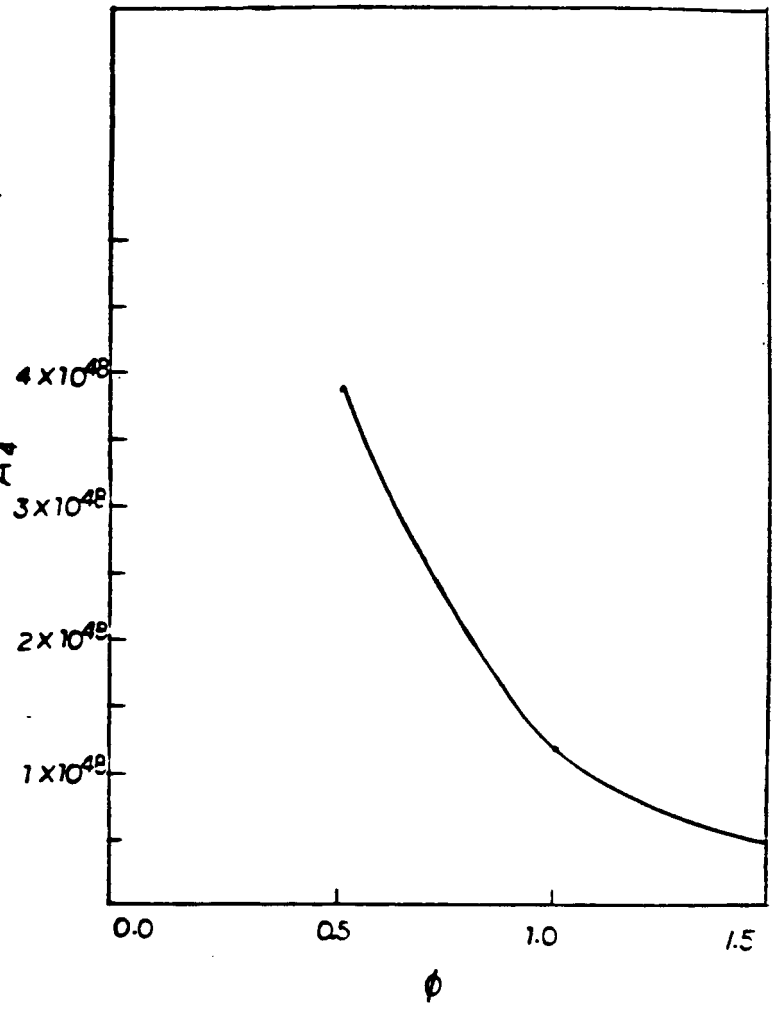

FIGURE 13 A_4 VERSUS ϕ

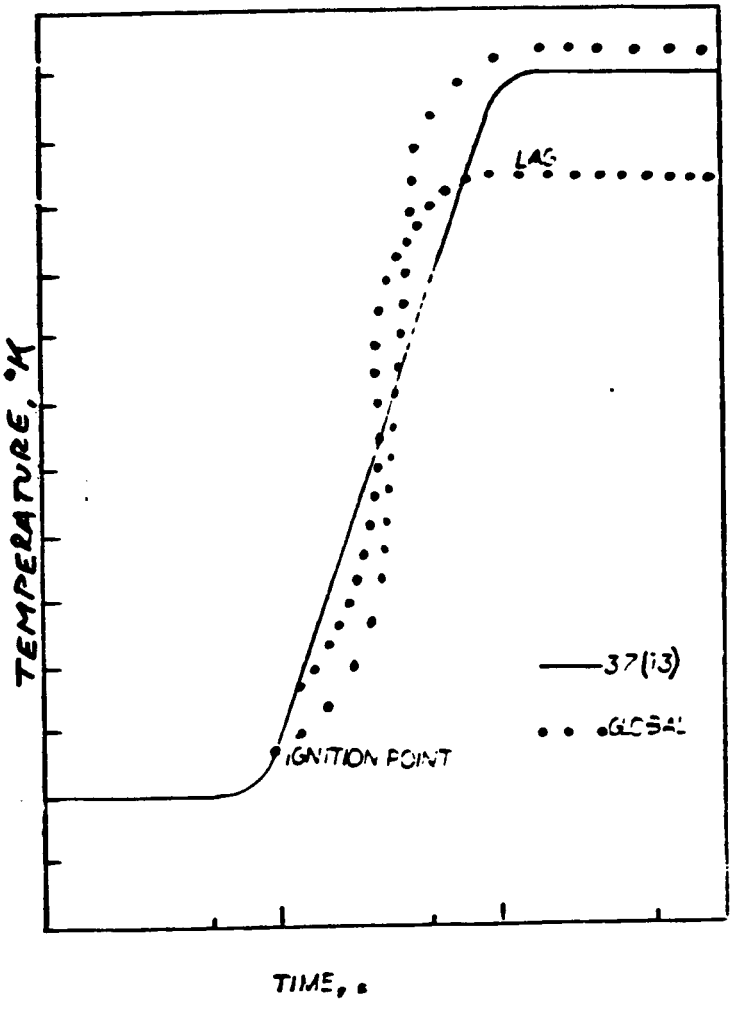

FIGURE 15 COMPARISON OF 37 [13] AND GLOBAL SYSTEMS IN COMBUSTION MODE

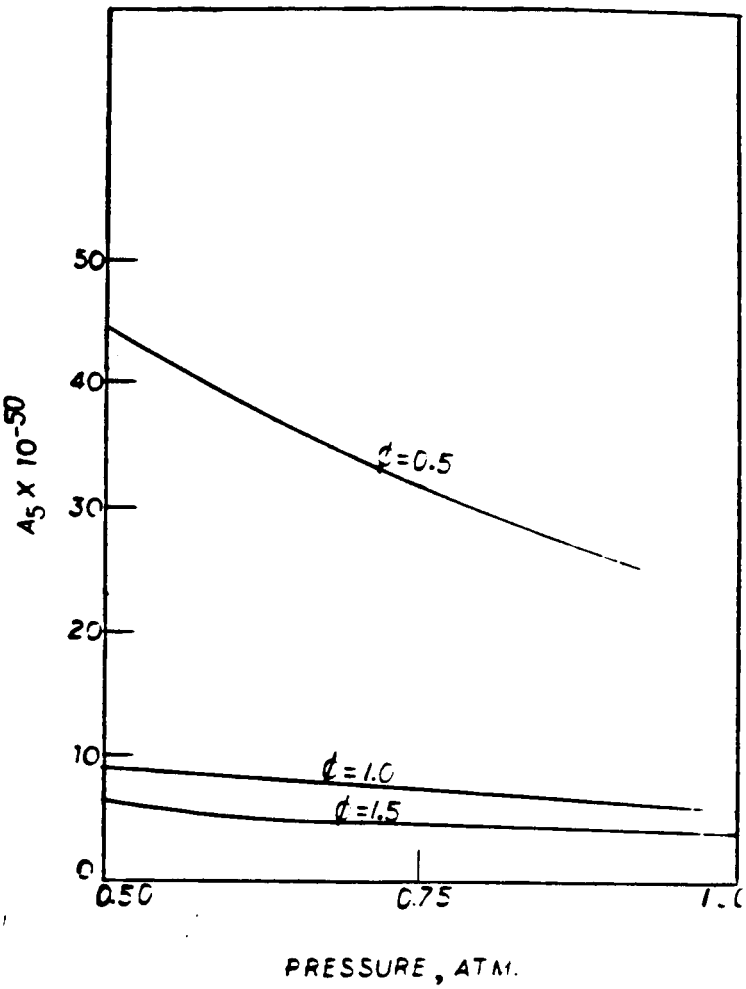

FIGURE 14 A_5 VS. P FOR VARIOUS ϕ'S

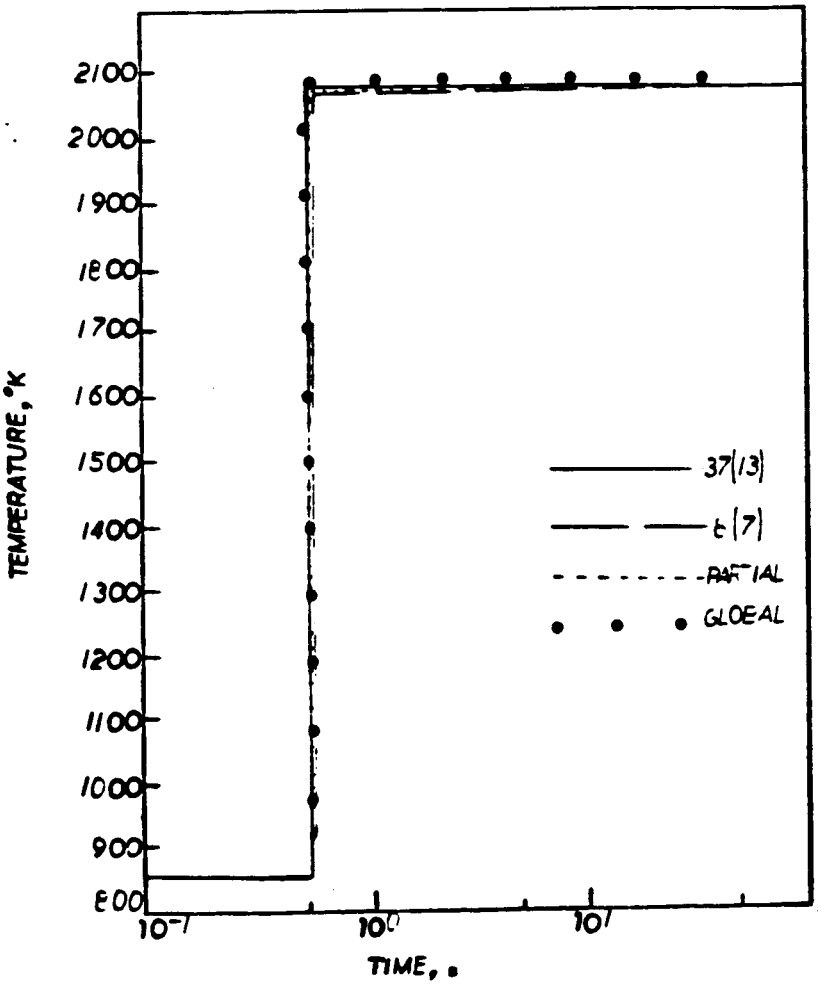

FIGURE 16 $\phi = 0.5, P = 0.75, T_0 = 850$

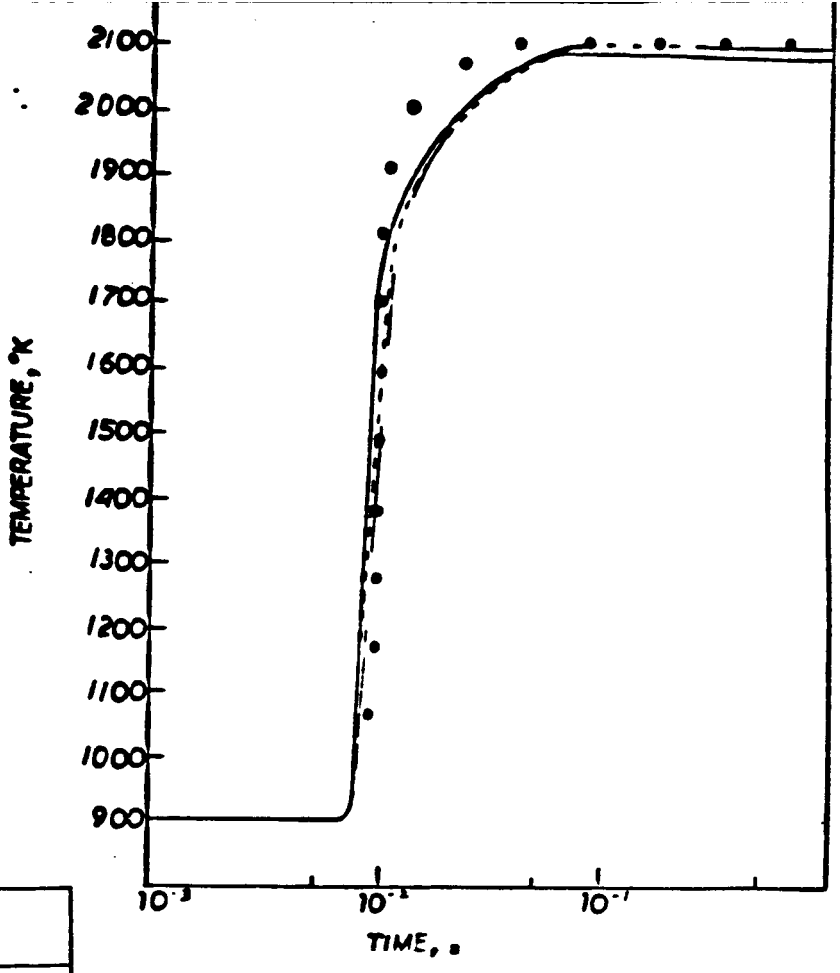

FIGURE 17 $\phi = 0.5, P = 0.50, T_c = 900$

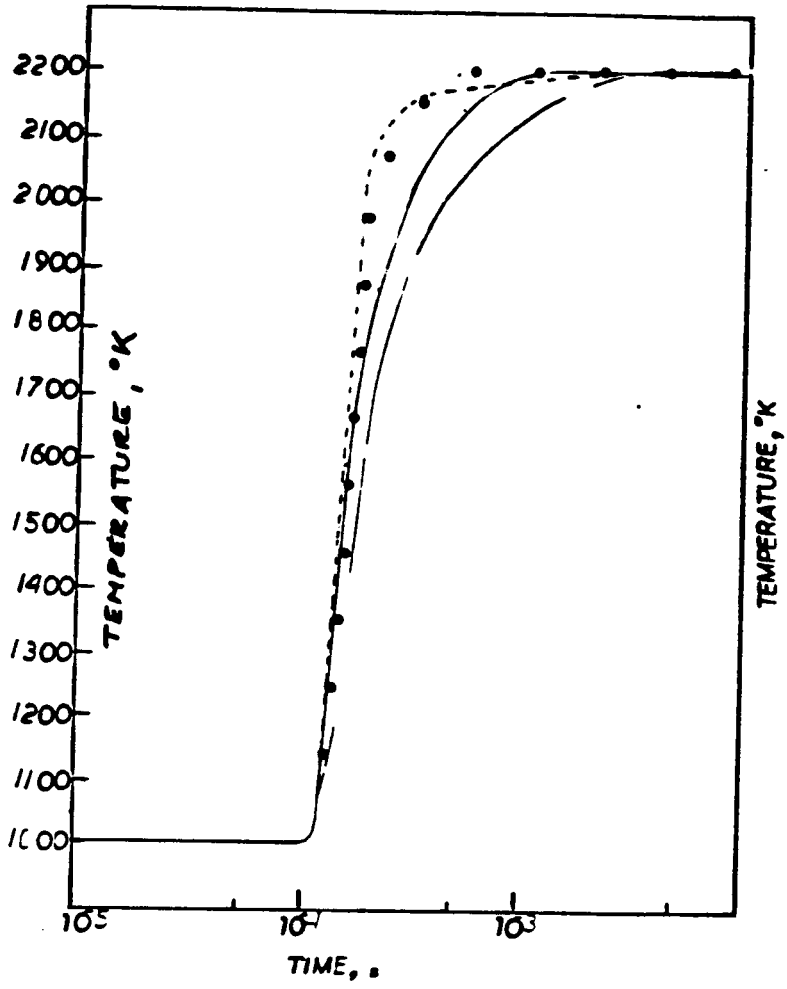

FIGURE 18 $\phi = 0.5$, $P = 1.00$, $T_0 = 1000$

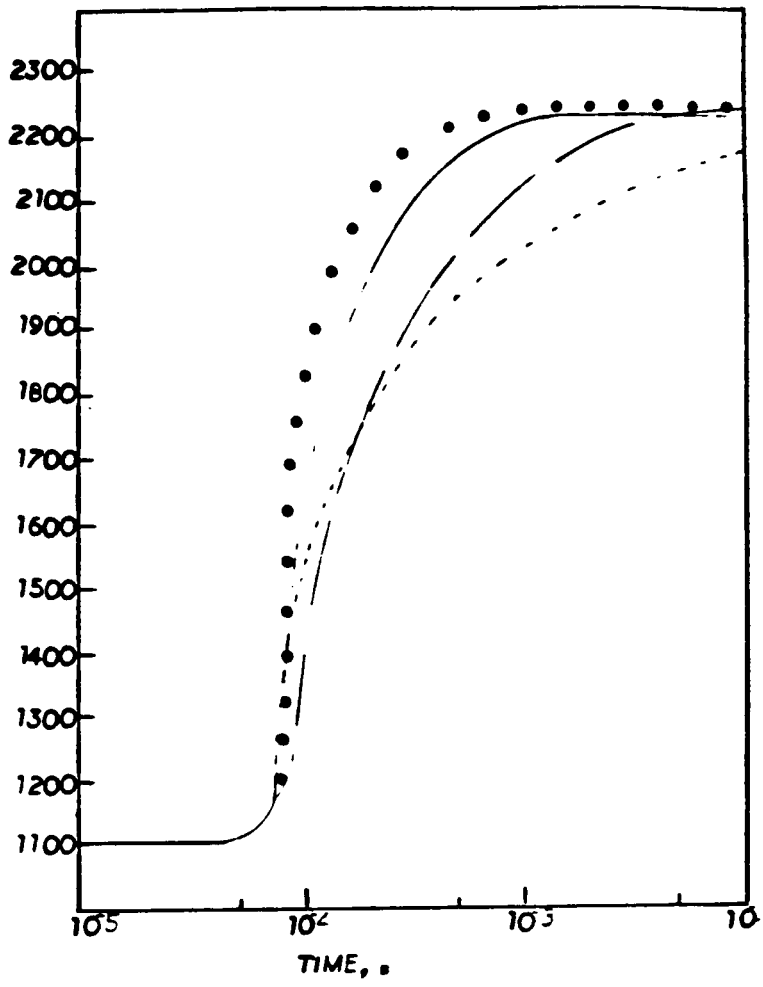

FIGURE 19 $\phi = 0.5$, $P = 0.75$, $T_c = 1100$

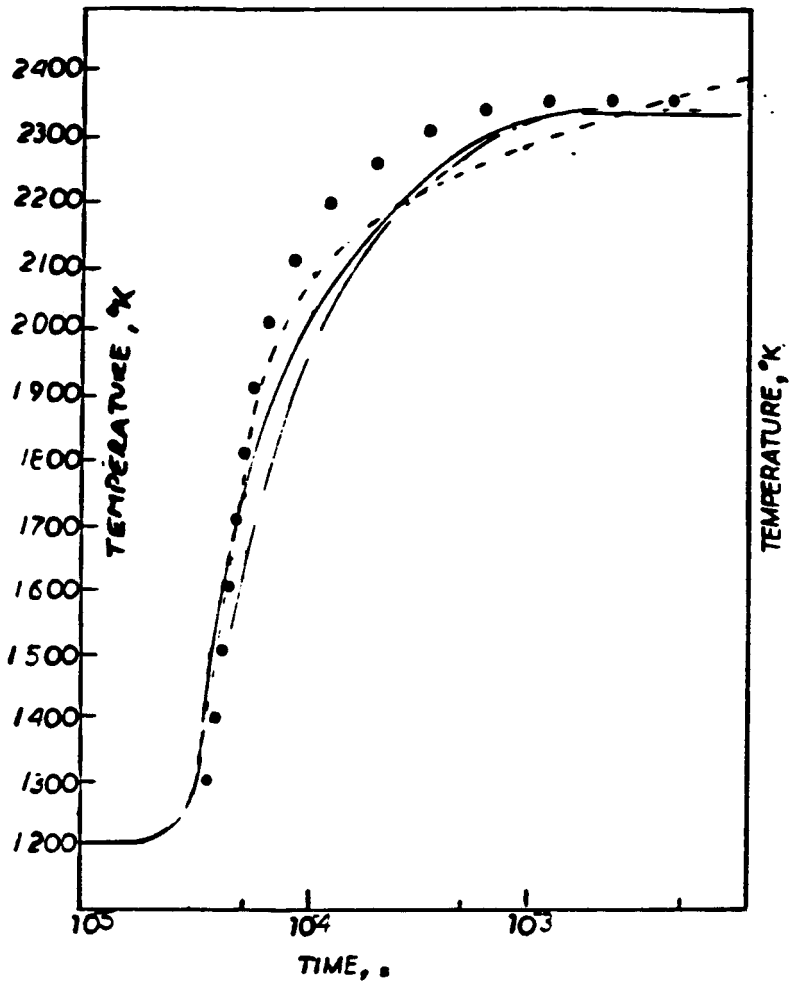

FIGURE 20 ϕ=0.5, P=1.00, T_c=1200

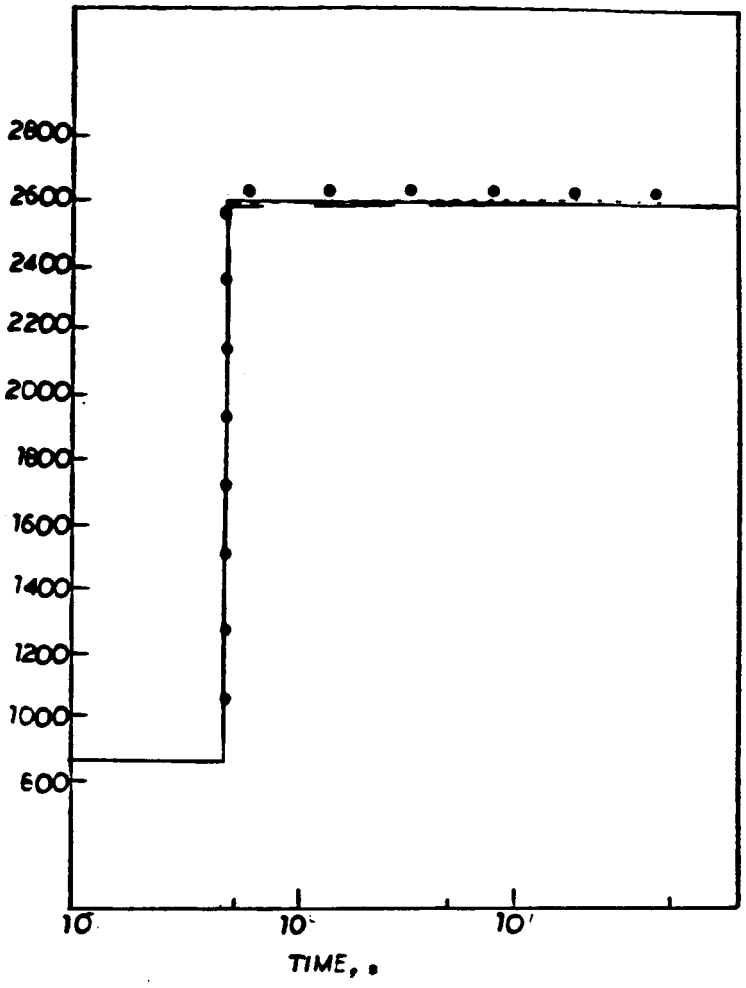

FIGURE 21 ϕ=1.0, P=1.00, T_c=850

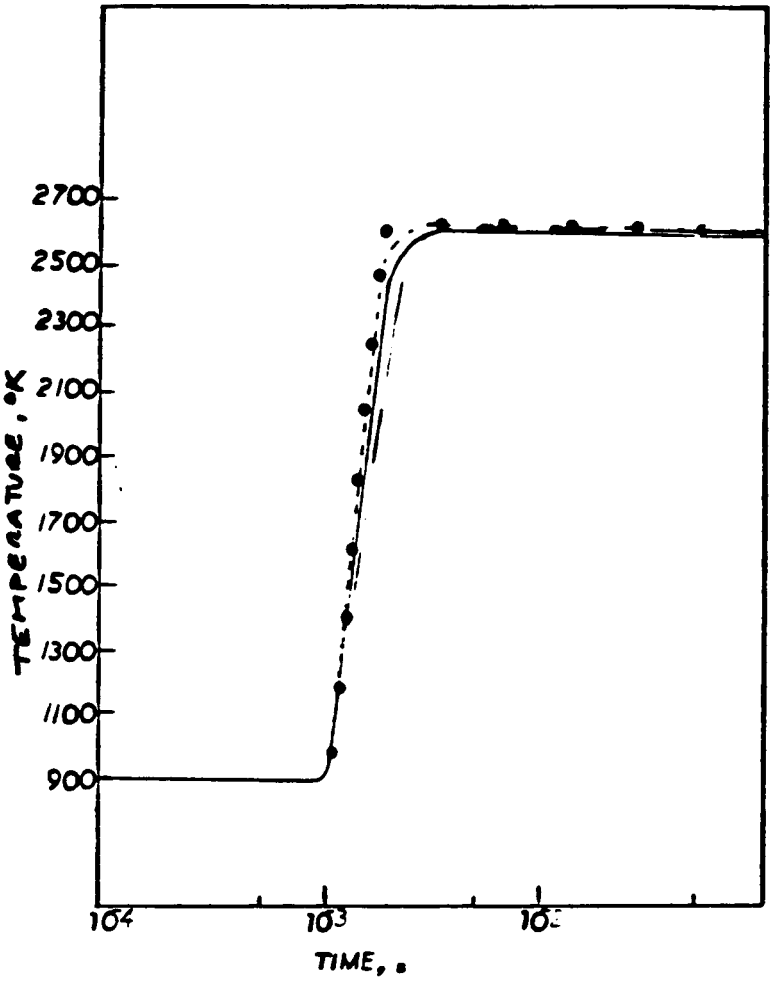

FIGURE 22 $\phi = 1.0, P = 0.75, T_c = 500$

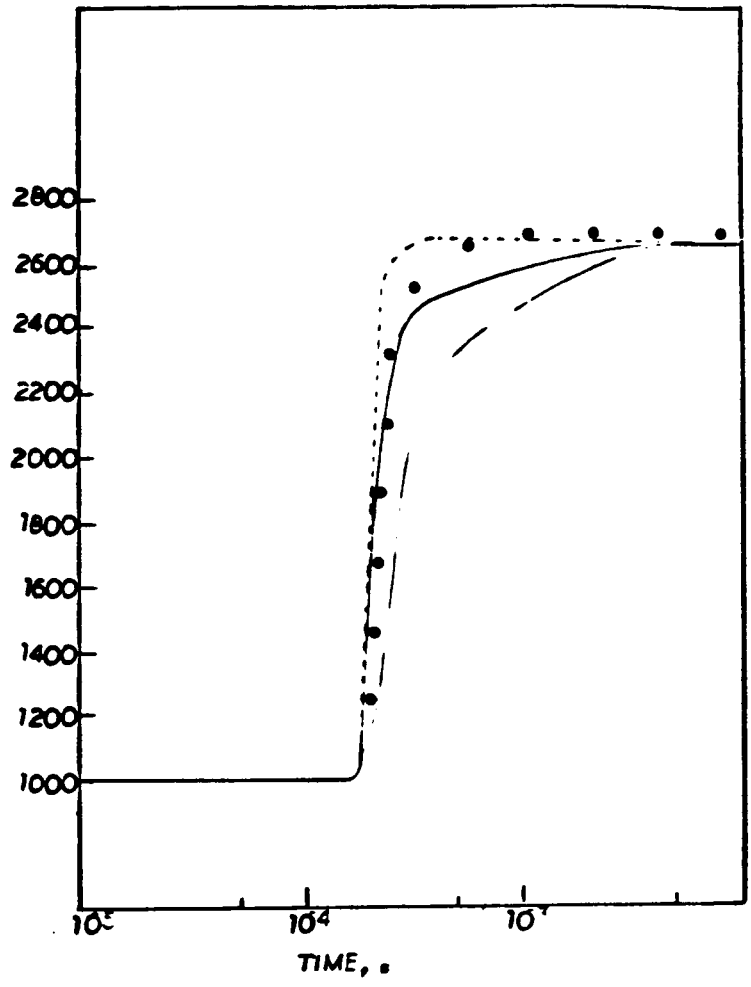

FIGURE 23 $\phi = 1.0, P = 0.75, T_c = 1000$

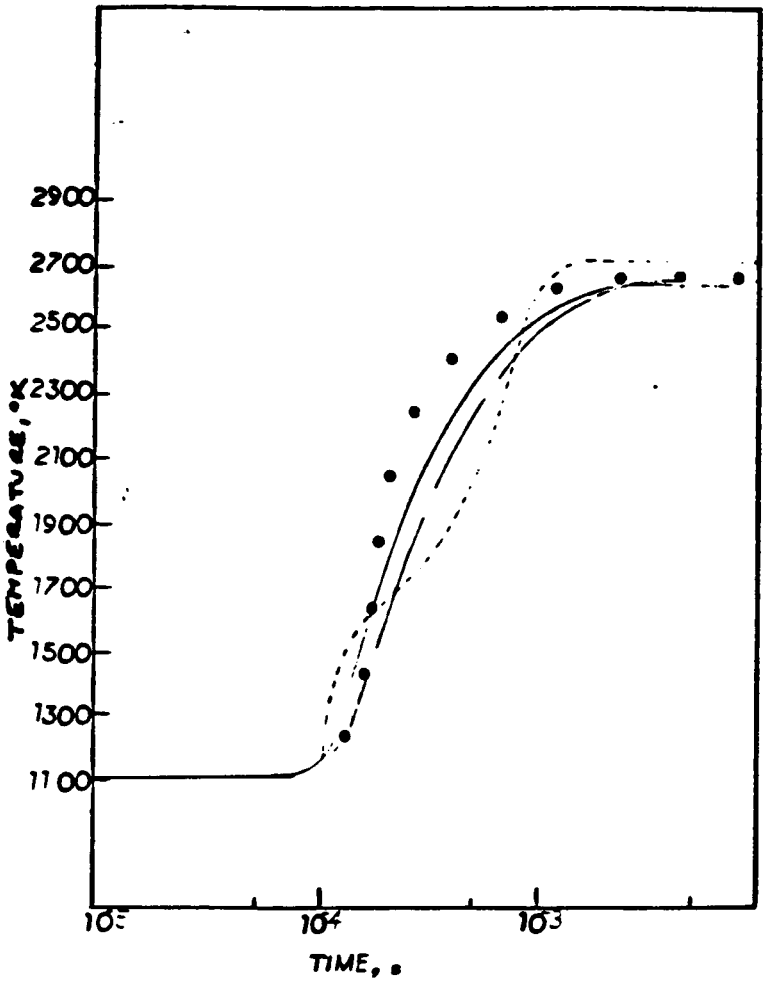

FIGUPE 24 ϕ=1.0, P=0.50, T_c = 1100

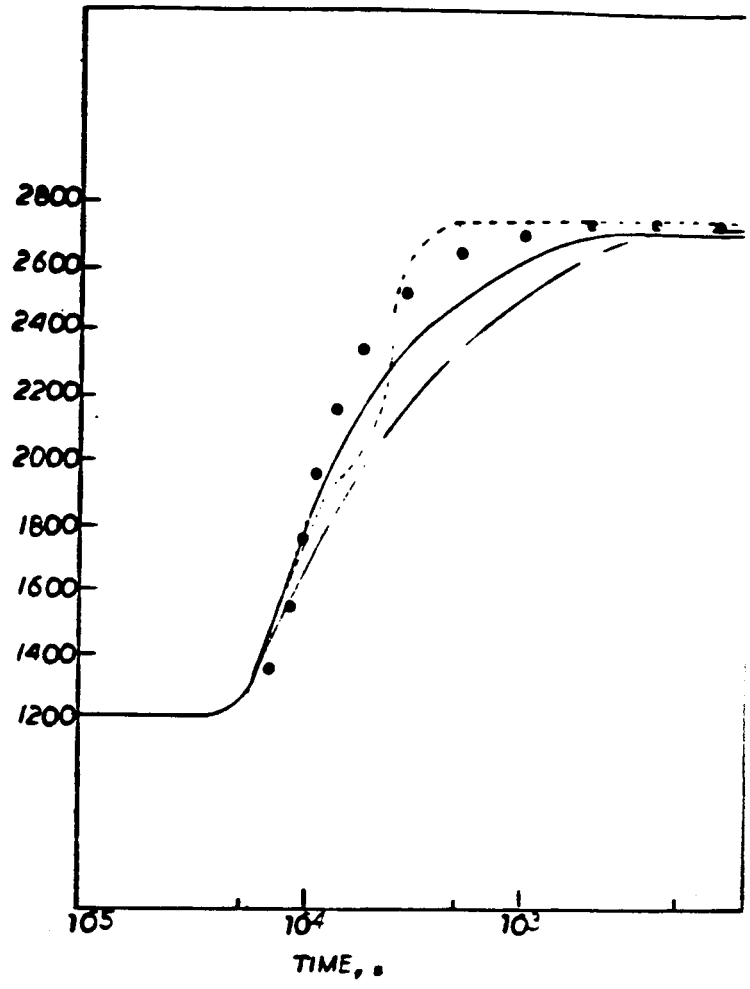

FIGURE 25 ϕ = 1.0, P=0.50, T_c = 1200

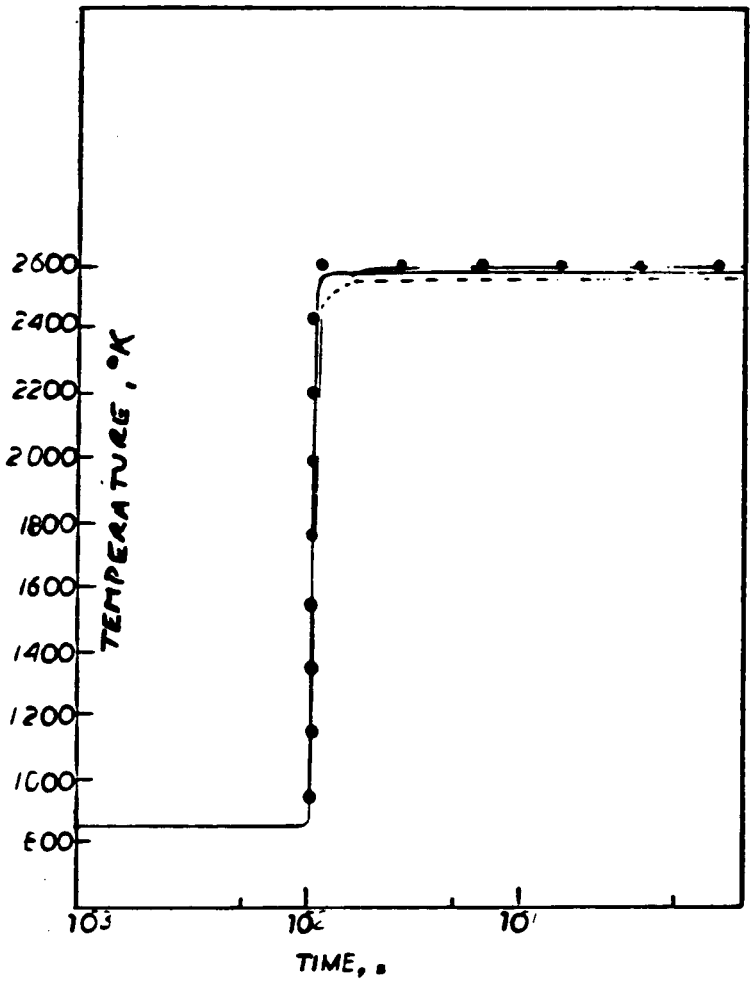

FIGURE 26 $\phi = 1.5$, $P = 0.50$, $T_c = 850$

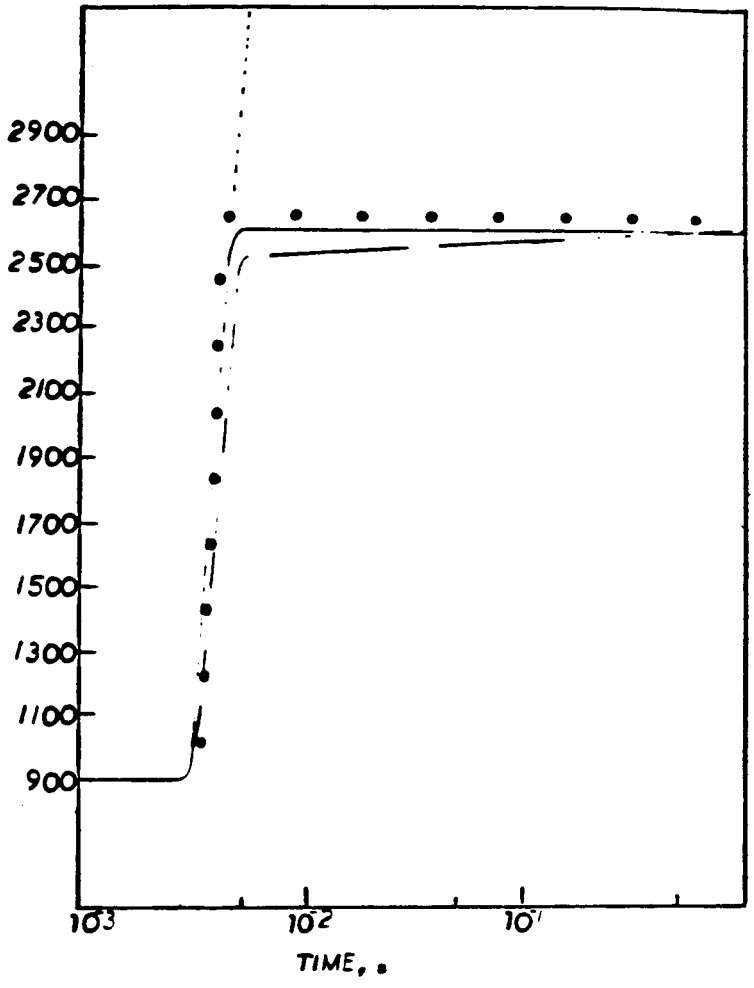

FIGURE 27 $\phi = 1.5$, $P = 1.00$, $T_c = 900$

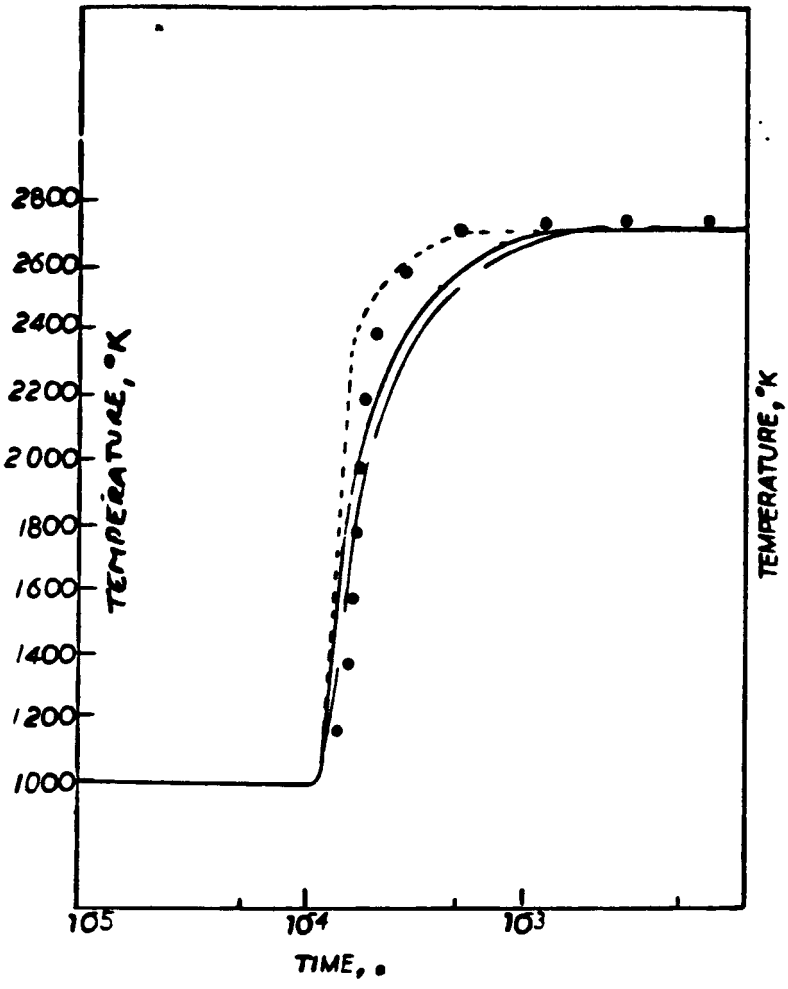

FIGURE 28 $\phi = 1.5, P = 1.0, T_0 = 1000$

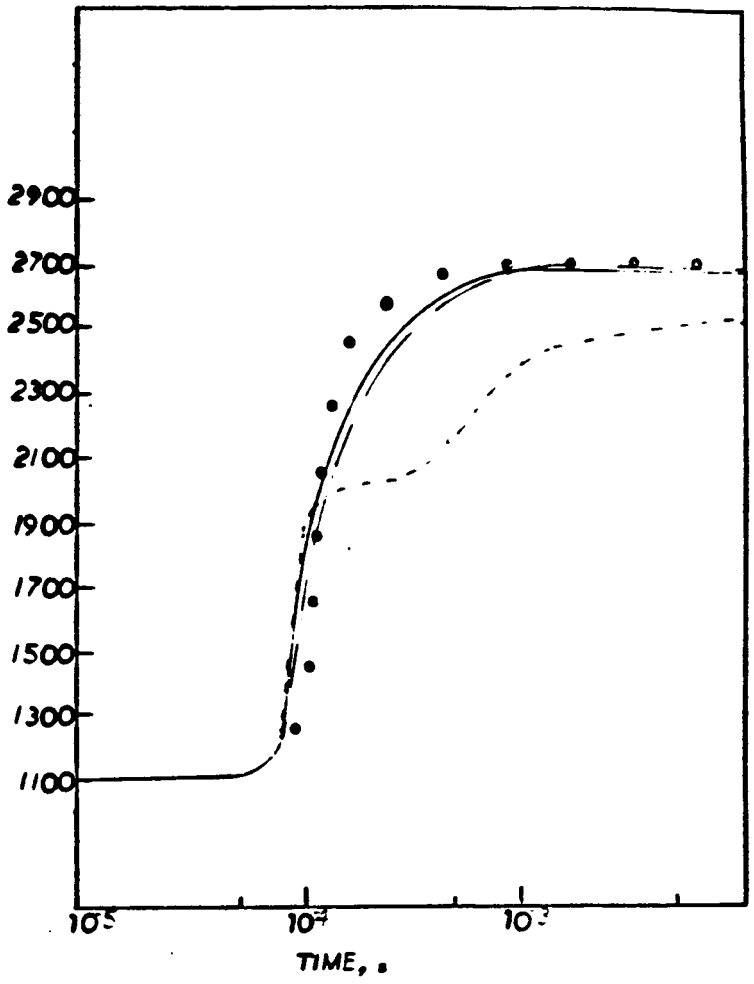

FIGURE 29 $\phi = 1.5, F = 0.75, T_c = 1100$

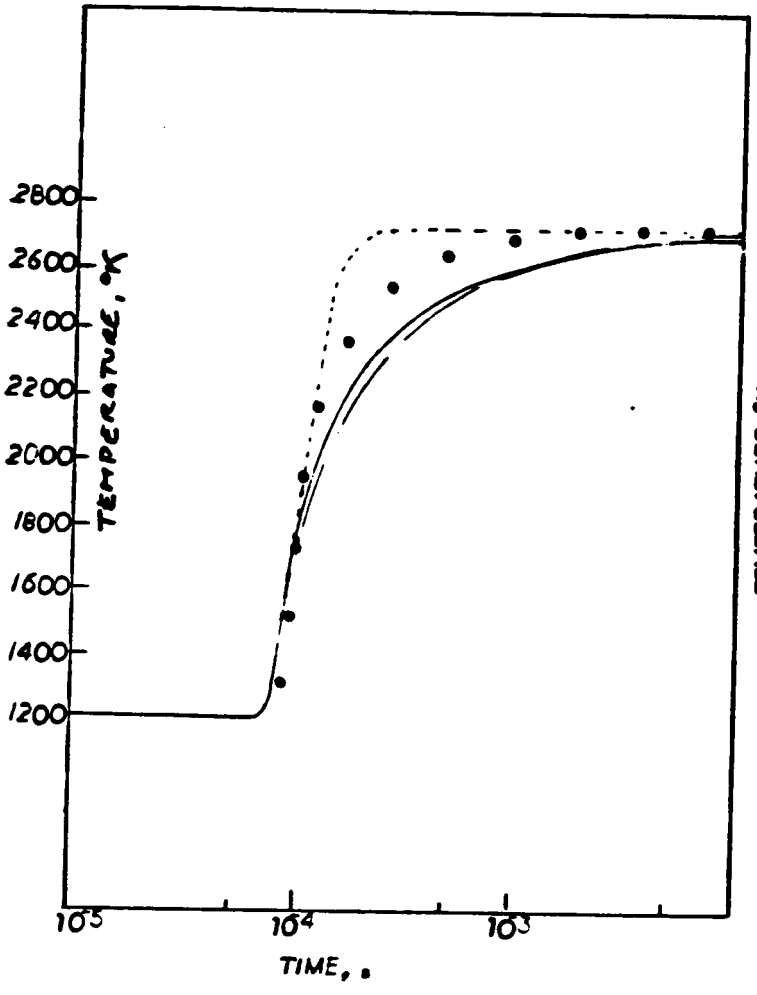

FIGURE 30 ϕ=1.5, P=0.50, T_c=1200

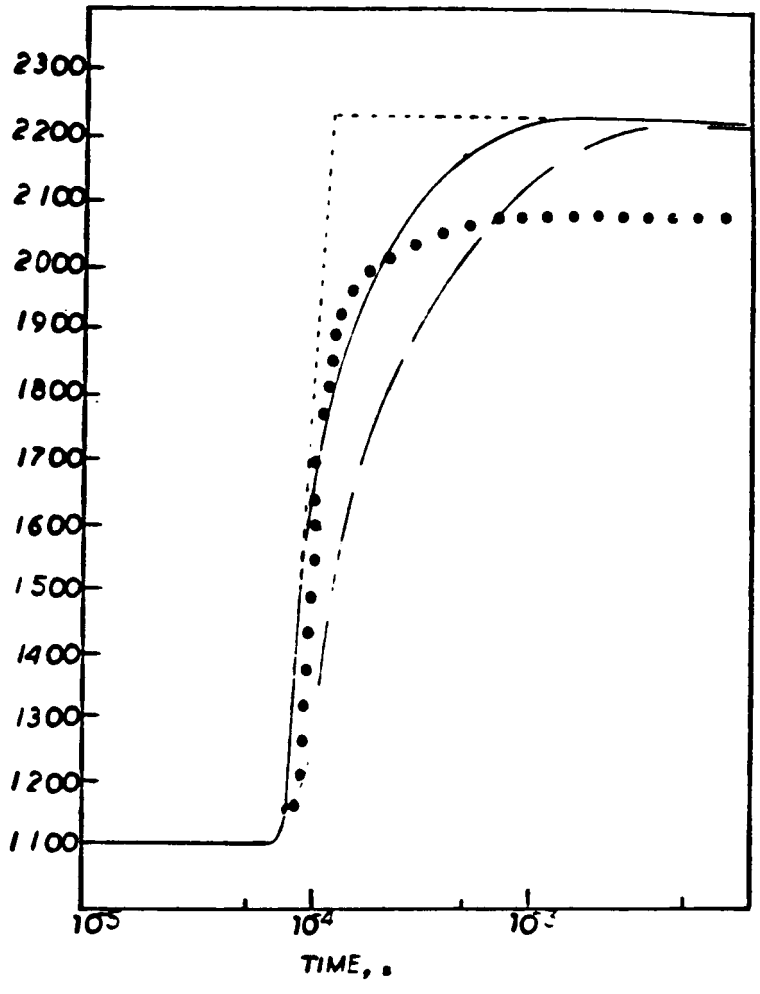

FIGURE 31 LAG FOR CASE NO. 11

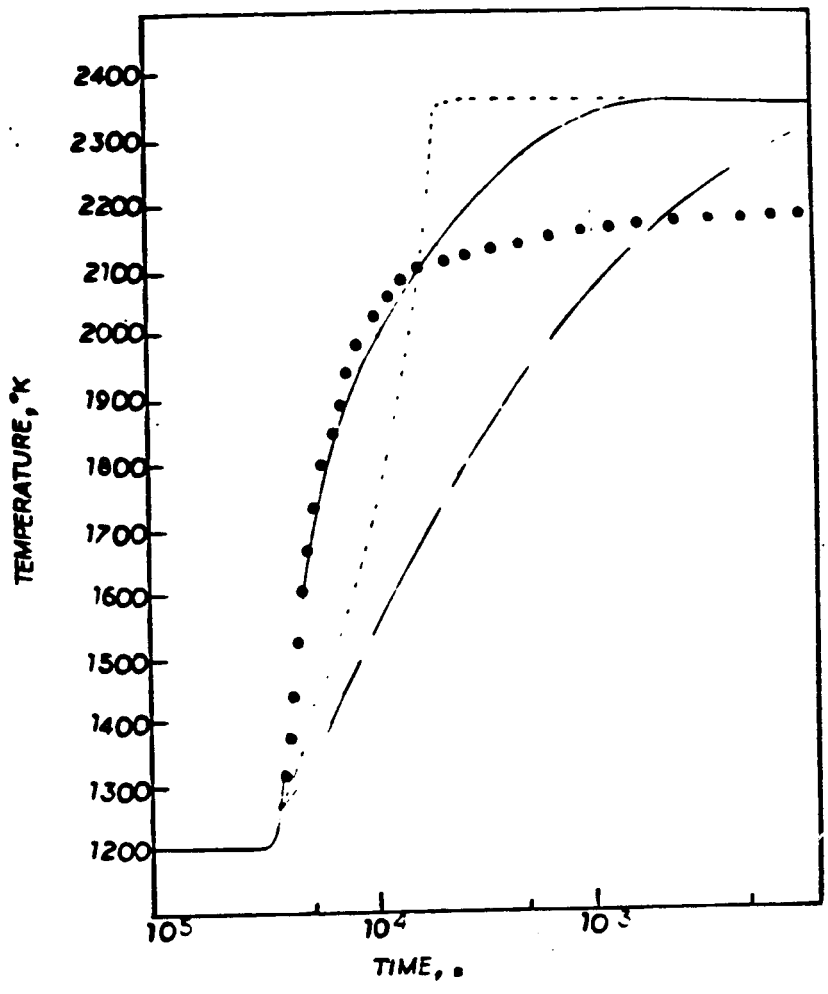

FIGURE 32 LAG FOR CASE NO. 15